University of Kentucky
UKnowledge

Theses and Dissertations--Mining Engineering | Mining Engineering

2013

Enhanced phosphate flotation using novel depressants

Lingyu Zhang
University of Kentucky, zly870110@gmail.com

Right click to open a feedback form in a new tab to let us know how this document benefits you.

Recommended Citation

Zhang, Lingyu, "Enhanced phosphate flotation using novel depressants" (2013). *Theses and Dissertations--Mining Engineering*. 10.
https://uknowledge.uky.edu/mng_etds/10

This Master's Thesis is brought to you for free and open access by the Mining Engineering at UKnowledge. It has been accepted for inclusion in Theses and Dissertations--Mining Engineering by an authorized administrator of UKnowledge. For more information, please contact UKnowledge@lsv.uky.edu.

STUDENT AGREEMENT:

I represent that my thesis or dissertation and abstract are my original work. Proper attribution has been given to all outside sources. I understand that I am solely responsible for obtaining any needed copyright permissions. I have obtained and attached hereto needed written permission statements(s) from the owner(s) of each third-party copyrighted matter to be included in my work, allowing electronic distribution (if such use is not permitted by the fair use doctrine).

I hereby grant to The University of Kentucky and its agents the non-exclusive license to archive and make accessible my work in whole or in part in all forms of media, now or hereafter known. I agree that the document mentioned above may be made available immediately for worldwide access unless a preapproved embargo applies.

I retain all other ownership rights to the copyright of my work. I also retain the right to use in future works (such as articles or books) all or part of my work. I understand that I am free to register the copyright to my work.

REVIEW, APPROVAL AND ACCEPTANCE

The document mentioned above has been reviewed and accepted by the student's advisor, on behalf of the advisory committee, and by the Director of Graduate Studies (DGS), on behalf of the program; we verify that this is the final, approved version of the student's dissertation including all changes required by the advisory committee. The undersigned agree to abide by the statements above.

Lingyu Zhang, Student

Dr. Daniel Tao, Major Professor

Dr. Thomas Novak, Director of Graduate Studies

ENHANCED PHOSPHATE FLOTATION USING NOVEL DEPRESSANTS

THESIS

A thesis submitted in partial fulfillment of the requirements for the degree of Master of Science in Mining Engineering in the College of Engineering at the University of Kentucky

By

Lingyu Zhang

Lexington, Kentucky

Director: Dr. Daniel Tao, Professor of Mining Engineering

Lexington, Kentucky

2013

Copyright © Lingyu Zhang 2013

ABSTRACT OF THESIS

ENHANCED PHOSPHATE FLOTATION USING NOVEL DEPRESSANTS

Froth flotation is the most efficient method for phosphate separation, which is a physic-chemical separation process based on the difference of surface properties between the valuable minerals and unwanted gangue minerals. However, the presence of clay slimes in the slurry after grinding consumes a large amount of reagents, decreases the collision probability between bubbles and minerals, prevents phosphate particle attachment to air bubbles, and thus considerably reduces flotation recovery and concentrate grade. Georgia Pacific Chemical, LLC has recently developed novel depressants, i.e., clay binders, which are a series of low molecular weight specialty polymers to help improve phosphate flotation performance by selectively agglomerating and depressing clay particles, thus lowering their surface area and reducing the adsorption of surfactants.

This thesis addresses the effects of clay binders on phosphate flotation performance and their adsorption behavior on different minerals in a sedimentary phosphate ore. Quartz Crystal Microbalance with Dissipation technique (QCM-D) was used to study adsorption characteristics of clay binders and batch flotation tests were performed under different conditions to investigate phosphate flotation performance. The experimental results have shown that clay binders significantly improved phosphate flotation selectivity and reduced the dosages of collector and sodium silicate used as dispersant in the industry.

Keywords: phosphate flotation, collector, depressant, clay binder, clay

Lingyu Zhang

Student's Signature

11/8/2013

Date

ENHANCED PHOSPHATE FLOTATION USING NOVEL DEPRESSANTS

By

Lingyu Zhang

Dr. Daniel Tao
Director of Thesis

Dr. Thomas Novak
Director of Graduate Studies

11/8/2013

ACKNOWLEDGEMENTS

I would like to express my greatest acknowledgement to my advisor Dr. Daniel Tao for his precious advice, motivation and continual support throughout this study. He let me to have the opportunity to make my dream come true, studying in the United States. This thesis was impossible to me without his academic guidance, fairness and responsiveness. His modest and prudent spirit always influences me and reminds me to work harder.

I would like to extend my deep gratitude to the thesis committee members, Dr. Rick Q. Honaker, professor of Mining Engineering, and Dr. B.K.Parekh, Senior Engineer, Center for Applied Energy Research, for their insightful comments, valuable guidance, suggestion and enthusiasm. I also would like to extend thank to Mr. Ed Thompson for his assistant in the laboratory, his effort of maintaining every single instrument. My appreciation is also expressed to all the other students, staffs and professors for their support.

Appreciation is extended to Georgia-Pacific Chemicals LLC. (GP) for supplying flotation chemicals employed in the study, and Yunnan Phosphate Company for providing phosphate specimens.

Finally, I would like to dedicate this thesis to my dearest family. The constant support and encouragement from my father and mother was always the greatest motivation for me to accomplish all.

TABLE OF CONTENTS

LIST OF TABLES

LIST OF FIGURES

CHAPTER 1 INTRODUCTION

1.1 BACKGROUND

Mineral resources are essential to human life and economic development. Phosphates are some of the most important minerals on the earth as they provide fertilizers for agriculture and essential feedstock for chemical production. Phosphates are used in many commercial and industrial products such as cleaning agents, dental creams, and flame retardants. Around 95% phosphate ore is used in the production of fertilizers or animal feed. The consumption of P_2O_5 in fertilizer in the world was projected to increase from 41.9 million tons in 2012 to 45.3 million tons in 2016 (Jasinski, 2013).

There are two main types of phosphate deposits: sedimentary phosphate and igneous phosphate. More than 80% of phosphate containing rocks in the world are sedimentary and are a non-renewable natural resource that needs to be processed prior to commercial applications. Igneous phosphate deposits are mainly found in Russia, the Republic of South Africa, Finland and Brazil. Igneous ores are mostly of low grade, but beneficiation can improve the P_2O_5 grade to 30%. The United States, China, Morocco and Russia produce 70% to 75% of the world's total phosphate (Cisse and Mrabet, 2004). China has produced more phosphate than other countries since 2006. In 2008, around 50 million tons of phosphate was produced in China, excluding small "artisanal" mines (Jasinski, 2009).

In the acidulation process of phosphorate, some special physical and chemical specifications for phosphate are critical to the phosphoric product quality. Insoluble impurities may cause erosion in stainless steel equipment and influence the filtration of gypsum. Soluble impurities in phosphate rock can influence the production of phosphoric acid and phosphoric fertilizer. Soluble impurities can also result in corrosion, sludge formation, process instability, increase in acid viscosity, etc (Theys, 2003).

Iron and aluminum content (R_2O_3) are the main cause of sludge and can be present throughout phosphoric acid production. The ratio of R_2O_3 to P_2O_5 needs to be less than 0.095 (Lehr and McClellan, 1973; El-Shall et al., 2003). Phosphate ores need to be processed to ensure that the ratio between CaO and P_2O_5 is less than 1.6 in order to avoid high sulfuric acid consumption during acidulation when they are used in fertilizer (Frazier and Lee, 1972). Chlorine is also harmful in phosphate ores due to its corrosive action on plant equipment and the content of chlorine should be less than 0.1-0.2% (Everhart, 1971). In phosphate ore, magnesium is undesirable as it can lead to the blinding of gypsum filters, since fluorine precipitates with magnesium. The MgO content should be less than 1.0% (McClellan and Germillion, 1980; El-Shall et al, 2003).

In order to effectively separate phosphate from gangues such as quartz, chert, clay, feldspar, mica, calcite, and dolomite, froth flotation is often used as a beneficiation method (Sis and Chander, 2003). It can be accomplished using anionic fatty acid as a collector for phosphate in direct flotation or cationic amine as a collector for quartz in reverse flotation or they can be used in combination as in the well-known "Crago" process used in the Florida phosphate industry.

The difficulty in phosphate beneficiation arises from three factors: i) in apatite lattice PO_4^{-3} are highly substituted for CO_3^{-2} and F^-; ii) the phosphate particle surface is porous and irregular leading to a larger surface area; iii) sedimentary minerals such as phosphate contain more slimes than crystalline minerals and therefore, require the use of higher dosages of reagents in processing (Henchiri, 2003).

Great effort has been made to improve phosphate flotation recovery and efficiency. However, many phosphate beneficiation processes are still low in phosphate recovery and grade, high in reagent consumption, and poor in process efficiency. The interactions between different mineral particles and reagents are not well understood and the rejection of some gangue minerals such as dolomite remains a challenge to the industry. Chinese phosphate minerals usually have to be finely ground to liberate phosphate from its matrix

prior to flotation owing to the fine grain size of phosphate in the ore. As a result, the consumption of flotation reagent is very high (Wang and Gu, 2010).

1.2 OBJECTIVES

The objective of this study is the improvement of phosphate flotation performance by means of testing and evaluating several novel clay binders, a special agglomerating depressant acquired from the Georgia Pacific Chemicals, LLC (GP). A number of process parameters such as the dosage of collector, the dosage of depressant, and the solution pH are investigated in details to optimize the reagent performance. Since water glass is used as dispersant in plant, the effect of clay binders combined with water glass was also evaluated. The use of water glass has serious detrimental effects on downstream processes such as tailings sedimentation and disposal and thus it is desirable to minimize its dosage. Advanced characterization and analysis techniques such as an automatic zeta potential meter and QCM-D were employed to better understand the interactions and adsorption of reagents on different minerals. It was expected that this study would lead to the identification and development of more effective reagents for phosphate flotation and an improved phosphate flotation process.

Copyright © Lingyu Zhang 2013

CHAPTER 2 LITERATURE REVIEW

2.1. GENERAL PHOSPHATE CHARACTERISTICS

Phosphate ores occur in nature primarily as marine sedimentary deposits. Most sedimentary phosphate deposits are located in northern Africa, China, the Middle East and the United States. Meanwhile, most igneous deposits are found in Brazil, Canada, Russia and South Africa. Worldwide, the scope of phosphate mining is predicted to increase to 228 million tons by 2015. No substitutes for phosphate have been found (Jasinski. S.M, 2011).

Phosphate ores can be divided into three groups according to quality and P_2O_5 grade: low-grade ores (12-16% P_2O_5), intermediate-grade ores (17-25% P_2O_5), and high-grade ores (26-35% P_2O_5). The deposits that consist of 28-38% P_2O_5 are considered commercial-grade phosphate deposits (Sengul et al., 2006).

The only economical source of the phosphorus used in manufacturing phosphatic fertilizers and chemicals, is phosphate rock. Around 95% of the world phosphate is utilized in the fertilizer industry. With an increase in world population, more fertilizer is required to promise agriculture product yields. Most extracted phosphate ore needs to be processed owing to a low grade for economic utilization. Phosphate rock without processing, except that found in moist, acidic soils, is not soluble enough to be made available to manufacturers.

Phosphoric acid made through treating phosphate rock with sulfuric acid is a basic component of phosphate fertilizers. Diammonium phosphate (DAP) and monoammonium phosphate (MAP) are phosphatic fertilizers produced from the reaction of phosphoric acid with ammonia and triple superphosphate (U.S. Geological Survey). The chemical grade of phosphate rock should be more than 24% P_2O_5, less than 3% Fe_2O_3 (Holmes et al. 1982).

2.2.CHINESE PHOSPHATE CHARACTERISTICS

Phosphate ores in China are characterized by a fine dissemination of intergrown minerals and a high content of carbonates. Flotation is reported to be the most efficient method of recovering phosphate from sedimentary siliceous-calcareous phosphate ores (Zheng et al., 1999). Chinese phosphates are mostly sedimentary apatites. There are three principal categories of sedimentary apatites: siliceous ores, carbonate ores and clayed phosphates. The major gangue minerals in siliceous ores are quartz, chalcedony and opaline. Clayed phosphates are associated with gangue minerals containing clays, hydrous iron and aluminum oxides in silt and clay size ranges (Lehr and McClellan, 1973). Phosphate resources in China are mostly of low and medium P_2O_5 grade and have a high MgO content; some impurities such as dolomite and silicates are contained in the fine particles (Gu et al., 1998).

Chinese phosphorus resources are mostly in the form of collophanite. Fines of carbonfluoapatite is the main phosphorus-bearing mineral with a dissemination size ranging from 0.2 to 2 μm (Lu and Sun, 1999). Since dolomite and calcite are commonly intergrown and finely distributed with the phosphorus-bearing minerals, fine grinding is needed to achieve acceptable liberation of carbonate minerals from the ore.

The problems with phosphate ores, specifically calcium and calcium-silicon sedimentary phosphate ores are as follows:

a. Increasing the substitution of CO_3^{-2} for PO_4^{-3} in the crystal lattice of phosphate minerals decreases the perfection of mineral crystals and the crystal size, thereby decreasing the floatability of phosphate;

b. Separating phosphate minerals from carbonate minerals by conventional flotation or other concentration methods is difficult due to their similar floatability;

c. Concentrating fine ground mineral particles is difficult. Combined collectors with improved collection ability and selectivity have been developed and applied in several plants in China (Lu and Sun, 1999).

The phosphate sample used in this study was a typical sedimentary phosphate ore acquired from Yunnan Province, China. Its characteristics are:

a. Long history. The phosphate ore has been formed over a span of at least 500 million years.

b. High content of carbonates. Around 85% of Chinese phosphate is siliceous-calcareous. Carbonates are mainly in the form of dolomite. MgO content is mostly more than 3% and some is even higher than 10%.

c. Fine particle size. Chinese phosphates are mainly colloidal agglomerate or francolite that is carbonate-fluorapatite. The impurities such as dolomite, quartz, calcedonite and clays are in the 0.6-0.04 mm size fraction. In order to liberate impurities from phosphate, phosphate ores must be ground to 0.05-0.01 mm.

2.3.FROTH FLOTATION FUNDAMENTALS

Flotation is the most widely used method for phosphate beneficiation. More than 50% the world's useable phosphate is produced from this process.

Froth flotation is a physic-chemical beneficiation technique that has great commercial benefits owing to its high separation efficiency and low costs. The flotation process is based on differences in surface hydrophobicity of different minerals. Hydrophobic particles are captured by air bubbles and ascend to the top of the pulp zone and are eventually discharged as froth product (Tao, 2004). Applications of flotation method are widely used in the mineral processing industry to separate different mineral particles ranging from sizes 10 μm to 100 μm. Many studies on the interactions between particles and bubbles, adsorption of reagents on minerals, novel flotation reagents, development of flotation machines and columns have been conducted with the aim of improving flotation efficiency and recovery.

Flotation is the result of interactions between particles and bubbles. The most critical steps in the flotation process are collision, attachment and detachment. The flotation

process contains two distinctly different zones: froth zone and collection zone. The overall recovery R in flotation process can be determined from Equation (1):

$$R = \frac{R_C R_F}{R_C R_F + 1 - R_C} \tag{1}$$

where R_C is recovery of collection zone and R_F is recovery of froth zone.

A typical flotation system is illustrated in Figure 2.1. The collection zone is the place where contact occurs between the air bubbles and the particles. In the froth zone, entrained materials are removed from the froth and some particles flow back to the collection zone (Harbort et al., 2004). If the recovery (R_F) in froth zone is low, then the particle may not be recovered in froth zone and would drop back to the pulp.

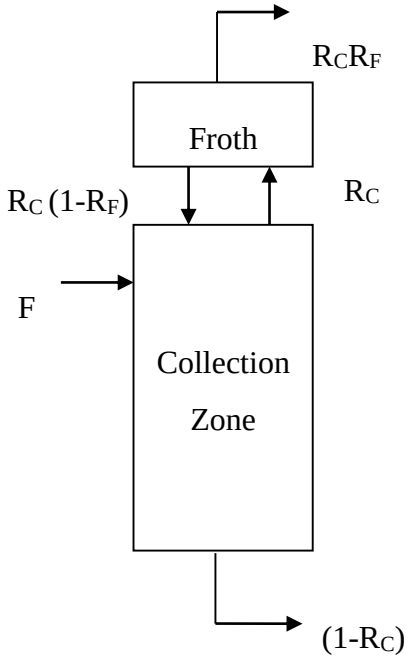

Figure 2.1. The procedure of determining the overall relationship

The recovery of a given component in the feed is a function of the flotation rate constant ($k_{i)}$, particle residence time (τ) and hydrodynamic conditions. Using Levenspiel's (1972) axial mixing equation, fraction recovery is determined by:

$$R = 1 - \frac{4ae^{(Pe/2)}}{(1+a)^2 e^{(a/2)Pe} - (1-a)^2 e^{(-a/2)Pe}} \tag{2}$$

$$a = (1 + \frac{4k\tau_m}{Pe})^{0.5} \tag{3}$$

$$Pe = (\frac{L}{D})^{0.53} (\frac{V_l}{(1-\varepsilon)V_g})^{0.35} \tag{4}$$

where Pe is the Peclet Number (a dimensionless term to quantify mixing in a chemical reactor), L is a characteristic's length and D is the axial dispersion coefficient for the characteristic of interest, V_l is superficial liquid velocity, V_g is superficial gas velocity. ε is the fractional of air hold-up, k is the process rate constant and τ_m is the mean residence time of the component within the reactor. When Pe=∞, it is the case of plug flow and when Pe=0 it is the case of perfectly mixed (Mankosa et al. 1992). Equation (2) can be simplified to Equations (5) and (6) for these two extreme conditions:

Plug flow: $R = 1 - \exp(-k\tau_m)$ (5)

Perfectly mixed: $R = \frac{k\tau_m}{1 + k\tau_m}$ (6)

Flotation rate is a measurement of how fast one particle can be recovered in the collection zone. It can be quantified by:

$$k = \frac{3V_g}{2D_b} P = \frac{1}{4} S_b P \tag{7}$$

in which P is the probability of flotation in the collection zone, V_g is superficial gas velocity, D_b is bubble diameter and S_b is the superficial bubble surface area rate.

The probability of flotation is a function of three individual processes that occur in the collection zone: collision, attachment, and detachment. It is expressed in Equation (8)

where P_C, P_A, and P_D are the probability of collision, probability of attachment and probability of detachment.

$$P = P_C P_A (1 - P_D) \tag{8}$$

To achieve great flotation separation efficiency, each of the three processes must be successful as shown in figure 2.2 (Tao, 2004).

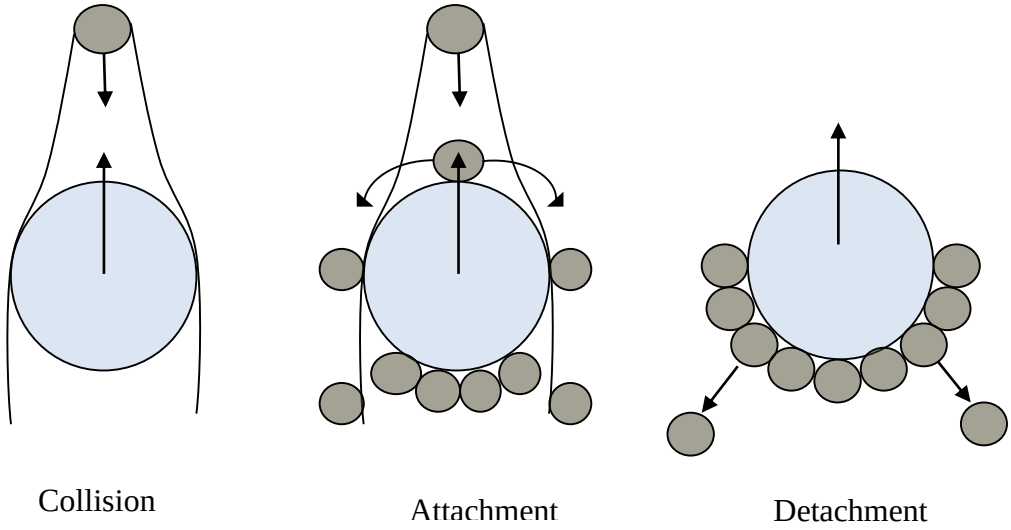

Figure 2.2. Three steps in flotation process

Collision is the first step in flotation. A collision occurs when a particle and a bubble are sufficiently close to each other. Gaudin (1957) proposed a model of collision probability for small bubbles in the Stoke's flow condition:

$$P_c = (\frac{D_p}{D_b})^2 \left[\frac{3}{2} + \frac{4\mathrm{Re}^{0.72}}{15} \right] \tag{9}$$

where D_b is the bubble size and D_p is the particle size.

Attachment occurs when the liquid film between the bubble and the hydrophobic particle becomes thin and ruptures. Induction time must be smaller than the sliding time so that the particle can attach to air bubble. The difference in P_A value of different

particles plays an important role in determining flotation selectivity. Yoon concluded that induction time and surface forces between particles and bubbles can determine or predict the probability of attachment (Yoon, 2000). The difference of P_A of different particles determines the selectivity of flotation.

Ralston et al. derived a general equation for calculating P_A:

$$P_A = \frac{\sin^2[2\tan^{-1}\exp(-[(2(u_p+u_b)+(u_p+u_b)(D_b/(D_b+D_p))3/(D_b+D_p)]t_i)]}{2\beta((1+\beta^2)^{\frac{1}{2}}-\beta)} \tag{10}$$

where $$\beta = \frac{12D_B}{D_p}\frac{\rho_f}{\rho_p-\rho_f}\frac{1}{\mathrm{Re}} \tag{11}$$

in which ρ_f and ρ_p are fluid and particle densities, D_b and D_P are diameters of bubble and particle, Re is Reynold's number, t_i is induction time, u_b and u_p is bubble and particle rise velocities.

Not all particles attached to bubbles move on to the froth phase. Some particles will detach from bubble surface and drop back to the collection zone. When total detachment forces are larger than maximum adhesive forces, detachment between particle and bubble occurs. Four categories of forces exist between the bubble and the particle. Capillary force (F_p), excess force (F_e) (the difference between the excess pressure in the bubble and hydrostatic force); real weight of particle in liquid medium (F_w); and other forces such as drag force (F_d). The four forces are calculated as follows:

$$F_p = \frac{\pi D_p \gamma(1-\cos\theta_d)}{2} \tag{12}$$

$$F_e = \frac{1}{4}\pi D_p^2(1-\cos\theta_d)(\frac{2\gamma}{D_p}-\frac{\rho_w g D_b}{2}) \tag{13}$$

$$F_w = \frac{1}{6}\pi D_p^3 \rho_p g - \frac{1}{8}\pi D_p^3 \rho_p g\left[\frac{2}{3} + \cos\left(\frac{\theta_d}{2}\right) - \left(\frac{1}{3}\right)\cos^3\left(\frac{\theta_d}{2}\right)\right] \quad (14)$$

$$F_d = 3\pi D_p \eta \mu \quad (15)$$

in which γ is the liquid surface tension; ρ_P and ρ_w are the densities of particle and water. When detachment occurs, the sum of capillary force and excess force is equal to the sum of weight and drag force.

$$\left(F_p + F_e\right) - \left(F_w + F_d\right) = 0 \quad (16)$$

Compared with F_w, F_d is so small that it can be ignored. Thus Eq. (16) can be simplified to:

$$\left(F_p + F_e\right) - F_W = 0 \quad (17)$$

The probability of detachment (P_D) may be found by the following equation:

$$P_D = \frac{1}{1 + F_{at}/F_{de}} \quad (18)$$

where F_{at} is the attachment force and F_{de} is the total detachment force. When $F_{at} = F_{de}$, $P_d = 0.5$; when $F_{at} >> F_{de}$, $P_D = 0$; and when $F_{at} << F_{de}$, $P_D = 1$. Equations (17) and (18) suggest that coarse particles are more likely to detach from air bubbles and small bubbles will increase flotation recovery of coarse particles.

Flotation reagents are often added to flotation slurry to modify surface hydrophobicity of different mineral particles. Since most minerals are hydrophilic, they need to be made hydrophobic by adding surface-active chemicals referred to as collectors. Most flotation reagents assist flotation through the adsorption of collector on minerals. Contact angle is utilized to measure the wettability of the mineral particles. The Young-Dupre equation shows the relationship of interfacial tension between gas (G), solid (S), and liquid (L) (Young, 1805):

$$\gamma_{SG} = \gamma_{SL} + \gamma_{LG}\cos\theta \quad (19)$$

Free energy is changed as a result of the creation of a solid-gas interface and the destruction of an equal area of both solid-liquid and liquid-gas interfaces. Free energy change is written as:

$$\Delta G_{ad} = \gamma_{SG} - \gamma_{SL} - \gamma_{LG} \tag{20}$$

$$\Delta G_{ad} = \gamma_{LG}(cos\,\theta - 1) \tag{21}$$

The work of adhesion (W_{SG}) is the work necessary to break the particle and bubble interface, and is equal to the work necessary to separate the solid-air interface and produce air-water and solid water separate interfaces.

$$W_{SG} = \gamma_{LG} + \gamma_{SL} - \gamma_{SG} = -\Delta G_{ad} \tag{22}$$

When θ was larger than zero, $\Delta G$was negative, meaning that the collector could be adsorbed on three separate interfaces and tension could be reduced. Particle-bubble attachment is determined by the adsorption of surfactants and polymers on the three interfaces. Highly hydrophilic solid needs low γ_{SG} or $\gamma_{LG}$to ensure enough collector adsorption and effective flotation. The wetting of solid surfaces with interfacial tension and contact angle is shown in Figure 3.

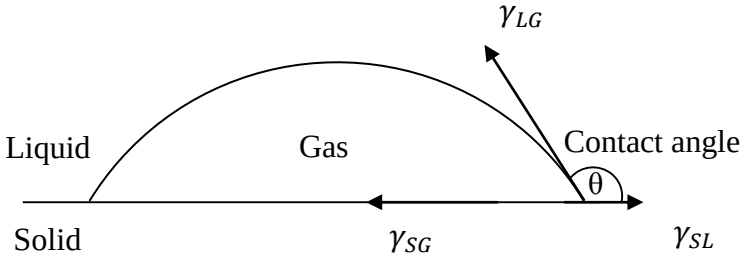

Figure 2.3. Wetting of solid surfaces from Young's equation

Adsorption of surfactant species can improve particle hydrophobicity by changing the solid interfacial tensions, which is a vital step to the flotation process. The surfactants adsorbed on the bubble surface can stabilize both the bubbles and the particle-bubble aggregate when the collision between particles and bubbles occurs. Adsorption reduces interfacial tension (γ), as shown in Gibbs adsorption equation (Gibbs, 1928):

$$\Gamma_A = -\frac{1}{nRT}\frac{d\gamma}{d\ln C_A} \tag{23}$$

in which n is the equivalents produced under the condition that one mole of the salt is dissolved in water, Γ_A is the adsorption density in mol/cm^2 , γ is interfacial tension in ergs/cm^2, C is the bulk concentration in mol/L, R is the gas constant in cal/deg mol, and T is the absolute temperature. Γ_A and C_A are adsorption density and bulk concentration of the surfactant ion A, respectively. The equation demonstrates that the slope for the relationship between Γ_A and $\ln C_A$ is negative when Γ is positive (Fuerstenau and Han, 2003).

2.4. PHOSPHATE FLOTATION TECHNOLOGY

There are various beneficiation schemes that can be applied to improve phosphate grade including: 1) physical methods such as size reduction, wet and dry screening, size classification, gravity separation, washing, desliming,magnetic separation (Unkelbach and Wasmuth, 1991); 2) chemical methods that include leaching of phosphorous with sulfuric or nitric acid (Al-Fariss, Ozbelge, and Abdulrazik, 1991; Abu-Eishah et al., 1991); 3) and thermal treatment or calcinations (Orphy, Yousef, and Lawendy, 1969; Doheim, Tarshan, and El-Gendy, 1978). Heavy media separation can be applied when phosphate minerals are porous. High-intensity magnetic separation can be utilized when carbonate minerals are combined with iron oxides (Abramov, et a., 1993). Their applications in the phosphate industry are limited due to relatively poor efficiency.

Flotation is one of the most effective technologies for phosphate processing. More than 60% of the commercial phosphate in the world is processed through flotation (Abdel-Zaher, 2008). It is generally used for siliceous phosphate when other cheaper or less complicated techniques fail to reach a very high phosphate concentrates suitable for chemical processing. The removal of carbonates from phosphate ores has been the focus of significant research efforts. However, selective flotation of carbonates from phosphate is difficult because of the similarity in the physicochemical properties of carbonate and phosphate ores. Carbonate and phosphate separation by flotation is employed

commercially in Finland and Brazil to process igneous phosphate rocks. Carbonate-containing sedimentary phosphate minerals are beneficiated by flotation in India and China. (Steven et al., 2010)

2.4.1.Direct flotation

Direct flotation is mostly used to upgrade phosphates, particularly finely ground silica-calcium collophanite by adding depressants and collectors. It has the advantage of being a simple procedure with high separation efficiency.

Du Rietz (1958) studied the separation of apatite and iron oxides using fatty acid flotation. The results indicated that apatite may be floated readily from iron oxide minerals by using oleate above pH 8 owing to the solubility of the Ca^{++} and Fe^{3+} fatty acid soaps. Thus apatite was floated successfully from iron oxide minerals and silicates by sodium oleate at pH 10 after going through the steps of desliming and magnetic separation.

Herbert, et al. (1969) discovered a two-stage anionic flotation process for phosphate beneficiating from silica and carbonates. In the first stage, both phosphate and carbonates are floated using an anionic collector at pH 9-10.5, followed by carbonate flotation with the same collector at a lower pH, around 5.5, while a soluble phosphate salt is used as phosphate depressant.

Jones (1975) investigated a single-stage flotation process. An anionic collector was used to float phosphate with a graft polymer added as silica depressant. Grade-recovery trends indicated that a single-digit insoluble concentrate could be achieved at percent recoveries in the low 70's.

Zhang et al. (2002) reported that Single-collector, All-anionic Phosphate Recovery or SAPR is one of the FIPR'S serious approaches to develop a viable alternative to the Crago "Double Float" process. This process could achieve A.I. rejection of more than 85% by using a blend of anionic collectors.

Albuquerque (2012) studied the direct flotation route of the concentration of a phosphate ore bearing a silicate-carbonate gangue by using flotation columns. The results of the tests indicate that under alkaline conditions an open, rougher-cleaner circuit yielded a final concentrate of 30.5% P_2O_5 and recovery was at 80.8% with a natural collector extracted from the distillation of coconut oil and depressant corn starch.

2.4.2.Reverse flotation

In reverse flotation of phosphate silica is often floated with cationic collectors (amines) while apatite is depressed. Successful reverse flotation of siliceous minerals from phosphate minerals have been documented in literature (El-Shall et al., 1996; Elgillani and Abouzeid, 1993; Anazia and Hanna, 1987).

Amine flotation of phosphate is selective due to strong electrostatic interactions between a positively charged amine colloid and negatively charged silica particles. However, the high costs and consumption of amine reduce the attractiveness of this separation method.

Samani et al. (1975) used sodium, potassium-tartrate and either aluminum or iron sulfate to depress the phosphate minerals. A mixture of oleic acid and pine oil was used to float carbonate gangue at a pH of 7.5 to 8.2. The formation of strong electronegative film on the phosphate surfaces prevents the adsorption of anionic collector that leads to the depression of phosphate.

Hanna and Anazia (1987) successfully conducted a study to float carbonate gangue from sedimentary apatite with fatty acid collector, using sulfuric acid to depress phosphate minerals in an acidic pulp at a pH of 3.5 to 4.5. Furthermore, conditioning of the pulp with the fatty acid collector was found unnecessary to achieve flotation of carbonate gangue from phosphate bearing minerals. Three Asian dolomitic and calcareous phosphate ores were studied using this process, yielding phosphate concentrates of 36% to 38% P_2O_5 and 0.8% MgO with 80% to 85% phosphate recovery

from a feed of 19% to 23% P_2O_5 grade. This process is referred to as the Mineral Resource Institute (MRI) process.

Zhang (2002) did research on an all-cationic flotation process using a relatively inexpensive amine condensate to float fine quartz from an "unsized" feed both with and without the use of a suitable phosphate depressant. This was followed by sizing the cell underflow product at 14 and 35 mesh, and subjecting the two size fractions (14×15 and 35×150) to the second stage cationic flotation using a higher quality cationic reagent to reject the remaining quartz and produce final concentrates of 30%-31% P_2O_5.

Mohammadkhani et al. (2011) studied reverse flotation of phosphate from a very low grade (5.01% of P_2O_5) sedimentary ore. Oleic acid and Armac-T were used as carbonate and silicate collectors, respectively. A few phosphate mineral depressants including sodium silicate, starch, tannic, aluminum sulfate, (Na, K) Tartarat, sodium tripolyphosphate, H_3PO_4, and H_2SO_4 were compared in acidic and alkaline conditions. Anionic-cationic and cationic-anionic methods were used to optimize the grade and recovery of phosphate. A mixture of (Na, K) tartarat and aluminum sulfate had the optimum effect on phosphate depression. The final concentrate grade and recovery reached 21.67% and 65.5% respectively. The results indicated that anionic-cationic method was more effective.

2.4.3.Combination of direct and reverse flotation

The Crago "double float" process is a matured technique for phosphate processing. In the Crago process, sized flotation feed is dewatered and conditioned at solid concentrate with 70% fatty acid and fuel oil at an alkaline pH, and then the phosphate is floated to produce a rougher concentrate and a sand tailing. About 30% - 40% of the silica floats with the phosphate at this step. Sulfuric acid is used to de-oil the concentrate and to remove collector from phosphate particles. Lastly, an amine is added to remove the silica at neutral pH.

Since, in the Crago process, about 30% - 40% by weight of the sands in the feed is floated by fatty acid and then by amine, it is not an efficient process when considering collector utilization. One of the biggest drawbacks of this process is the step of de-oiling. It consumes a large amount of sulfuric acid that requires special safety precautions and equipment maintenance. If the de-oiling is not sufficient, it can lead to a poor concentrate grade. De-oiling can cause loss of fine phosphate particles. Further, amine costs more than fatty acid, and is sensitive to water quality.

Some other methods developed to replace the conventional Crago process include combinations of anionic-cationic flotation methods. Zhang, et al. (1997), studied an amine-fatty acid double flotation process using Florida phosphate. An amine was used to float the silica at a neutral pH, and then a fatty acid was added for phosphate flotation. The authors reported that a reverse Crago process was more efficient and economic benefits were better. It 1) reduced the total cost and amount reagent consumed; 2) increased flotation recovery by 2% - 5%; 3) reduced the numbers of conditioners (in amine flotation conditioners are not required. Amine can be adsorbed readily onto silica, thus it is sensitive to the existence of slime); 4) no acid scrubbing circuit is necessary; and, 5) it reduced the size of equipment by 50% - 100% (there is no need to separate coarse from fine feed in amine flotation).

Abdel-Khalek et al. (2000) studied three circuits for phosphate flotation to separate calcite from the phosphate. The flotation circuit, comprised of two stages including one for carbonate and the other one for either phosphate or silica, presents the best strategy to improve calcitic siliceous phosphate grade. The results showed that the application of the processes can reduce carbonates from 13.6% to about 6.9%-8.9%. The results also showed that phosphoric acid, when used, has a significant effect on phosphate separation. Concentrates of P_2O_5 above 30% are obtained with a flotation strategy for a feed ground to -0.15 mm.

2.5.DEPRESSANTS IN PHOSPHATE FLOTATION

2.5.1.Phosphate, carbonate and silicate depressants

Flotation reagents are associated with the surface characteristics of the ore and interactions between its minerals and the pulp medium. Several types of flotation reagents are used in phosphate flotation, including collectors, pH modifiers, depressants, promoters, and rheological modifiers. These reagents modify the surface characteristic of minerals to improve recovery, selectivity and handling properties (Sotillo et al. 2009).

Depressants play a vital role in phosphate flotation by preventing the flotation of unwanted minerals in direct flotation or of phosphate minerals in reverse flotation. They are designed to enhance the separation of minerals in an ore. When a depressant has the same functional group as a collector but the hydrophobic part of the collector is replaced with a hydrophilic component, this depressant can have a good selectivity. For instance, fatty acids have a carboxylated functionality that can collect calcite, dolomite, apatite and hematite. Thus, a carboxylated depressant such as CMC is effective on these minerals. Phosphoric acid and its derivatives, diposphonic acid [DPA] and orthophosphoric acid [OPA], are most widely used to depress apatite in the reverse flotation of phosphate. Cationic amine collectors are used to collect siliceous minerals while depressants based on cationically modified polysaccharides are effective for depressing siliceous minerals. In carbonate-phosphate systems, apatite can be depressed through the adsorption of $CaHPO_4$ and carbonate can be floated by using fatty acids as collectors in acidic environments between pH 5.5-6.0 (Zhang et al. 1997, Somasundaran and Zhang, 1999). Typical depressants in phosphate flotation are shown in the following table (Sis and Chander, 2003):

Table 2.1. Depressants commonly used in phosphate flotation

Mineral	Depressant
Apatite	Aluminum sulfate and sodium
	Potassium tartrate
	Fluosilicic acid
	Sulfuric acid
	Phosphoric acid
	Sodium carbonate/bicarbonate
	Sodium tripolyphosphate
	Diphosphonic acid
	Dipotassium hydrogen phosphate
	Starch
Silica	Sodium silicate
Carbonates	Sodium silicate
	Hydrofluoric acid
	Gum Arabic
	Starch
	Polysaccarides
	Aromatic sulfonate polymers
	Citric acid

Sodium silicate is often used to improve flotation selectivity for different scarcely soluble minerals or between scarcely soluble and silicate minerals. The combined use of sodium silicate and a mixture of fatty acid and fuel oil were found to be beneficial to phosphate flotation performance (Sis and Chander, 2003).

Jones (1975) created a single stage flotation process using an anionic collector to float phosphate with a graft polymer as a silica depressant. Acid insoluble recovery could be achieved in low 70%'s. Nagaraj et al. (1988) used polymers, including copolymers or terpolymers, derived from acrylamide units and N-acrylamidoglycolic acid units to depressed silica in order to improve anionic flotation process. Insoluble concentrate can be achieved at 15-30%.

Lu and Sun (1999) studied a series of depressants, i.e., tannin, quebracho, lignin and humic acid on carbonates in reverse-direct flotation and reverse flotation. Among these depressants, L339 was efficient in removing carbonate impurities such as dolomite. The main compounds of L339 were derivatives of lignosulphonate that interacted with fatty acid to improve collector adsorption on fluorapatite and enlarge the hydrophilic difference between apatite and carbonate gangue minerals. Mohammadkhani (2011) did research using H_2SO_4 and H_3PO_4 as depressants in reverse flotation experiments. The collector adsorption is prevented as a result of adsorption of aqueous $CaHPO_4$ on the surface of phosphate particles.

Filho and Chaves (1993) studied several depressants used in phosphate flotation and found that dipotassium hydrogen phosphate depressed phosphate more effectively than starch and hydrofluosilicic acid. Corn starch depressed some high-dolomite Brazilian phosphate well. Albuquerque et al. (2012) used a reagents scheme consisting of corn starch and coconut oil that was effective for the separation of apatite and the contaminant calcite, as well as the float of silicates present in this phosphate ore from igneous origin. Corn starch depressed the gangue minerals markedly.

Flouosilicic acid was studied as a phosphate depressant by Celerici (1984). Carbonate flotation was conducted with 500 g/t tall oil as a collector and H_2SiF_6 as a phosphate depressant at 300 g/t and at pH of 6.5. The concentrate grade was acceptable, but the overall P_2O_5 recovery was less than 28%. Atalay and coworkers (1985) reported that fluosilicic acid was not as efficient as diphosphonic acid or phosphoric acid in depressing a Turkish phosphate ore. The concentrate grade was less than 26% while the recovery was below 57%.

The University of Utah researchers, Miller et al. (2001), found the addition of certain nonionic polymers PEO (polyethylene oxide) can increase flotation recovery of coarse phosphate particles and reduce fatty acid/fuel oil consumption. PEO in the phosphate rougher flotation system may influence both the hydrophobicity of the particle and frothing behavior, which is good for improving the recovery of coarse phosphate particles. In the case of a coarse feed (16×35 mesh), 85% phosphate recovery can be achieved with 1200 g/t of fatty acid and fuel oil blend, but only 500 g/t PEO was needed.

2.5.2.Clay depressants

The adverse effects of clay slimes on flotation include high consumption of reagents due to high specific surface area and interference effects on bubble-mineral contact. The tiny size of slime particles increases the difficulty of particles to be captured by bubbles as a result of low collision probability (Tao and Zhou, 2010). Current desliming practices prior to flotation to reduce the concentration of clay in flotation feed are not efficient enough to eliminate clay slime coating problems. As a result, remaining slimes still deteriorate flotation performance and cause higher acid insoluble content in phosphate product. Slime particles also change flotation froth properties that contribute to a poor flotation separation performance. Use of special clay depressing reagents is one way to alleviate the clay problems (Tao et al, 2007; Zhang et al. 1999).

Clay in phosphate ore causes many problems. It makes tailing disposal difficult, and causes tremendous loss of P_2O_5. The slimes may attach to coarse particles and prevent

originally hydrophobic minerals from being floated. The sheet structure of clays provides large surface area that can adsorbs polymers like a sponge (Brown et al., 1954). Table 2.2 shows the size and specific surface area of different minerals in phosphate ore (Lamont et al., 1975; Gruber et al., 1995). It is obvious that clay particles have much greater specific surface area than other minerals. Chinese phosphate is usually ground to smaller than 74 μm to make sure minerals are liberated and some particles are smaller than 2 μm, close to the clay particle size. It is necessary to use depressants to improve flotation efficiency because of a significant amount of clay or clay size minerals present in the flotation feed.

Table 2.2. Size and specific surface area of different minerals in phosphate

Sample	Size, mesh	Specific surface area, m^2/g
Feed	-24+150	2.38-8.59
Concentrate	-24+150	3.5-13.7
Quartz	-24+150	0.17-0.28
Clays	-150	31.6-69.4
Sphere, external	150	0.022

Previous studies have shown the success of separating phosphate from clay minerals by flocculation (El-Shall and Bogan, 1994). Gu and Doner (1993) reported that organic polyanions worked as dispersion agents for Na-clays and Na-soils. Water soluble acrylic polymer was able to keep various materials within an aqueous system, including mud, silt, or clay minerals (Hann and Natoli, 1984). One study showed that calcite and kaolinite could be dispersed well by certain humates (Pan, 1984). Anderson (1992) demonstrated that polyacylic acid adsorbs on clay and the presence and exchange of surface Ca^{2+} cause the adsorption, which might be exchanged for Na^{+}.

Clay binder produced by Georgia Pacific Chemicals, LLC is a series of low molecular weight specialty polymers. They are the condensation products of an amide, an aldehyde and or an amine urea and formaldehyde. The binder plays a role of slime depressant that agglomerates clay slimes to increase the size, lower the surface area, clean bubble and particle surfaces, and reduce the adsorption of surfactants, as shown in Figure 2.4.

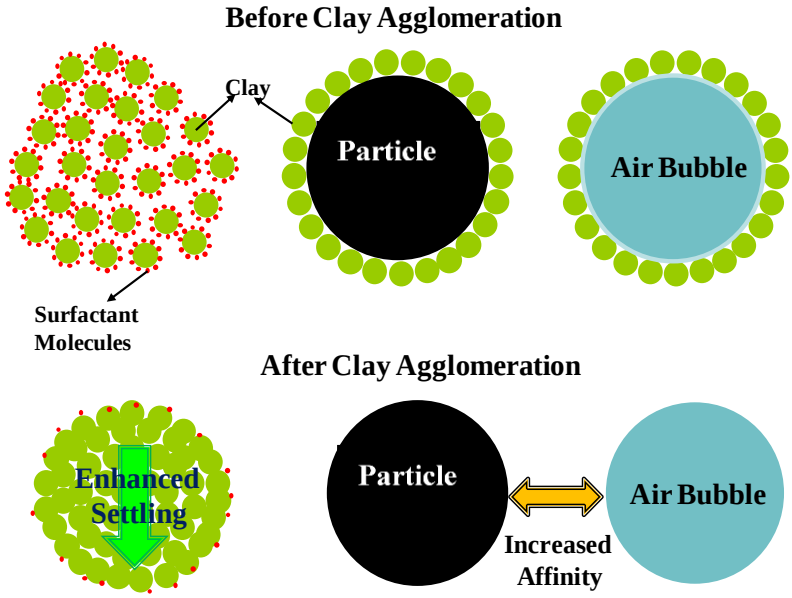

Figure 2.4. Illustration of how clay agglomeration improves flotation performance by removing slime coating from mineral particle and bubble surface and increasing clay particle size.

The main chemical components of binder backbone are carbonyl oxygen, etherified oxygen, amido nitrogen and amines that can hydrogen bond to siliceous oxygen or chelate to electrophilic metals such as Mg, Fe, or Al on clay surfaces. The structure of one of the clay binders is shown as follows:

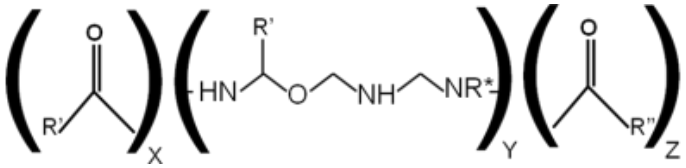

Two main adsorption mechanisms of clay binder are dipole-dipole interaction and strong hydrogen bond. Because of amphiprotic characteristic and multiple binding and chelating sites, binding can be very selective. Thus, clay binder can promote phosphate flotation separation as a result of larger clay particle size and higher surface hydrophilicity. The main factors that affect the performance and specification of clay binders are the molar ratio between formaldehyde and urea, functionalization degree, addition of functional groups, molecular weight and crosslink density. Some new formulations have been developed for use in flotation of different minerals such as phosphate, potash and coal. (Tao et al, 2007)

Tao et al. (2007) used GP clay binders in flotation tests with coal and potash, and they observed higher flotation recovery in the presence of clay binders. Use of clay binders can produce higher concentrate yield than without clay binder. Figure 2.5 shows the coal flotation results with different impeller rotation speeds with and without clay binder. Obviously clay binders significantly improved the flotation performance.

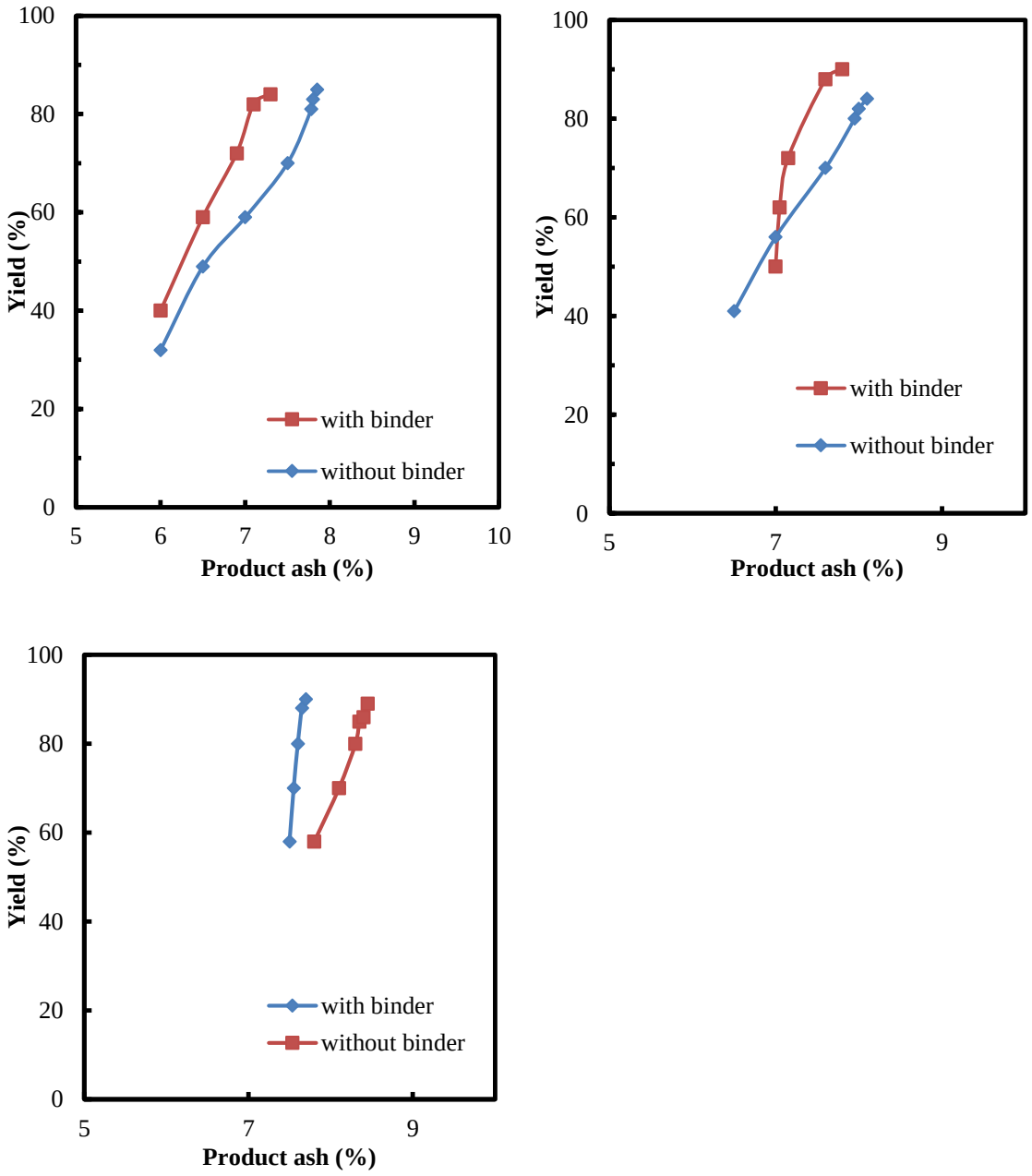

Figure 2.5. Clean coal yield vs. product ash curve from kinetic flotation tests with and without clay binder GP 374G41 at a) 1000 rpm, b) 1200 rpm, c) 1500 rpm (Tao et al., 2007)

Tao and Zhou (2010) also studied the effect of clay binders that were cationic polymers produced in acidic conditions in iron ore flotation. The results have shown that when the clay binder was used in combination with corn starch, the iron ore recovery

increased by more than six absolute percentage points. Similar tests were performed with phosphate by Tao et al. (2010). The use of 0.1 lb/t clay binder increased phosphate yield and recovery by 1.7 % and 5.5 %, respectively.

2.6.MECHANISM STUDY

2.6.1 Current research and development

The chemical reagent plays a critical role in flotation by interacting with different minerals that is the key to flotation selectivity. Fundamental understanding of physicochemical principles can help study mineral surfaces, aquatic chemistry, speciation of complexes and solubility and interactions (Sotillo et al, 2007). Characterization studies of mineral surface chemistry are critical to improve flotation process. These studies provide information on reagent adsorption on mineral surface such as reaction, product and mechanism. There are many aspects of surface chemistry in flotation, including crystal chemistry, surface oxidation, interfacial phenomena role, adsorption/desorption in the electrical double layer, hydrocarbon chain association and aqueous solution equilibrium and so on. There are many techniques that can be used to investigate flotation surface chemistry, including contact angle, FTIR, XPS, AFM, SEM, TEM, zeta potential, adsorption isotherm (Sotillo et al, 2007). The techniques can reveal the mineral surface changes with pulp chemistry such as pH value, reagent dosage, and ionic strengths. The surface properties of phosphate are influenced by its own solution chemistry and chemistry of dissolved species such as calcite and dolomite. Selectivity can be attributed to the difference in the surface chemical properties of the component minerals (Somasundaran and Zhang, 1999). Water chemistry also has a significant impact on the floatation of apatite-calcite systems through the surface chemistry of the solids (Gu et al., 1998).

Yoon and Ravishanker (1995) used dodecylamine hydrochloride to study the forces on mica surfaces. At pH 5.7, “short range” hydrophobic forces were observed with decay lengths of about 1.3 nm. At pH 9.5, a “long range” hydrophobic force with a decay length of 5.5 nm was observed. At pH 10.1, no significant hydrophobic forces were

observed when dodecylamine hydrochloride was above 2×10^{-5} M. Thus long-range hydrophobic forces may be necessary for good flotation, because the pH at which the long range hydrophobic force was observed corresponds to the one where quartz flotation had the best recovery.

Chibowski and Holysz (1985) studied the mechanism and flotation effects on quartz and the dodecylamine hydrochloride in the solution of methyl alcohol. Their results indicated that when the thickness of the adsorption layer was 0.25 times the monomolecular layer thickness, the recovery of quartz was 90% and the free energy of quartz surface decreased fast. When the adsorption layer was theoretical monomolecular layer, the flotation effect of quartz was the best.

Hamid and Eric (2006) investigated the adsorption of cationic and anionic collectors on the surface of smithsonite by FTIR and XPS. The FTIR showed the presence of RNH_2 on the surface of smithsonite and the adsorption of dodecylamine. XPS showed the presence of a ZnS layer on the surface after amine adsorption. FTIR shows the presence of COO^- on the surface of smithsonite after adsorption of oleic acid on the surface and the most adsorption occurred at around pH 10 when RCOO- is predominant in solution and has ample chances for interaction with the mineral surface. XPS confirmed the presence of ZnS layer on the surface after sulphidising in amine adsorption and transferring the surface to CuS in potassium amyl xanthate adsorption, suggesting that Cu^{2+} exchanged with zinc during copper activation of smithsonite.

Somasundaran and Mofty (2002) used zeta potential to study the electrokinetic properties of natural pure calcite which are a function of pH in the absence and presence of different surfactants and species of dissolved ionic in order to understand and improve the beneficiation of carbonaceous phosphate. They found that electrochemical property of calcite is not only a function of pH and concentration of different constituent species but also pulp densities. Calcite particles had a negative surface charge in low pulp densities and a positive surface charge at higher concentrations. Both oleate and

sulfonate adsorption were caused by chemical interaction and amines adsorb mainly due to electrostatic attractions.

Using adsorption isotherm, zeta potential and FTIR, Rao et al. (1991) did a series of mechanism studies of fatty acid on mineral surfaces. They found that oleic acid group can form monomolecular adsorption on calcite surface and form double-layer adsorption on the surface of fluorite, apatite and scheelite. Calcium oleate was formed during the adsorption procedure. The adsorption area was 33 $Å^2$ and the main structure of monomolecular adsorption layer was the closely packed oleic acid molecule. For the double-layer adsorption, the first layer was formed from chemisorptions and closely packed, and the second layer was from physical deposition and unorganized. Due to the surface characteristic and the effect of pH value, oleic acid group may have chemisorptions or the coordination reaction with the Ca^+ on the surface.

2.6.2 QCM-D analysis

QCM-D (Quartz crystal microbalance with dissipation monitoring) can monitor adsorption/reaction process and characterize the adsorbed layer in real time. QCM-D has widely been used in studies of adsorption because of its stability and simplicity, high precision, good sensitivity and ease of analysis. With QCM-D technology changes in adsorbed mass can be measured through changes in the frequency and the rigidity of the formed film can be measured through changes in the energy dissipation. When operated at multiple harmonics, QCM-D technique can quantify the changes in thickness, density and viscosity. QCM-D provides a novel tool for studying molecular interactions and changes in adsorbed layer.

QCM-D was developed from QCM, which has been used as a research tool since 1959 when Sauerbrey relates frequency and mass in the following equation:

$$\Delta m = -\frac{\rho_q t_q \Delta f}{f_0 n} = -\frac{\rho_q v_q \Delta f}{2 f_0^{\,2} n} = -C \frac{1}{n} \Delta f \qquad (24)$$

where ρ_q and t_q are the density and thickness of quartz crystal, respectively, v_q is the transverse wave velocity in quartz, C is a constant with value 17.8 ng cm^{-2} Hz^{-1} for a 5 MHz quartz and n is the overtone number (n=1,3,5,7). Δf is the change in the resonance frequency and Δm is the change of adsorbed mass on quartz crystal.

The QCM sensor consists of a thin quartz disc sandwiched between a pair of electrodes as shown in Figure 2.6. A picture of the quartz sensor is shown in Figure 2.7. The electrodes are normally made of gold since gold can be coated with many different materials. By applying an AC voltage across the electrodes, oscillation can be created as a result of the piezoelectric properties of quartz. Piezoelectricity means an object produces an electric charge when a mechanical stress is applied. On the other hand, if an electric field is applied a mechanical deformation can happen to shrink or expand the object.

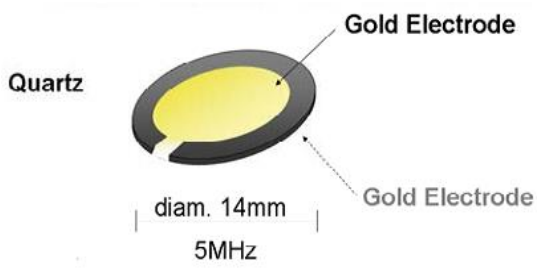

Figure 2.6. Composition of the QCM-D sensor (q-sense.com)

Figure 2.7. Picture of QCM-D sensor (q-sense.com)

The resonance frequency (f) of the sensor is determined by the total oscillating mass. The frequency decreases when a thin film is attached to the sensor. If the film is thin and rigid, the decrease of the frequency is proportional to the mass of the film. Sauerbrey equation is applicable to this condition. If the film is "soft" (viscoelastic), it will not fully couple to the oscillation of the crystal. In this situation, the damping or energy dissipation (D) of the sensor's oscillation is used to reveal the film's softness or viscoelasticity.

The dissipation factor D is proportional to the dissipation of power in an oscillatory system. The information about the rigidity of the adsorbed film can be known from factor D:

$$D = \frac{E_{dissipated}}{2\pi E_{stored}} \tag{25}$$

where $E_{dissipated}$ is the energy dissipated and E_{stored} is the energy stored in oscillating system. Thus the changes in the property of adsorbed layer determine the change of D. Changes in resonance frequency Δf and dissipation ΔD are measured simultaneously at nanoscale in real time as a result of adsorption on a crystal surface. QCM-D can provide the mechanical structural information of the adsorbed layer after analyzing the data of energy dissipation which relates to frequency shift.

According to the research of Voinova et al. (1999), Kevin-Voigt model can reveal the relationship between QCM-D response and viscoelastic properties of the adsorbed soft film layer as follows (Voinova et al., 1999):

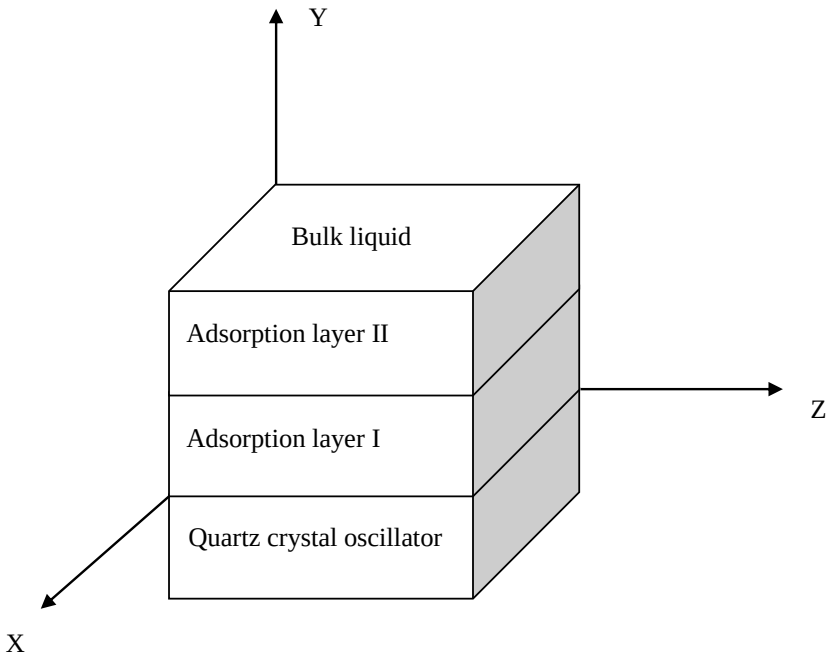

Figure 2.8. A schematic diagram of the Kevin-Voigt model related to two adsorption layers on a quartz crystal surface

$$\Delta f \approx -\frac{1}{2\pi\rho_0 h_0}\left\{\frac{\eta_3}{\delta_3}+\sum_{j=1,2}\left[h_j\rho_j\omega-2h_j\left(\frac{\eta_3}{\delta_3}\right)^2\frac{\eta_j\omega^2}{\mu_j^2+\eta_j^2\omega^2}\right]\right\} \tag{26}$$

$$\Delta D \approx \frac{1}{2\pi f\rho_0 h_0}\left\{\frac{\eta_3}{\delta_3}+\sum_{j=1,2}\left[2h_j(\frac{\eta_3}{\delta_3})^2\frac{\mu_j\omega^2}{\mu_j^2+\eta_j^2\omega^2}\right]\right\} \tag{27}$$

Δf and ΔD both depend on the density (ρ_0), thickness (h), elastic shear modulus (μ) and shear viscosity (η) of adsorption layer. j is the number of adsorbed layer. η_3 is the viscosity of the bulk liquid and δ_3 is the viscous penetration depth of the shear wave in the liquid. ω is the angular frequency of the oscillation. Sauerbrey equation and Voigt model are the theoretical basis for data modeling with Software QTools 3.0 (Q-Sense Co.). A value of ΔD greater than 1×10^{-6} suggests that adsorption leads to greater shift in ΔD due to the viscous and soft layer. Using this model, physical properties (mass,

thickness and density) and mechanical properties (viscosity and shear modulus) of the adsorbed layer can be known.

The application of QCM is most common in electrochemistry, under the name EQCM where E is electro chemical, as a tool for the measurement of interfacial processes at electrode surfaces. It is also commonly used to study the viscoelastic properties of protein adsorbed on a biosensor's surface, and the adsorption interaction of surfactants and polymers in aqueous solutions. Paul et al. (2008) did research about the adsorption behavior of lysozyme, bovine serum albumin (BSA), and immunogamma globulin (IgG) onto a liquid crystal phthalocyanine surface. They used QCM-D to detect the viscoelastic variation, interfacial hydration and structural details. They extracted physical and mechanical properties of the adsorbed film from Δf and ΔD values with viscoelastic modeling. The data from QCM-D showed that lysozyme adsorbed on a $CuPcR_8$ surface formed a rigid multilayer by hydrophobic interaction. The slope K ($K= \Delta D / \Delta f$) and small value from Δf -ΔD plots of lysozyme indicated that lysozyme adsorbed on $CuPcR_9$ surface by direct adhesion to form a rigid and compact adsorption layer.

Sharmistha et al. (2008) studied adsorption and viscoelastic properties of proteins onto liquid crystal phthalocyanine using QCM-D. It was the first time to present in situ adsorption kinetics of three proteins lysozyme, bovine serum albumin (BSA), and immunogamma globulin (IgG) onto a $CuPcR_8$ film surface. The time-resolved adsorption behavior included kinetic, viscoelastic variation, interfacial hydration, and structural details obtained by quartz crystal microbalance dissipating monitoring (QCM-D) technique with the Voigt model. The adsorption behavior of lysozyme was direct adhesion and formed a rigid multilayer by hydrophobic interaction. The adsorption of IgG and BSA was slow with orientation change of proteins containing hydrodynamically coupled water.

The density and structural property of the oleate layer adsorbed on a hydroxyapatite surface at six different concentrations and three pH's (pH 8, 9 and 10) were studied by Kou et al. (2012). The real-time measurements of frequency and dissipation shifts with a

hydroxyapatite coated sensor demonstrated that the adsorption of sodium oleate was chemisorption. At low concentrations and high pH value, the adsorption layer of sodium oleate was a rigid and thin one. At concentrations higher than critical micelle concentrations and lower pH's, the surface of calcium oleate formed a thick but dissipated adsorption layer with a high hydration level. The critical concentrate at pH 8 was 0.33 mM, while it was 0.821 mM and 3.3 mM at pH 9 and 10, respectively.

Kou et al. (2010) used QCM-D to study adsorption of collectors on the surface of hydroxyapatite. They investigated the adsorption behavior of the plant collector and a refined tall oil fatty acid on a hydroxyapatite-coated sensor surface. Figure 2.8 demonstrated the real-time response curves of frequency shift Δf and dissipation shift ΔD with refined tall oil fatty acid and the plant collector adsorbed onto a hydroxyapatite surface at the concentration of 500 ppm. Arrow A shows the beginning of injection of collector solution in the system. After the injection of refined tall oil fatty acid, Δf had a sharp decrease simultaneous with a sharp increase in ΔD as shown in Figure 2.8B. This change indicates the quick adsorption of refined tall oil fatty acid on the apatite surface and the high ΔD means the formation of a dissipated layer. Using Voigt model, the thickness of the highest adsorption at arrow b was calculated to be 70 nm. The steady state was reached at arrow c. The adsorption thickness at the stable frequency was estimated to be 11 nm.

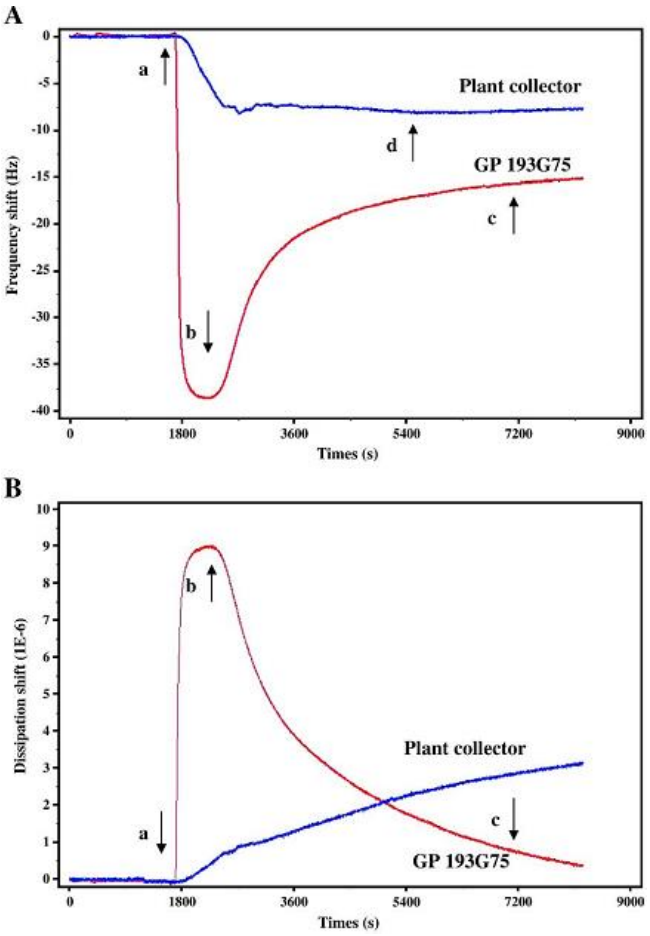

Figure 2.9. QCM-D analysis of collectors on the surface of hydroapatite

Copyright © Lingyu Zhang 2013

CHAPTER 3 METHODS AND MATERIALS

3.1.PARTICLE SIZE ANALYSIS

Figure 3.1 shows the CILAS 1064 laser particle size analyzer that was used to analyze the size distribution of the fine phosphate sample. It is based on the principle of laser diffraction to analyze particles from 0.04 to 500 µm within several minutes.

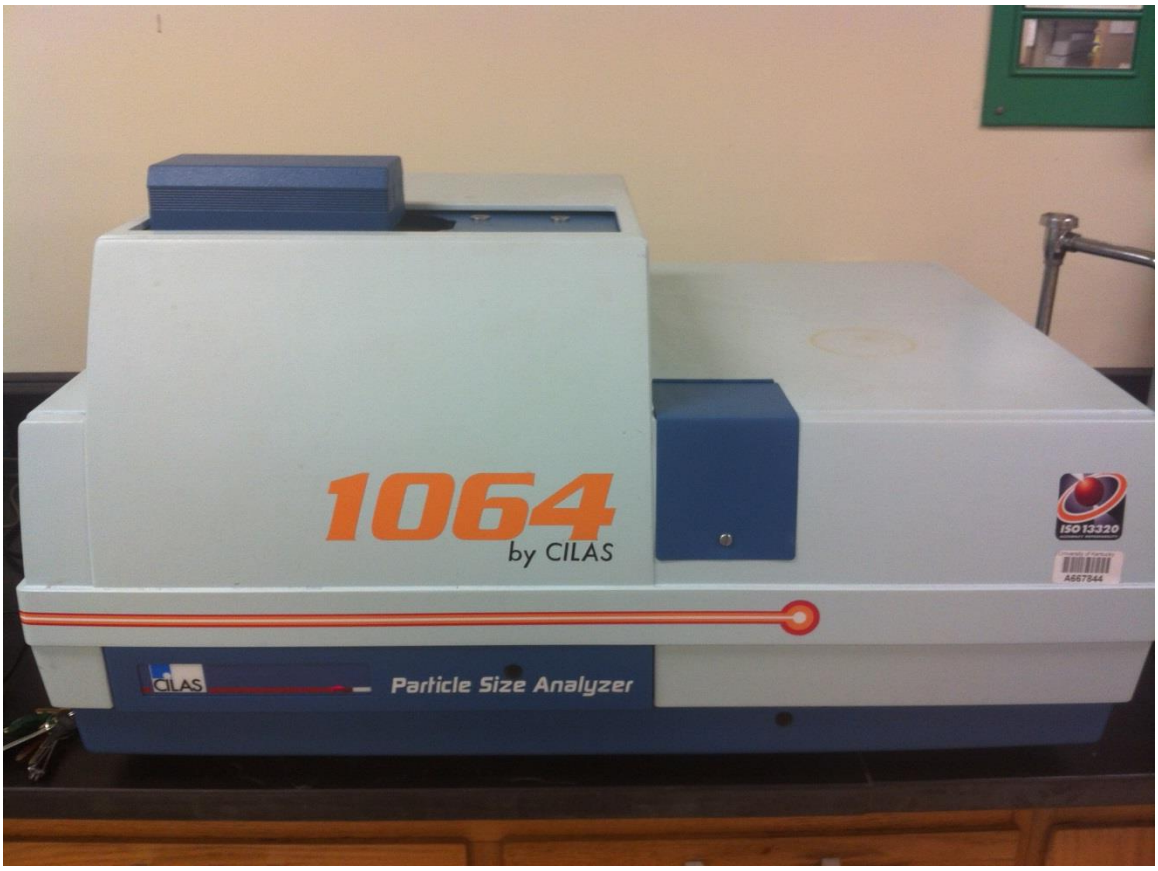

Figure 3.1. CILAS 1064 particle size analyzer

3.2.XRD ANALYSIS

A Bruker D-8 Discover X-2 advanced diffraction x-ray cabinet system was utilized to analyze mineral elements in the phosphate sample used in flotation tests.

Figure 3.2. Bruker D-8 Discover X-2 advanced diffraction x-ray cabinet system

3.3.XRF ANALYSIS

The chemical composition of the phosphate sample was analyzed with a S4 pioneer-wavelength dispersive X-ray fluorescence spectrometer.

Figure 3.3. S4 pioneer-wavelength dispersive X-ray fluorescence spectrometer

3.4.ZETA POTENTIAL

Zeta potential measurements were made with a Brook Haven Instruments Corporation zeta-plus analyzer shown in Figure 3.2. The experiments were conducted at room temperature and atmosphere and a 1 mM KCl solution was used. A 0.5 g apatite, silica, or clay mineral powder sample was mixed in an 80 ml 1 mM KCl solution. A NaOH or HCl solution was used to adjust the pH value. The mineral suspension was poured into a rectangular cell for zeta potential measurements. The leftover solution was measured for the final pH.

Figure 3.4. Zeta-plus analyzer of Brook Haven Instruments Corporation

3.5.INDUCTIVELY COUPLED PLASMA (ICP) ANALYSIS

The Varian ICP-AES Vista PRO was used to analyze P_2O_5 content in phosphate flotation tests.

Figure 3.5. Varian ICP-AES Vista PRO

3.6.FLOTATION TESTS

3.6.1 Flotation procedure

Rougher phosphate flotation tests were conducted under various operating conditions to evaluate the flotation performance of the GP reagents and the plant reagent. The process parameters examined in this study included the pH value, the collector type and dosage, the clay binder type and dosage, and the combination of clay binder and dispersant.

A three-factor three-level Box-Behnken experimental design, created with Design-Expert 8.0 software, was utilized for the laboratory flotation tests. The three factors were plant fatty acid dosage, water glass dosage, and clay binder dosage. The details of experimental design are shown in Table 3.1.

Table 3.1 Levels of variables for a three-factor three-level Box-Behnken experimental design of flotation tests with a laboratory flotation cell at the optimum pH value

Variables	Code	Units	Level		
			Low Level	Middle Level	High Level
Water glass	A	kg/t	0	3	6
Plant fatty acid	B	kg/t	1	2	3
727G25	C	kg/t	0	0.25	0.5

Flotation tests were conducted using a Denver D-12 lab flotation machine equipped with a 1-liter tank used in rougher phosphate flotation and a 2-7/8" diameter impeller. In the rougher phosphate flotation test, the slurry was conditioned to 60% solid percentage in a bucket. Collectors at variable dosages and pH values were added into the slurry and then the slurry was conditioned for additional 3 minutes. The conditioned slurry was then transferred to a 1-liter flotation cell and water was added to dilute the slurry. Flotation tests lasted for 2 minutes. Tap water was used in all flotation tests and the rotor speed of the flotation machine was set at 1,200 RPM. The whole procedure is shown in Figure 3.6.

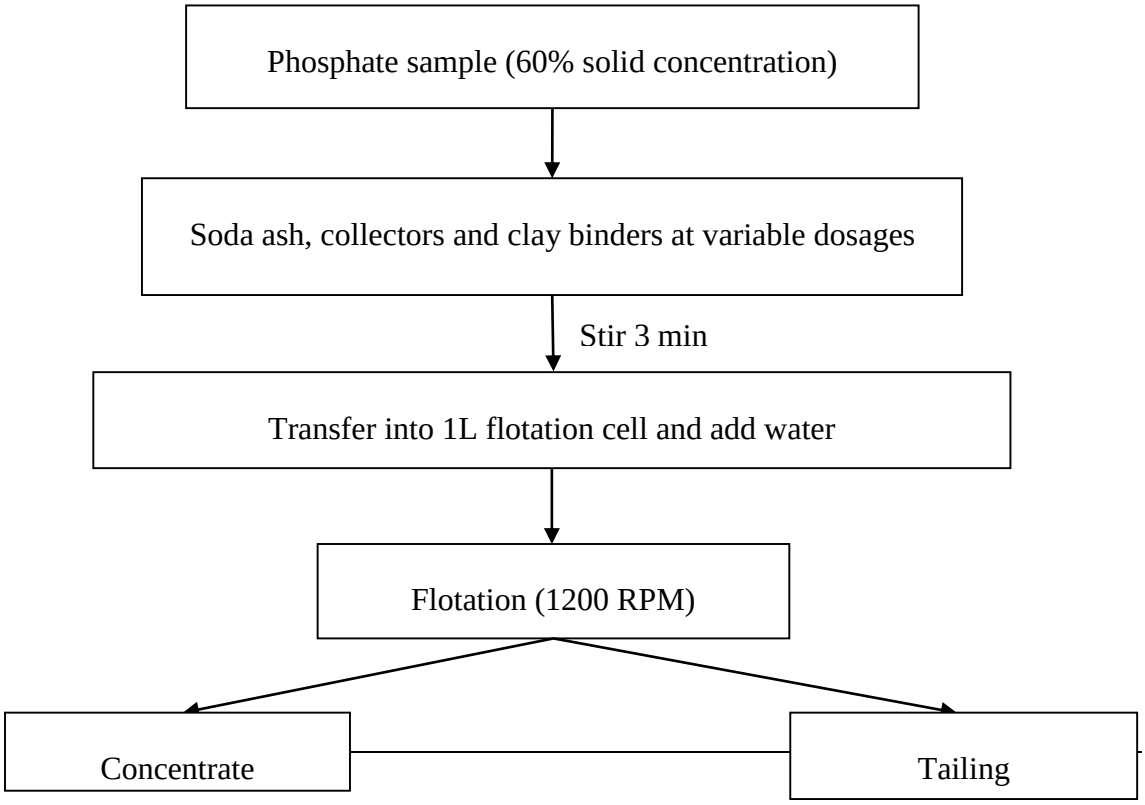

Figure 3.6. Flowsheet of the phosphate flotation procedure

For chemical assays, a phosphate sample was ground with a mortar and pestle for 90 seconds and one gram of sample was digested in a 250 ml volumetric flask using an acid composed of 40% (vol) HNO_3, 20% (vol) HCl, and 40% (vol) H_2O. The solution settled in the flask for approximately 30 minutes. Afterward, a 2.5 ml of the supernatant was transferred into a 100 ml volumetric flask and de-ionized water was added to bring the solution to the final volume. This dilution was made for P_2O_5 analysis using the ICP (Inductively Coupled Plasma) instrument (Vista-Pro) made by Varian, Inc. (Palo Alto, CA).

Acid insoluble (A.I.) was measured from the rest of the diluted solution in the 250 ml volumetric flask. The solution was filtered using filter paper. The filter paper, still containing the undissolved solids, was transferred to a porcelain crucible that was placed in a 600 ℃ muffle furnace for 30 minutes. The temperature was then increased to 900 ℃

for 1 hour. The crucible was cooled to room temperature and weighed. The percent insoluble was found to be the weight difference between the crucible with undissolved solid and the empty crucible.

The P_2O_5 recovery of the experiment was calculated using dry weights of floated and non-floated fractions in Eq. (28) in which C and T are fractions of the concentrate and tailing products respectively; c and t are P_2O_5 grades of concentrate and tailings in percentages.

$$\text{Recovery} = \frac{C \times c}{C \times c + T \times t} \times 100\ \% \tag{28}$$

A.I. rejection can be calculated using Eq. (29) in which t' and c' are the A.I. of tailing and concentrate.

$$\text{A.I. Rejection} = \frac{T \times t'}{C \times c' + T \times t'} \times 100\,\% \tag{29}$$

Flotation separation efficiency is a composite parameter used for evaluating flotation performance. Flotation separation efficiency is the sum of recovery and A.I. rejection minus 100% (Eq. (30)).

Flotation separation efficiency = P_2O_5 recovery + A.I. rejection–100% (30)

3.6.2 Flotation reagents

Table 3.2 lists the reagents used in this study.

Table 3.2 Flotation reagents used in the study

Reagent type	Reagent name
Collectors	Plant fatty acid, XTOL 100, GP 654G16 , XTOL 0621
Clay binders	727G24, 727G25, 727G26, 727G27, 727G28
Dispersant	Water glass (Sodium Silicate, Na_2SiO_3, 40%)
pH modifiers	Soda ash (Na_2CO_3, 30%)

3.7.QCM-D MEASUREMENT

QCM-D was used to measure the adsorption of reagents on apatite, silica and Al_2O_3 sensor surfaces. Q-sense E4 shown in Figure 3.7 was used in this study. The QCM-D experiments were conducted at 25 ° C. The stock solutions of different reagents (collectors and clay binders) were diluted in de-ionized water. The diluted solution was left in an ultrasonic bath for 5-10 minutes to ensure the dissolution of reagents. The reagent solution was injected into the measurement system through a precision chemical feeding pump.

Figure 3.7. Q-sense E4 equipment in the lab

Copyright © Lingyu Zhang 2013

CHAPTER 4 RESULTS AND DISCUSSION

4.1 CHARACTERIZATION OF PHOSPHATE SAMPLE

4.1.1 Particle size and ICP analysis

The phosphate ore sample used in this study was dry phosphate ore provided by the Yunnan Phosphate Company, China. Wet sieving was conducted and the particle size distribution data and the plot of the samples are shown in Table 4.1 and Figure 4.1. The P_2O_5 grade of the sample is 21.47%. The dominant particle size fraction is minus 200 mesh (0.074 mm), which accounts for 57.20% of the total weight. The size fraction between 100 mesh (0.15 mm) and 170 mesh (0.088 mm) has the second highest particle population, accounting for 26.05% particles.

Table 4.1. Wet screening results of phosphate as received samples

Particle size (mesh)	Wt (%)	A.I. (%)	P_2O_5 Grade (%)	∑Wt. (%)	∑A.I. (%)	∑P_2O_5 grade (%)
100	8.75	33.74	24.37	8.75	33.74	24.37
100-170	26.05	41.56	20.59	34.8	39.59	21.54
170-200	8.00	40.56	20.65	42.8	39.77	21.38
-200	57.2	32.75	21.54	100	35.76	21.47

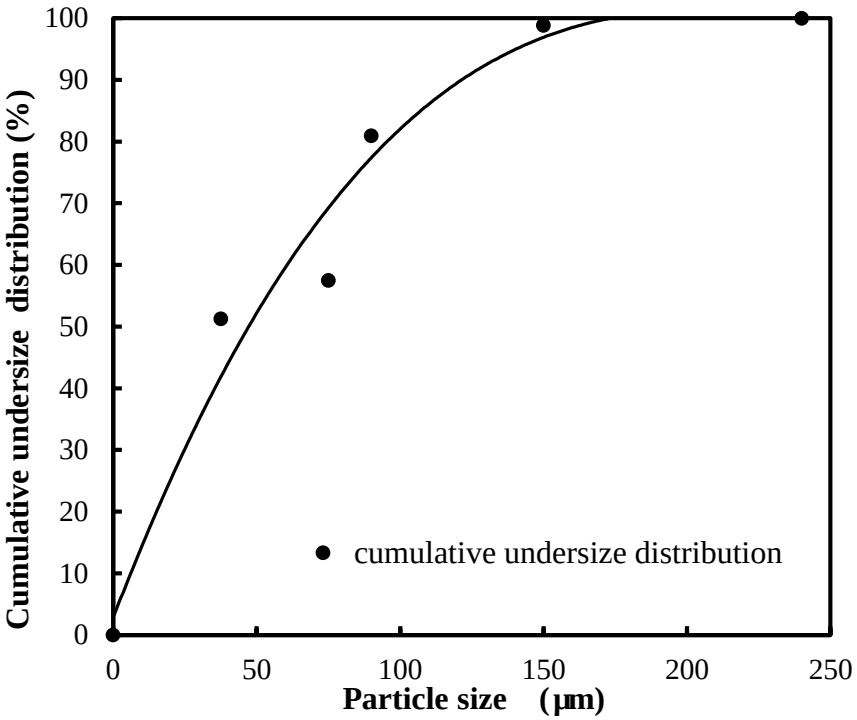

Figure 4.1. Particle size distribution of phosphate sample

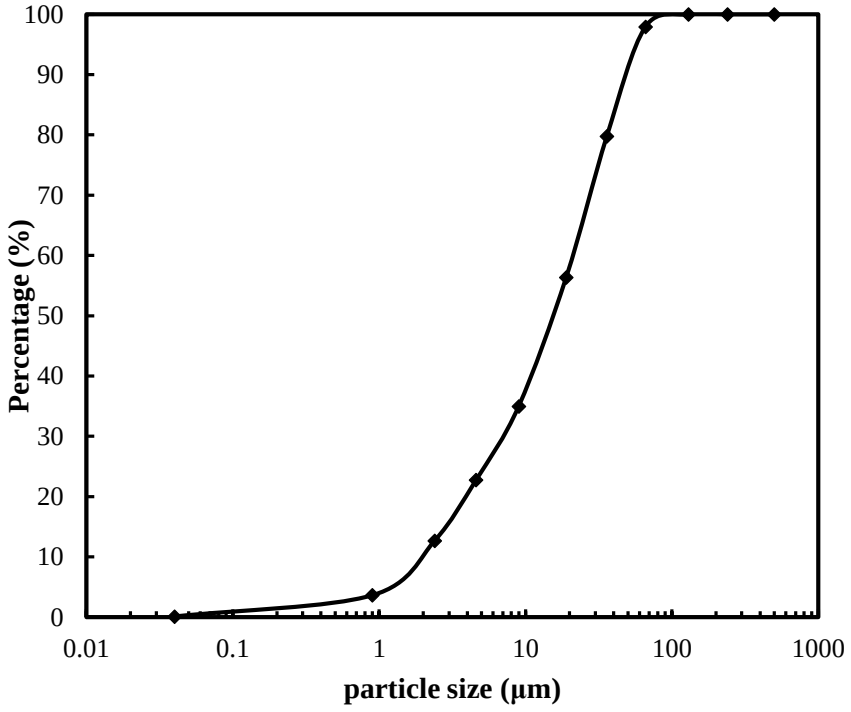

Figure 4.2. Size distribution for ground flotation feed sample

Fine grinding is required for the liberation of phosphate from gangue minerals. The as-received sample was subjected to grinding in a 1.3 gal ball mill that rotated at 50 RPM for 2 hours in a 50% solid slurry. Figure 4.2 shows the size distribution of the ground sample measured using a CILAS 1064 particle size analyzer. The D_{50} value is about 18 μm and more than 95% particles are smaller than 70 μm at which phosphate is well liberated.

4.1.2 XRD and XRF analysis

The XRD pattern of the sample used in this study is shown in Figure 4.3. The pattern indicates that the main form of phosphate is fluorapatite ($Ca_{10}(PO_4)_6F_2$) and the main gangue is quartz (SiO_2). The major peaks are at λ= 3.4489, 2.8001, 2.7044, 2.6241 Å for fluorapatite and at λ=3.3459, 4.259, 1.8018, 1.5429 Å for quartz.

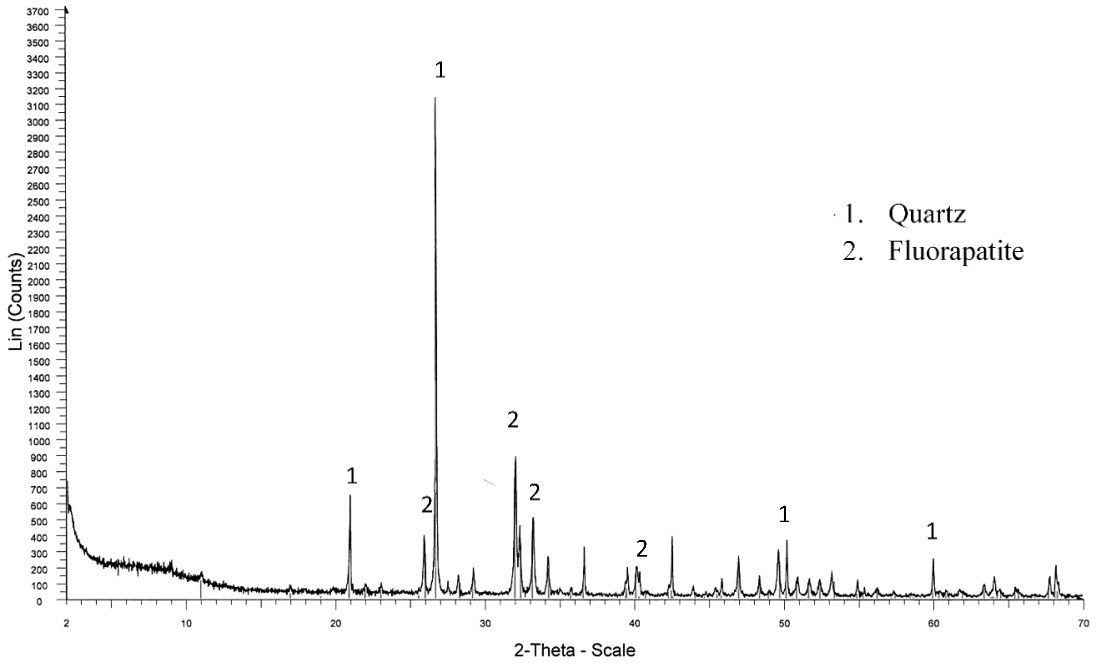

Figure 4.3. XRD pattern for Yunnan phosphate sample

From the XRF analysis, the elemental contents can be estimated, as shown in Table 4.2 for the main chemical composition of the phosphate sample.

Table 4.2. XRF results for Yunnan phosphate sample

Element	SiO_2 (%)	P_2O_5 (%)	Al_2O_3 (%)	Fe_2O_3 (%)	CaO (%)	MgO (%)
Content	36.18	19.32	3.46	1.42	30.99	0.34

4.2 ZETA-POTENTIAL MEASUREMENTS

A Zeta potential analyzer measured the change in zeta potentials between pH 2 to 12 of pure apatite, silica and clay minerals. The clay sample mainly consisted of chlorite, illite, kaolinite, feldspar, quartz, dolomite and siderite. The isoelectric point for apatite was at pH 3.9. The phosphate flotation feed was conditioned in an alkaline medium where the phosphate particles were negatively charged. At a pH value above 4.3 quartz and clay minerals exhibited zeta potentials that were more negative than apatite. This means that the repulsive electrostatic force between clay minerals and quartz is much stronger than that of clay minerals and apatite. Clay minerals attach to a quartz surface more preferentially than apatite surface. Removing clay particles from apatite can significantly improve the flotation selectivity.

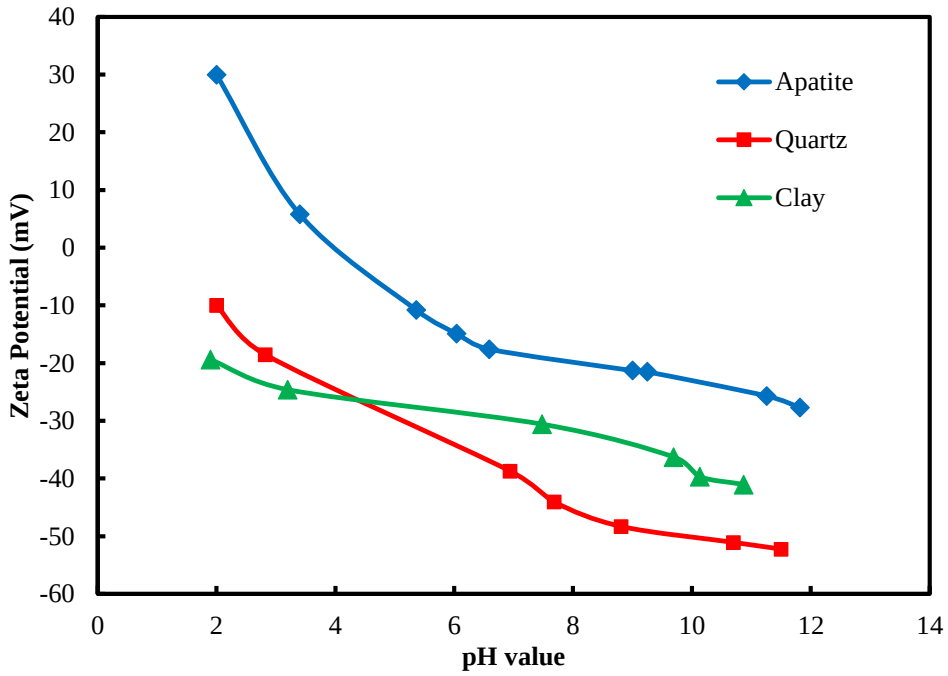

Figure 4.4. Zeta potential of apatite, quartz and clay as a function of pH

4.3 FLOTATION TESTS

4.3.1 Phosphate flotation without clay binders

4.3.1.1 Effect of pH values on collector

A number of baseline flotation tests were conducted to investigate the effect of major flotation process parameters on flotation performance in the absence of a GP clay binder.

Figure 4.5 shows the effect of pH value on flotation with 2 kg/t plant fatty acid. Impeller speed was maintained at 1,200 RPM. The product yield, recovery and separation efficiency increased as the pH value increased from 9 to 11. The concentrate grade slightly increased as the pH value increased. The data in Figure 4.5 shows that at pH value 11 the highest recovery and highest concentrate grade was achieved. Table 4.3 shows the triplicate flotation results with plant fatty acid at different pH value.

Table 4.3. Flotation results with plant fatty acid at different pH values

	pH	1st test	2nd test	3rd test	Average	St Dev
Yield (%)	9	28.60	27.39	28.25	28.08	0.62
	10	39.60	42.02	42.80	41.47	1.67
	11	49.44	50.68	51.52	50.55	1.05
Recovery (%)	9	31.78	28.94	30.75	30.49	1.44
	10	47.98	49.38	49.46	48.94	0.83
	11	60.74	60.94	61.50	61.06	0.39
A.I. rejection (%)	9	68.33	71.80	70.13	70.09	1.74
	10	59.89	59.06	56.90	58.62	1.54
	11	55.13	53.53	52.13	53.60	1.50
Separation Efficiency (%)	9	0.10	0.74	0.88	0.57	0.42
	10	7.86	8.44	6.36	7.55	1.07
	11	15.87	14.47	13.63	14.66	1.13
Concentrate Grade (%)	9	25.50	23.17	23.50	24.06	1.26
	10	25.88	25.07	25.02	25.32	0.48
	11	26.78	27.12	26.55	26.82	0.29

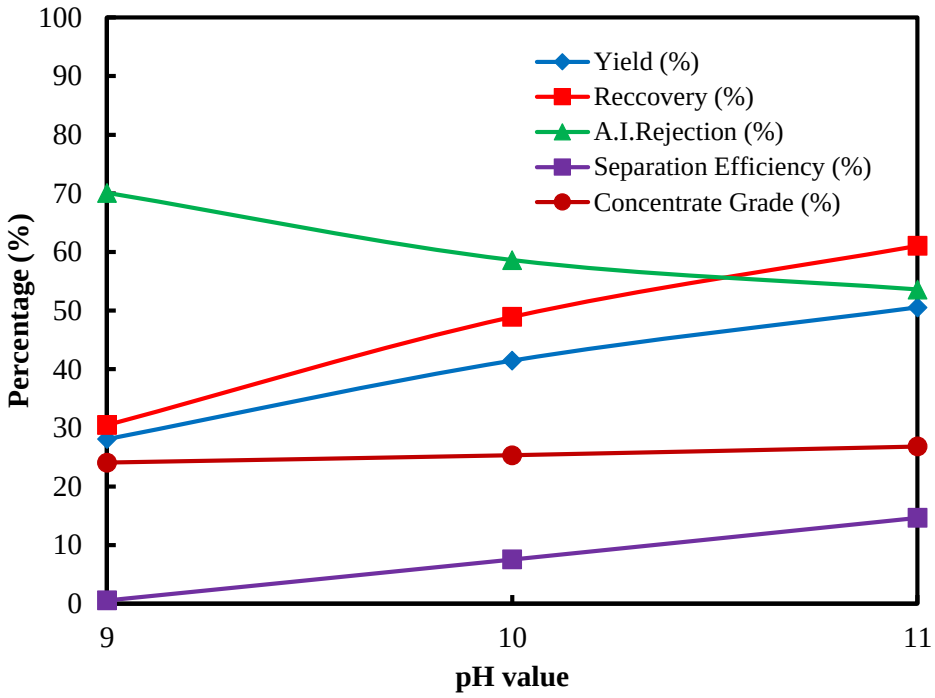

Figure 4.5. Flotation results with plant fatty acid at different pH values

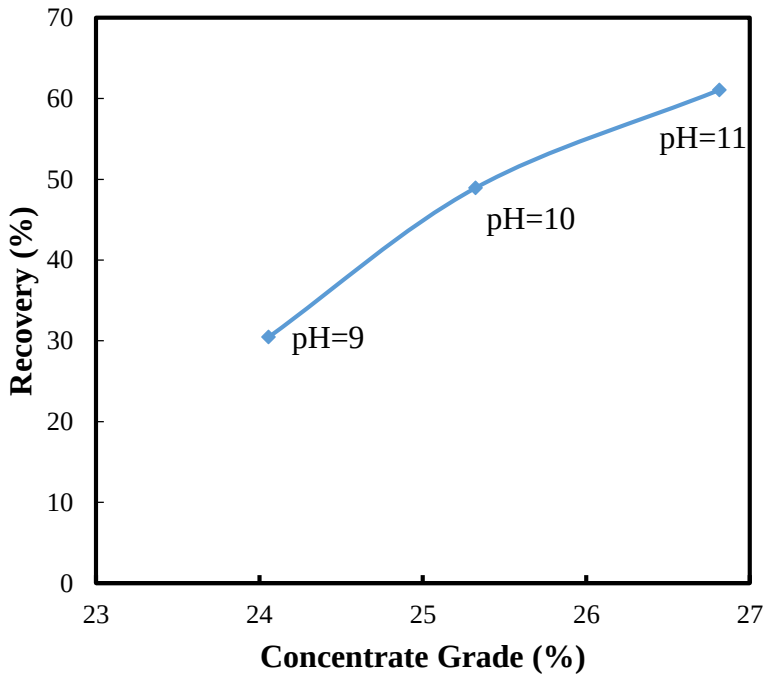

Figure 4.6. The relationship between concentrate grade and recovery with plant fatty acid at different pH values

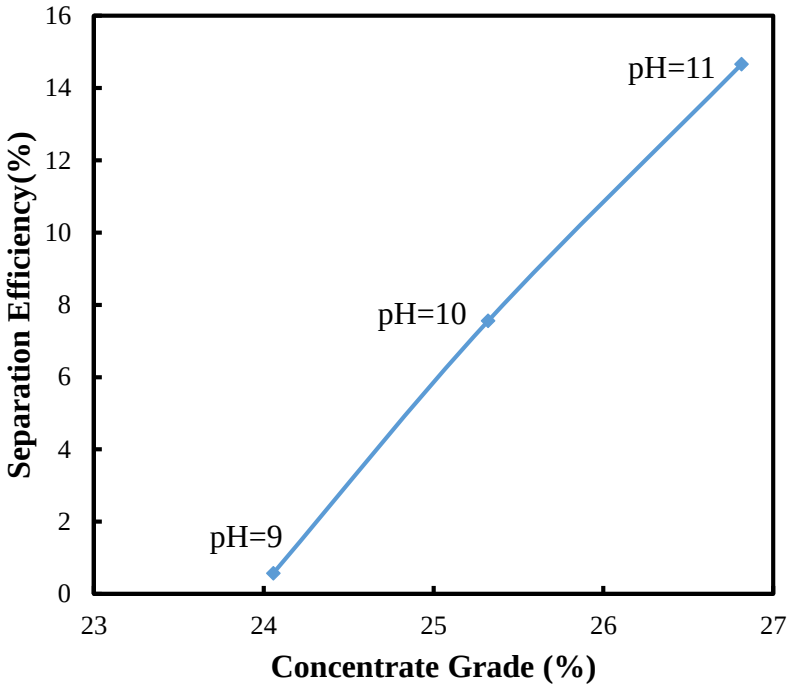

Figure 4.7. The relationship between concentrate grade and separation efficiency with plant fatty acid at different pH values

Figure 4.6 and 4.7 show the effect of pH value on the relationship between recovery and concentrate grade and also separation efficiency and concentrate grade, respectively. Recovery, separation efficiency and concentrate grade all increased with an increasing pH value. The plots shown in Figure 4.6 and 4.7 also suggest that the highest recovery, separation efficiency and concentrate grade were achieved at pH 11 with plant fatty acid.

4.3.1.2 Effect of collector dosages

Table 4.4 shows the flotation results with four different collectors at dosages 1, 2 and 3 kg/t at pH 11.

Table 4.4. Flotation results with four collectors at different dosages

	Dosage (kg/t)	Yield (%)	P_2O_5 Recovery (%)	A.I. Rejection (%)	Separation Efficiency (%)	Concentrate Grade (%)
Plant FA	1	41.25	44.33	63.33	7.66	22.54
	2	45.52	48.59	59.83	8.42	24.65
	3	54.91	60.82	51.69	12.51	26.13
XTOL 100	1	53.97	57.08	51.65	8.73	22.98
	2	58.31	61.27	48.72	9.99	24.76
	3	62.77	68.21	44.49	12.7	24.01
GP 654G16	1	45.09	46.56	57.65	4.21	23.91
	2	64.75	65.51	37.65	3.16	24.04
	3	71.02	73.28	31.95	5.23	25.16
XTOL0621	1	44.37	43.77	56.64	0.41	23.61
	2	52.14	54.93	50.64	5.57	22.59
	3	56.27	55.79	49.58	5.37	22.24

Figure 4.8 shows the variation tendency with different collector dosages on the flotation yield. Higher yields could be produced by increasing collector dosage. Figure 4.8 suggests that at a dosage of 3 kg/t the yield was increased by around 10% for all collectors. The highest yield was 71.02% achieved with GP 654G16.

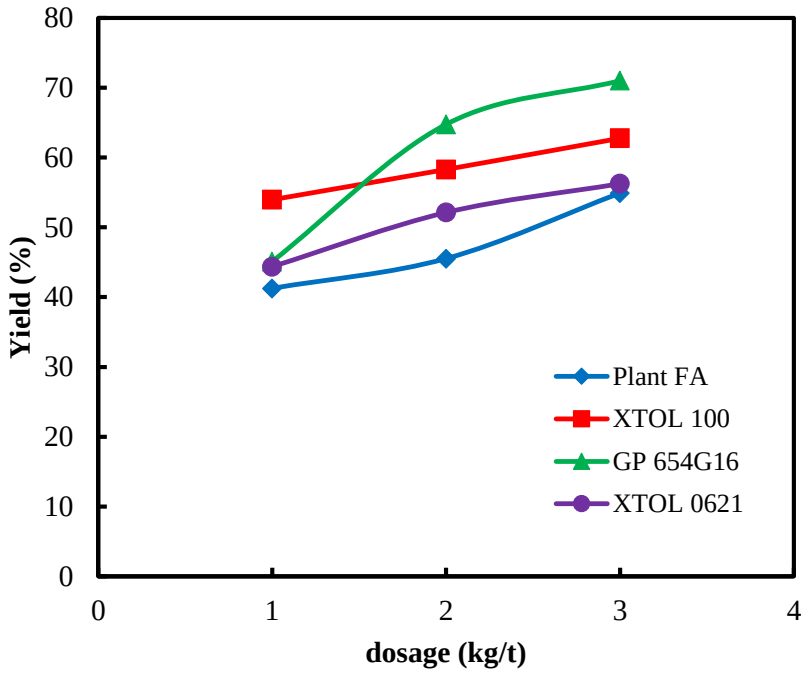

Figure 4.8. Effect of collector dosages on flotation yield with varying collectors

Figure 4.9 and Figure 4.10 indicate the effect of the collector dosage on the flotation recovery and A.I. rejection. For all collectors, recovery increased with an increase in collector dosage. GP 654G16 exhibited the highest recoveries of 65.51% and 73.38% at dosages of 2 kg/t and 3 kg/t. XTOL 100 and GP 654G16 showed higher recoveries while XTOL 0621 and plant fatty acid had lower recoveries. Plant fatty acid yielded the highest A.I. rejection of 63.33% at 1 kg/t.

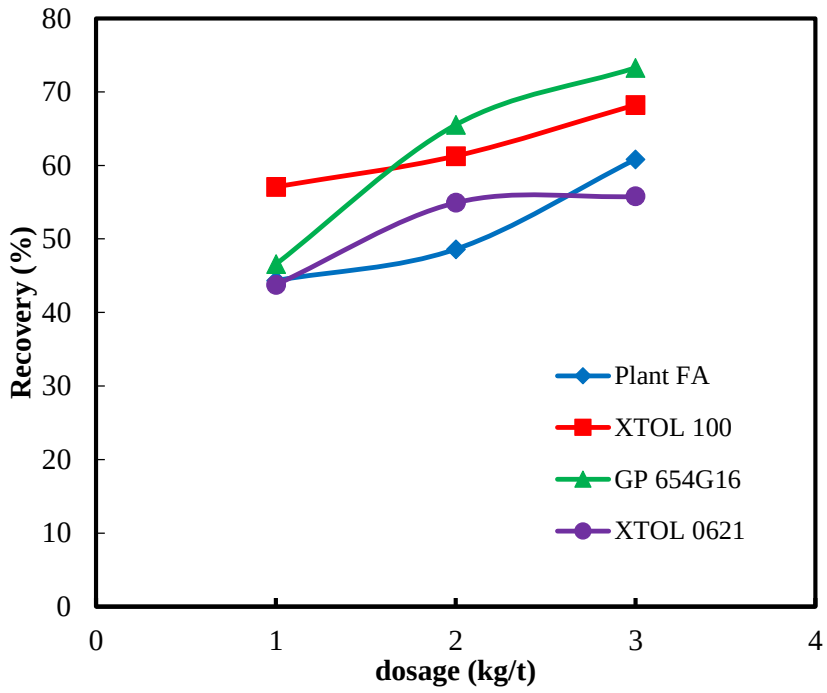

Figure 4.9. Effect of collector dosages on flotation recovery with varying collectors

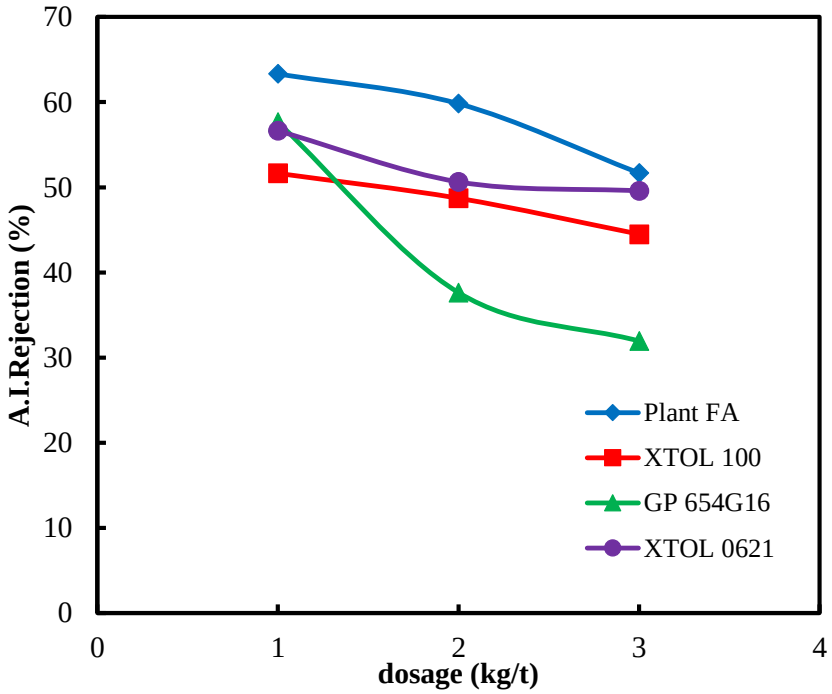

Figure 4.10. Effect of collector dosages on A.I. rejection with varying collectors

Figure 4.11 shows the effect of collector dosage on separation efficiency with four different collectors. The highest separation efficiency of 12.70% was generated with XTOL 100 at a dosage of 1 kg/t. XTOL 100 generated the highest separation efficiency of the four fatty acid collectors. Separation efficiency was improved with higher collector dosages.

Figure 4.12 demonstrates the effect of collector dosage on concentrate grade with four different collectors. At 1 kg/t, the concentrate grades of the four collectors are similar. When the dosage was increased to 2 kg/t, XTOL 100 and plant fatty acid produced a higher concentrate grade. The highest grade of 26.13% was produced in the presence of the plant fatty acid.

Figure 4.13 shows the relationship between recovery and A.I. rejection. The curve closer to the upper right corner represents sharper separation. Plant fatty acid and XTOL 100 showed sharper separation. XTOL 0621 exhibited both lower recovery and lower A.I. rejection compared to the other three collectors.

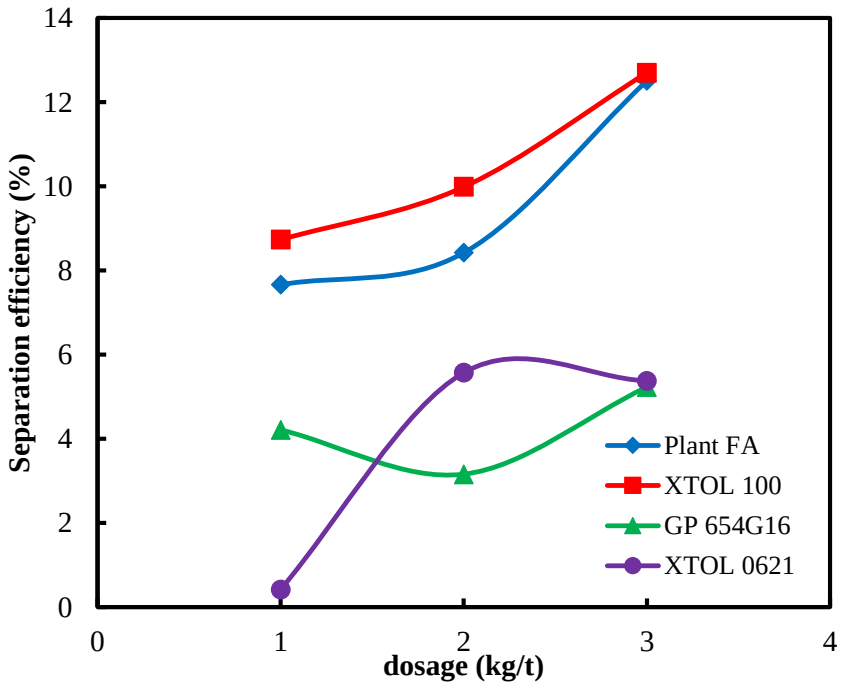

Figure 4.11. Effect of collector dosages on separation efficiency with varying collectors

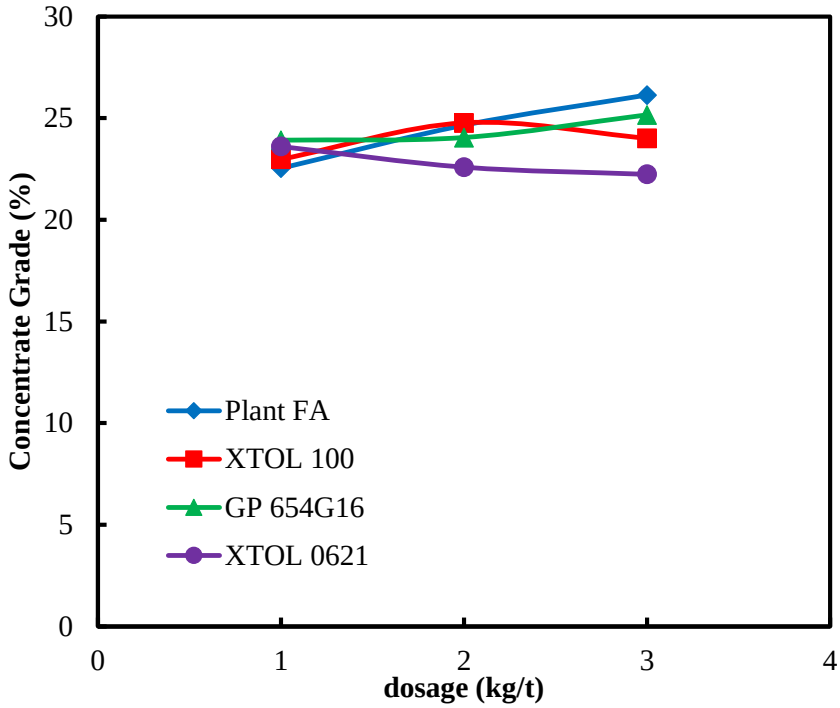

Figure 4.12. Effect of collector dosages on concentrate grade with varying collectors

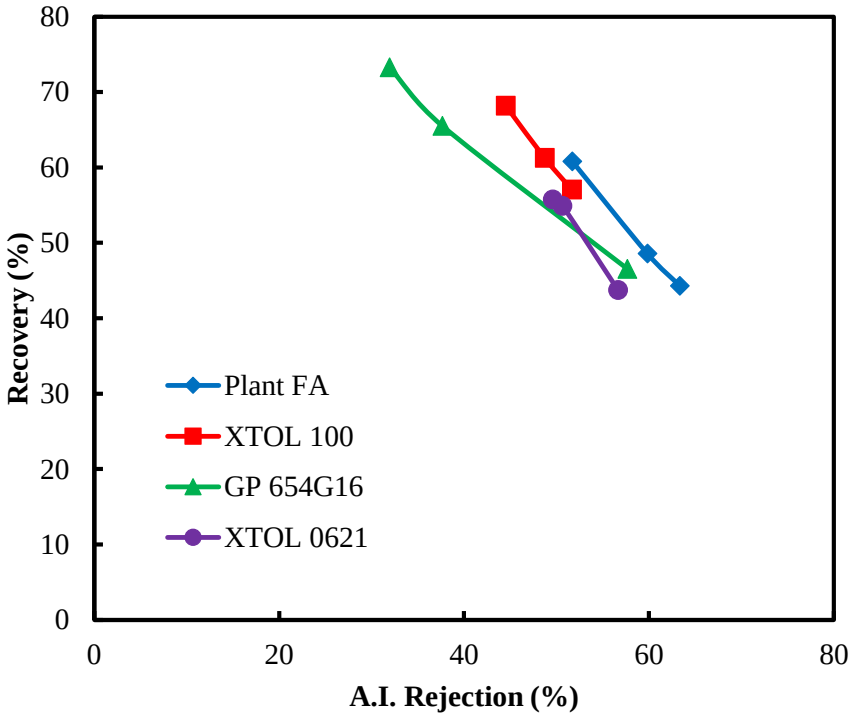

Figure 4.13. The relationship between A.I. rejection and recovery with varying collectors

4.3.2 Phosphate flotation with clay binders

4.3.2.1 Identify optimum clay binder dosage

Table 4.5 shows the flotation results with five collectors at dosages of 0.25, 0.5, 1 and 2 kg/t in the presence of 3 kg/t XTOL 100 collector at pH 11 adjusted with soda ash.

Table 4.5. Flotation results with four collectors at different dosages

	Clay binder dosage (kg/t)	Yield (%)	P_2O_5 Recovery (%)	A.I. Rejection (%)	Separation Efficiency (%)	Concentrate Grade (%)
XTOL 100 3kg/t + 727G24	0.25	66.29	74.30	40.13	14.43	25.59
	0.50	63.73	72.08	40.66	12.74	25.80
	1.00	61.40	70.34	42.06	12.40	26.95
	2.00	50.11	64.11	45.76	9.87	27.20
XTOL 100 3kg/t + 727G25	0.25	64.70	76.79	39.63	16.42	25.67
	0.50	61.61	74.70	40.42	15.12	26.21
	1.00	57.43	72.06	41.61	13.67	27.91
	2.00	52.66	70.26	42.74	12.99	28.08
XTOL 100 3kg/t + 727G26	0.25	68.31	76.01	38.77	14.78	23.07
	0.50	60.15	75.87	38.60	14.47	23.62
	1.00	56.67	74.77	39.03	13.80	25.28
	2.00	52.50	73.10	40.60	13.71	26.83
XTOL 100 3kg/t + 727G27	0.25	73.84	78.80	37.11	15.91	22.88
	0.50	60.93	76.68	38.37	15.06	23.22
	1.00	57.88	75.17	39.20	14.37	24.17
	2.00	56.05	74.60	39.94	14.54	25.88
XTOL 100 3kg/t + 727G28	0.25	73.46	75.18	37.46	12.63	23.23
	0.50	63.15	73.87	37.96	11.83	24.10
	1.00	57.67	72.67	38.80	11.46	25.26
	2.00	54.50	71.35	39.24	10.59	25.83

Figure 4.14 depicts the effect of clay binder dosage on flotation yield. The figure shows that 0.25 kg/t was the optimal dosage for yield at which all clay binders showed their highest yield. The highest yield was 73.84% with 727G27 at a dosage of 0.25 kg/t. Yield was decreased by around 20% as the dosage increased from 0.25 to 2 kg/t. All five clay binders showed higher yields than without a clay binder.

Figure 4.15 shows the effect of the clay binder dosage on flotation recovery. The recovery was decreased with the increase of clay binder dosage. 727G27 generated the highest recovery of 78.80%. The plot shows that use of clay binder at all dosages from 0.25 kg/t to 2 kg/t increased phosphate recovery except 2 kg/t 727G24.

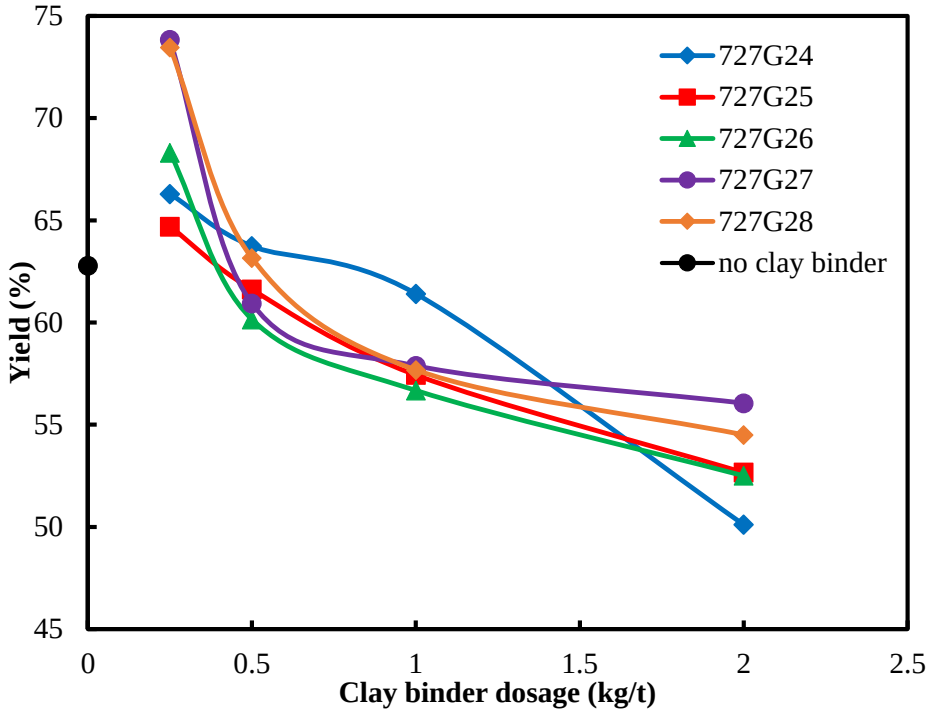

Figure 4.14. The effect of clay binder dosage on flotation yield with five clay binders

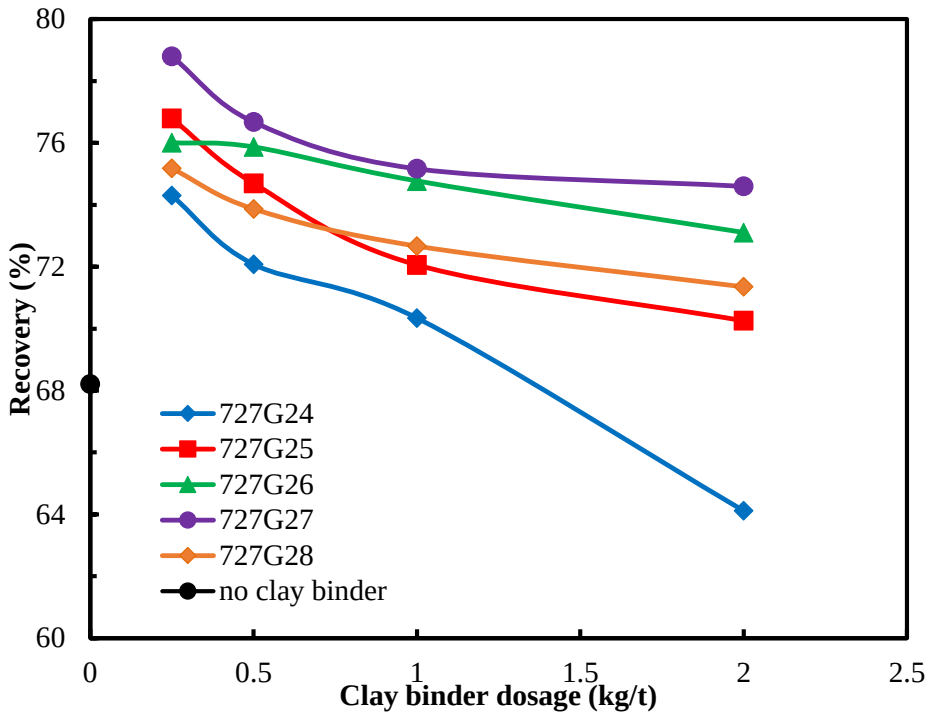

Figure 4.15. The effect of clay binder dosage on flotation recovery with five clay binders

Figure 4.16 shows the effect of a clay binder dosage on A.I. rejection. 727G24 generated the highest A.I. rejection of 45.76% among five clay binders. A.I. rejection increased by about 2% - 5% as the clay binder dosage increased from 0.25 kg/t to 2 kg/t. Use of clay binders reduced A.I. rejection since more minerals were recovered.

Figure 4.17 shows separation efficiency as a function of clay binder dosage. When the dosage was less than 0.5 kg/t, 727G25 produced highest separation efficiency of 16.42%. Clay binder 727G27 produced the best selectivity at a dosage of greater than 0.5 kg/t. 727G28 generated the lowest separation efficiency. The presence of a clay binder, at lower dosages, increased separation efficiency by 4%.

Figure 4.18 shows the concentrate grade as a function of clay binder dosage. The concentrate grade increased as the clay binder dosage increased from 0.25 kg/t to 2 kg/t. The highest grade of 28.08% was achieved by 3 kg/t XTOL 100 combined with 2 kg/t 727G25. Use of 727G25 increased concentrate grade by around 2% - 4%.

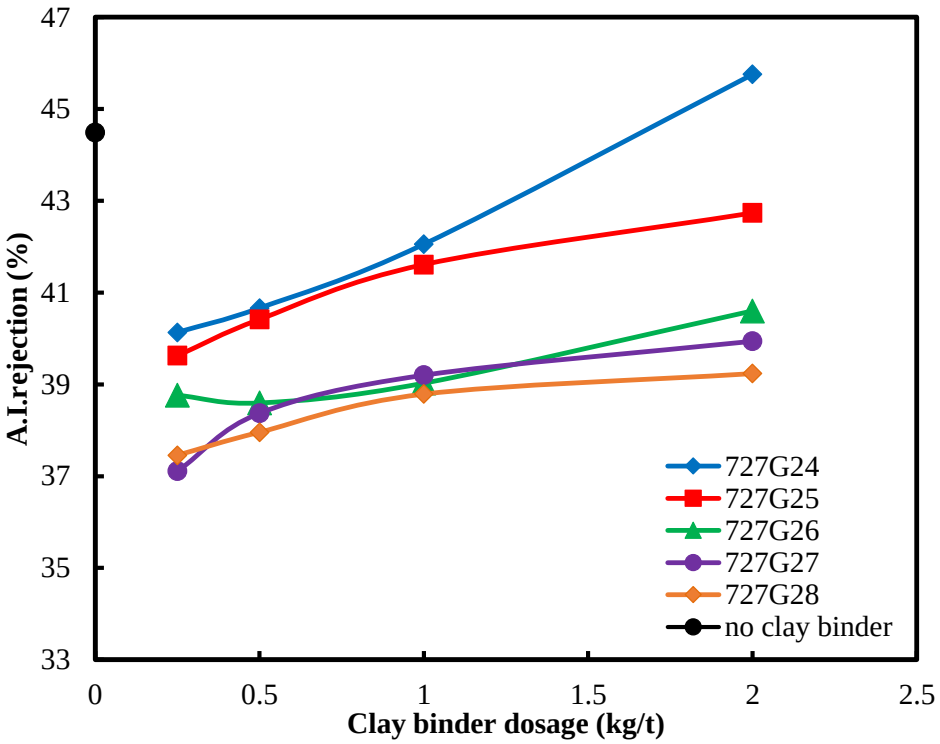

Figure 4.16. The effect of clay binder dosage on A.I. rejection with five clay binders

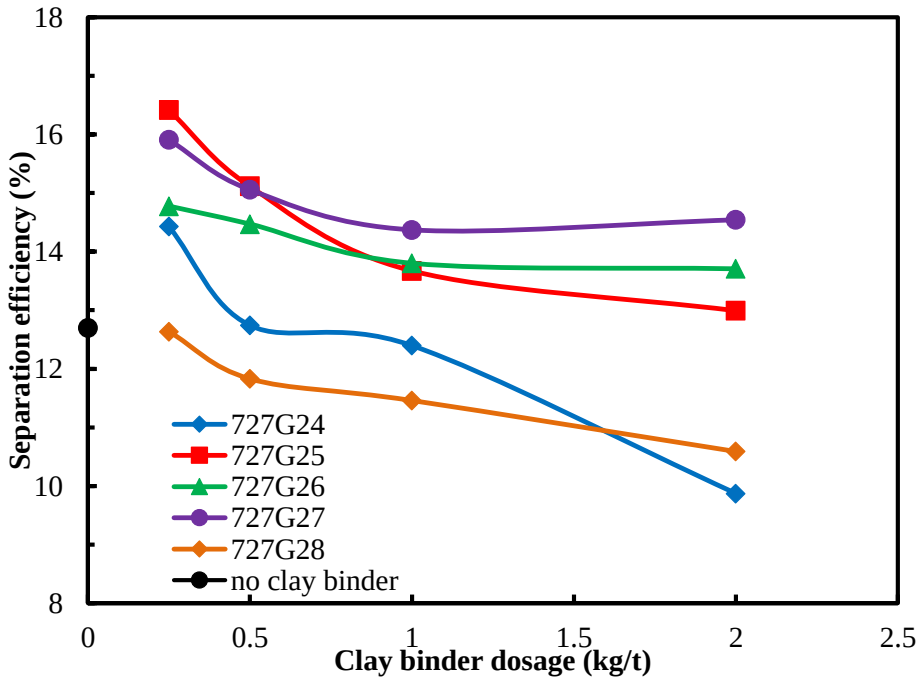

Figure 4.17. The effect of clay binder dosage on separation efficiency with five clay binders

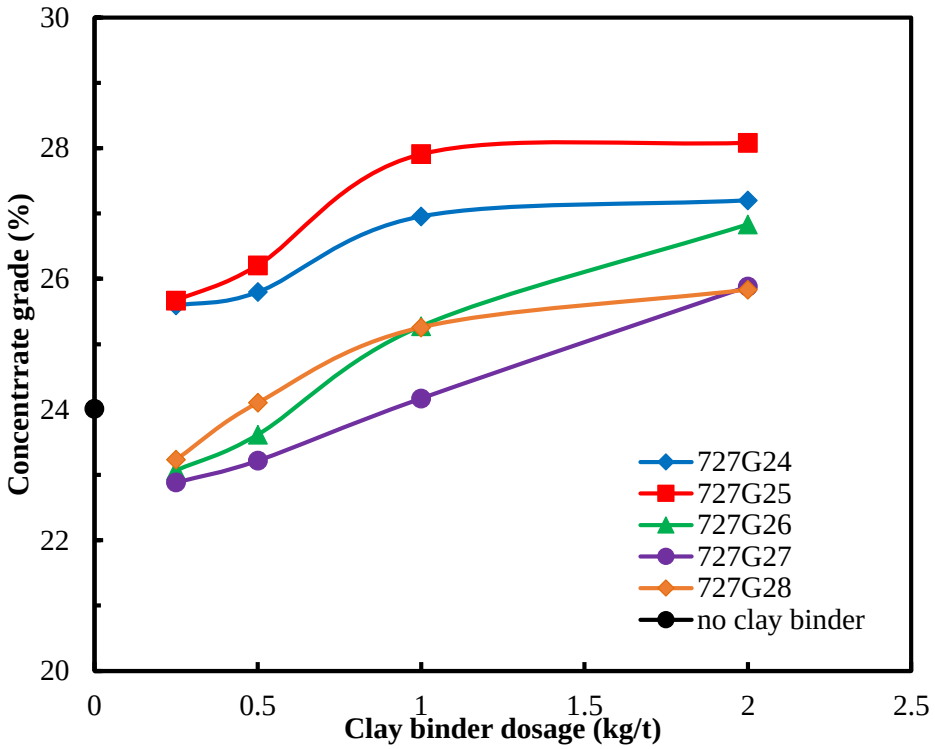

Figure 4.18. The effect of clay binder dosage on concentrate grade with five clay binders

Figure 4.19 depicts the relationship between A.I. rejection and recovery with and without clay binders. The points in the upper right corner represents higher recovery and higher A.I. rejection, indicating better separation performance. 727G25 had the best flotation performance among five clay binders. In all cases, flotation recovery was improved significantly in the presence of clay binders.

Figure 4.20 shows the relationship between concentrate P_2O_5 grade and recovery. Higher concentrate grade and recovery are the primary goals of the flotation process. 727G25 produced higher concentrate grade and recovery than other four clay binders. Tests conducted without a clay binder had a lower recovery and concentrate grade; therefore, it can be concluded that clay binders markedly enhanced flotation selectivity.

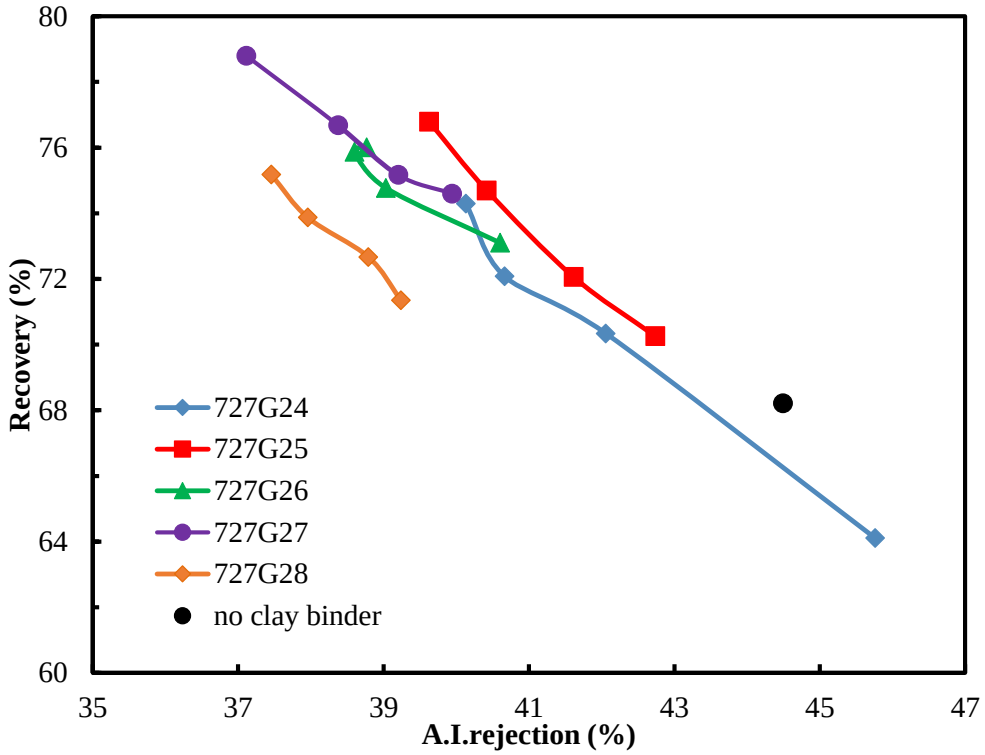

Figure 4.19. The relationship between recovery and A.I. rejection with five clay binders at varying dosages

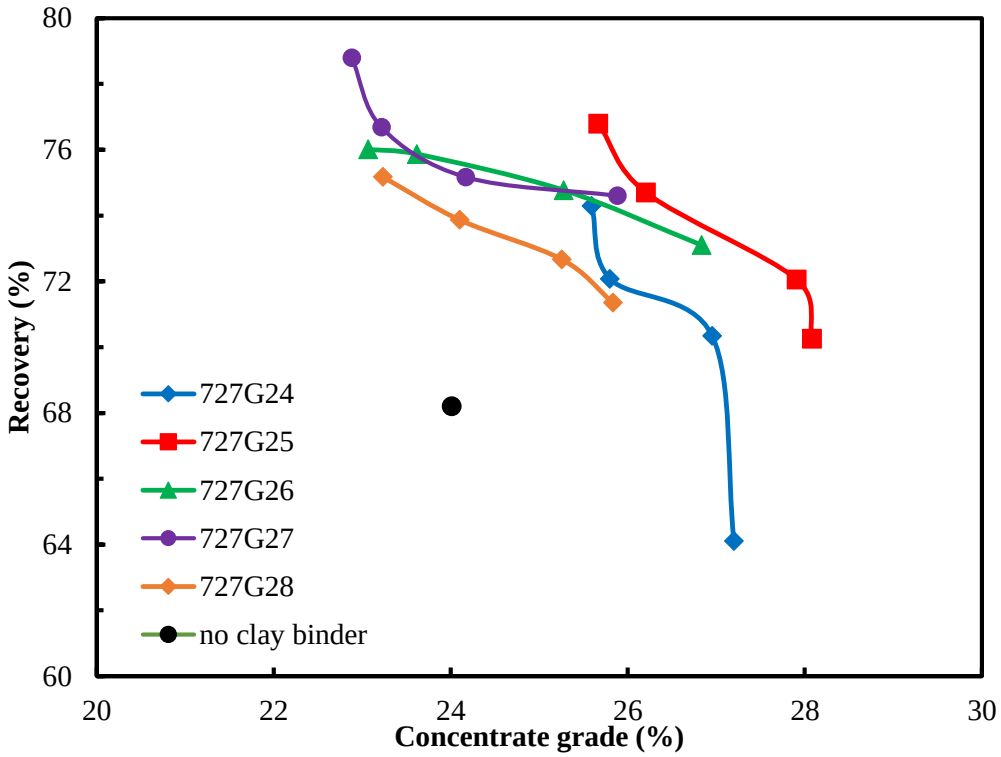

Figure 4.20. The relationship between recovery and concentrate grade with five clay binders at varying dosages

4.3.2.2 Identify optimum clay binder by comparing data at 0.25 kg/t dosage

Table 4.6 shows the flotation results obtained with 3 kg/t XTOL 100 as collector in the presence of five different clay binders at optimal dosage 0.25 kg/t. Baseline flotation results without a clay binder are also shown for comparison.

Table 4.6. The flotation results with five clay binders at optimal dosage of 0.25 kg/t and without clay binder

Clay binder	Clay binder dosage (kg/t)	Yield (%)	P_2O_5 Recovery (%)	A.I. Rejection (%)	Separation Efficiency (%)	P_2O_5 Grade (%)
727G24	0.25	66.29	74.30	40.13	14.42	25.59
727G25	0.25	64.70	76.79	39.63	16.42	25.67
727G26	0.25	68.31	76.00	38.77	14.78	23.07
727G27	0.25	73.84	78.80	37.11	15.91	22.88
727G28	0.25	73.46	75.18	37.46	12.63	23.23
No clay binder		62.77	68.21	44.49	12.70	24.01

Figure 4.21 compares the flotation results of different tests. 727G25 produced the best separation efficiency. 727G27 produced the highest yield and recovery but lowest A.I. rejection and concentrate grade. Use of clay binder at a dosage of 0.25 kg/t significantly increased recovery and concentrate grade. This is particularly true especially when compared to the results obtained with the plant fatty acid only.

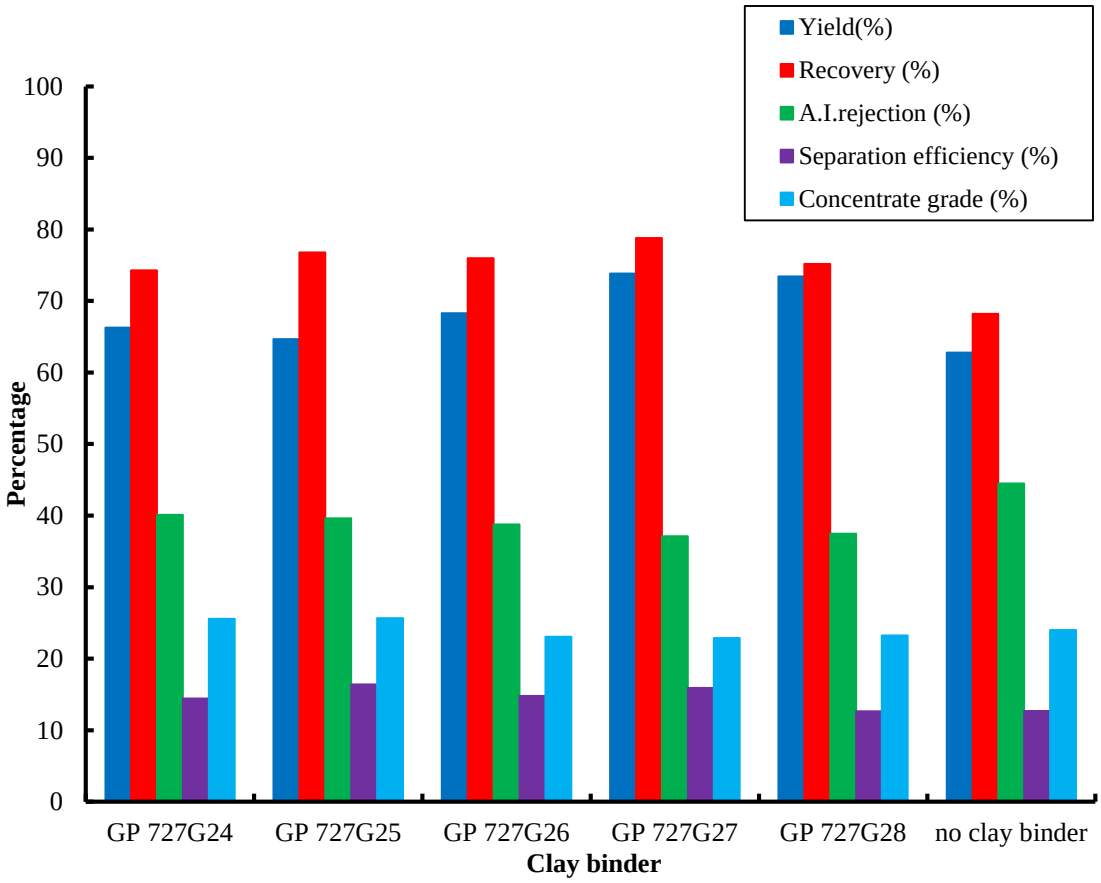

Figure 4.21. Flotation results with five clay binders at 0.25 kg/t and no clay binder

4.3.3 Effects of clay binder and water glass

Table 4.7 shows the results of flotation tests based on statistical design(generated by Design-Expert software) of three factors, including water glass (F1), plant fatty acid (F2), and clay binder 727G25 (F3), at three levels. The five responses of yield (R1), recovery (R2), AI. Rejection (R3), seperation efficiency (R4) and concentration grade (R5) were examined in statistical analyses at pH 11 which was the optimum value for plant fatty acid.

Table 4.7. The flotation results with different dosages of plant fatty acid, water glass and clay binder 727G25 from statistical experimental design

		F1	F2	F3	R1	R2	R3	R4	R5
Std	Run	A: water glass	B: Plant FA	C: 727G25	Yield	Recovery	A.I. Rejection	SE	Conc. Grade
					%	%	%	%	%
8	1	6	2	0.5	27.87	38.71	74.98	13.69	25.49
10	2	3	3	0	86.64	92.54	20.48	13.03	24.46
3	3	0	3	0.25	88.59	96.05	19.35	15.4	22.58
12	4	3	3	0.5	48.75	68.23	61.44	29.67	26.48
9	5	3	1	0	33.35	39.84	67.66	7.5	23.99
4	6	6	3	0.25	29.01	31.45	74.7	6.15	23.07
6	7	6	2	0	38.42	69.77	63.92	33.69	22.39
17	8	3	2	0.25	42.02	67.75	68.17	35.91	19.98
7	9	0	2	0.5	82.6	89.95	21.39	11.34	24.19
11	10	3	1	0.5	30.05	30.98	74.59	5.57	24.24
13	11	3	2	0.25	43.2	57.3	63.38	20.69	26.41
2	12	6	1	0.25	34.01	35.79	68.16	3.95	21.64
15	13	3	2	0.25	45.44	62.97	65.22	28.19	27.95
5	14	0	2	0	51.4	49.61	53.58	9.19	24.68
1	15	0	1	0.25	73.17	75.89	32.82	8.71	23.88
16	16	3	2	0.25	38.74	45.1	70.84	15.94	22.72
14	17	3	2	0.25	45.61	49.75	61.32	11.07	24.97

The flotation recovery model, created using Design-Expert software, is shown in the following table:

Table 4.8. Analysis of variance of P_2O_5 recovery (%) for flotation tests

Response	Recovery					
ANOVA for Response Surface Reduced Cubic Model Analysis of variance table [Partial sum of squares - Type III]						
Source	**Sum of Squares**	**df**	**Mean Square**	**F Value**	**p-value Prob > F**	
Model	3935.044	11	357.7313	8.882907	0.0129	significant
A-water glass	279.0001	1	279.0001	6.927914	0.0464	
B-Plant FA	1627.217	1	1627.217	40.4058	0.0014	
C-727G25	142.8094	1	142.8094	3.546132	0.1184	
AB	0.087836	1	0.087836	0.002181	0.9646	
AC	183.5531	1	183.5531	4.557849	0.0859	
BC	9.529887	1	9.529887	0.236639	0.6472	
A^2	36.27208	1	36.27208	0.90068	0.3862	
C^2	5.782768	1	5.782768	0.143593	0.7203	
A^2B	985.0298	1	985.0298	24.4595	0.0043	
A^2C	60.9149	1	60.9149	1.512592	0.2735	
AB^2	280.673	1	280.673	6.969455	0.0460	
Residual	201.3594	5	40.27187			
Lack of Fit	*0.282907*	*1*	*0.282907*	*0.005628*	*0.9438*	*not significant*
Pure Error	*201.0765*	*4*	*50.26911*			
Cor Total	4136.403	16				

Since the Model F-value is 8.88, the model is significant. Only 1.29% chance that a "Model F-Value" could be this large owing to noise. "Prob > F" is less than 0.0500 indicating that model term are significant and A, B, A^2B and AB^2 are significant model terms. The "Lack of Fit F-value" is 0.01 implying that the Lack of Fit is not significant relative to the pure error. A 94.38% chance for a "Lack of Fit F-value" this large could occur due to noise.

According to a statistical analysis of the experimental data, the final equation, in terms of coded factors, is as follows:

Recovery =

56.61304	
-8.35165	* A
20.16939	* B
-5.97514	* C
-0.14819	* A * B
-6.77409	* A * C
-1.54353	* B * C
-2.931	* A^2
-1.1703	* C^2
-22.1927	* A^2 * B
5.518827	* A^2 * C
-11.8464	* A * B^2

The final equation in terms of actual factors:

Recovery =

61.22772	
-30.7319	* water glass
-0.33157	* Plant FA
45.4494	* 727G25
19.59798	* water glass * Plant FA
-23.749	* water glass * 727G25
-6.1741	* Plant FA * 727G25
4.014118	* water glass^2
-15.6602	* 727G25^2
-2.46585	* water glass^2 * Plant FA
2.452812	* water glass^2 * 727G25
-1.21307	* water glass * Plant FA^2

Figure 4.22 depicts the normal probability of residual in recovery. Figure 4.23 shows the relationship between the actual and predicted values of the model.

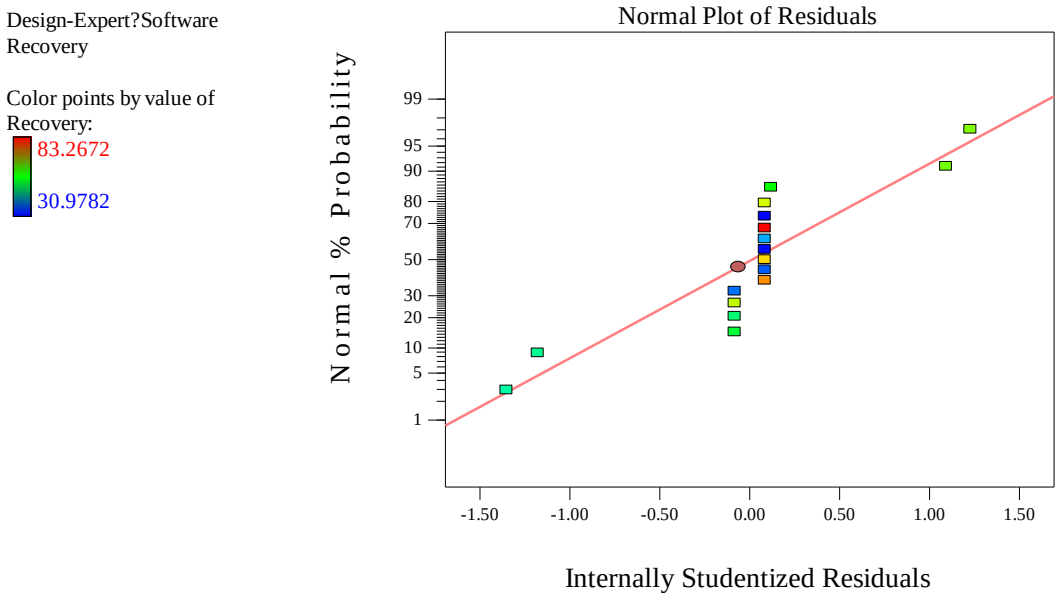

Figure 4.22. Normal probability plot of residual for P_2O_5 recovery of the phosphate flotation

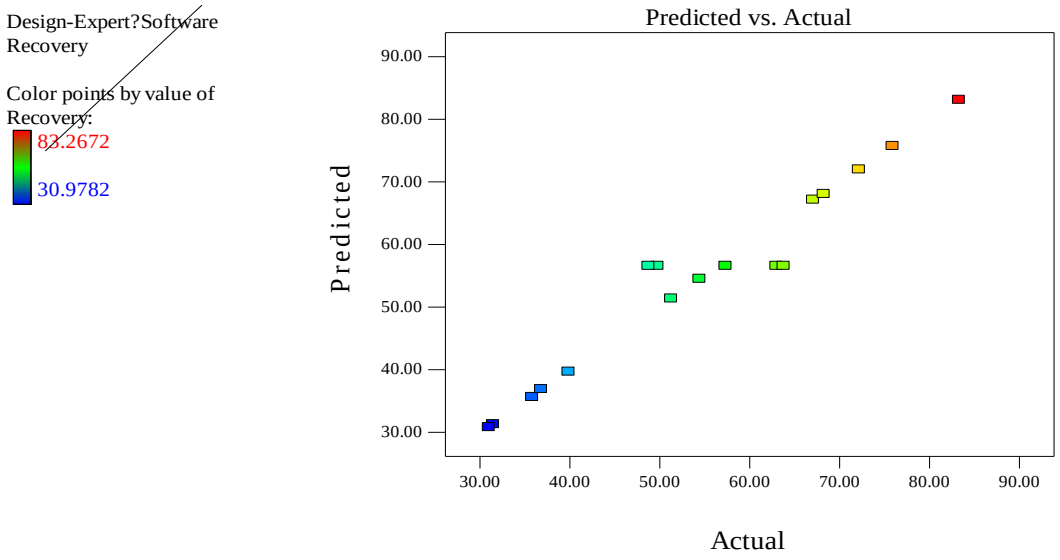

Figure 4.23. Relationship between the actual and the predicted values of the flotation recovery model.

Figures 4.24, 4.25 and 4.26 indicate the effect of water glass and clay binder 727G25 on recovery with dosages at 1 kg/t, 2 kg/t and 3 kg/t. The contour graphs were generated

as a function of collector dosage. The minimum and maximum P_2O_5 recoveries were 30.98% and 83.27%. Recovery increased as the collector dosage increased. Flotation recovery decreased by 20% - 50% when a higher dosage of water glass was used. When collector dosage was 1 kg/t, the clay binder increased recovery by approxiametely 15% without water glass. If a recovery of 70% is required, it can be generated using 1 kg/t plant fatty acid and 0.1 kg/t 727G25 without the use of water glass. Therefore, the presence of a clay binder can reduce collector usage and water glass dosage.

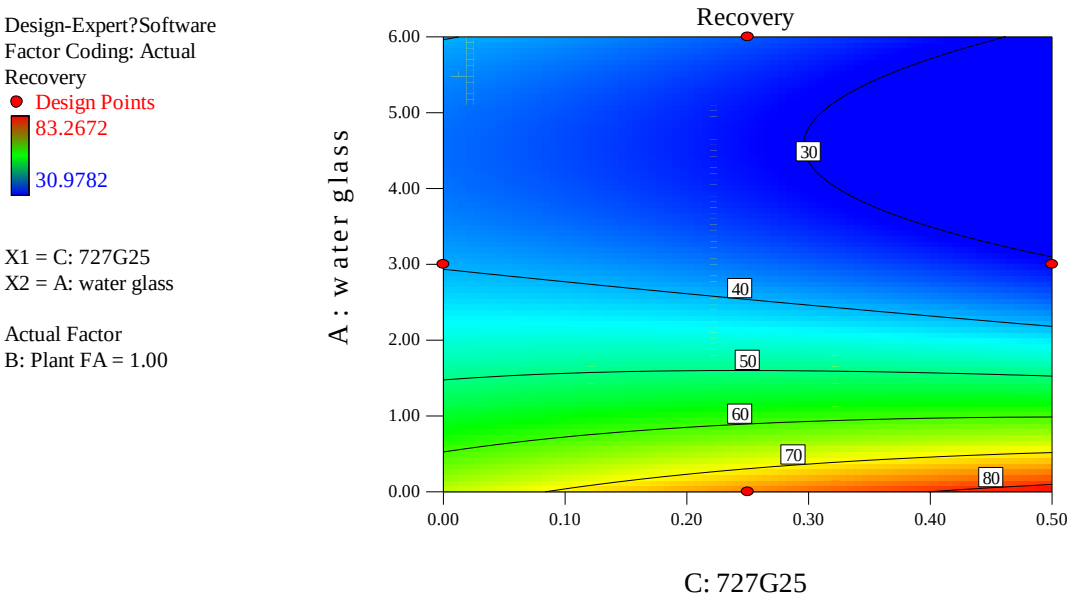

Figure 4.24. Effect of water glass and 727G25 on recovery with 1 kg/t plant fatty acid

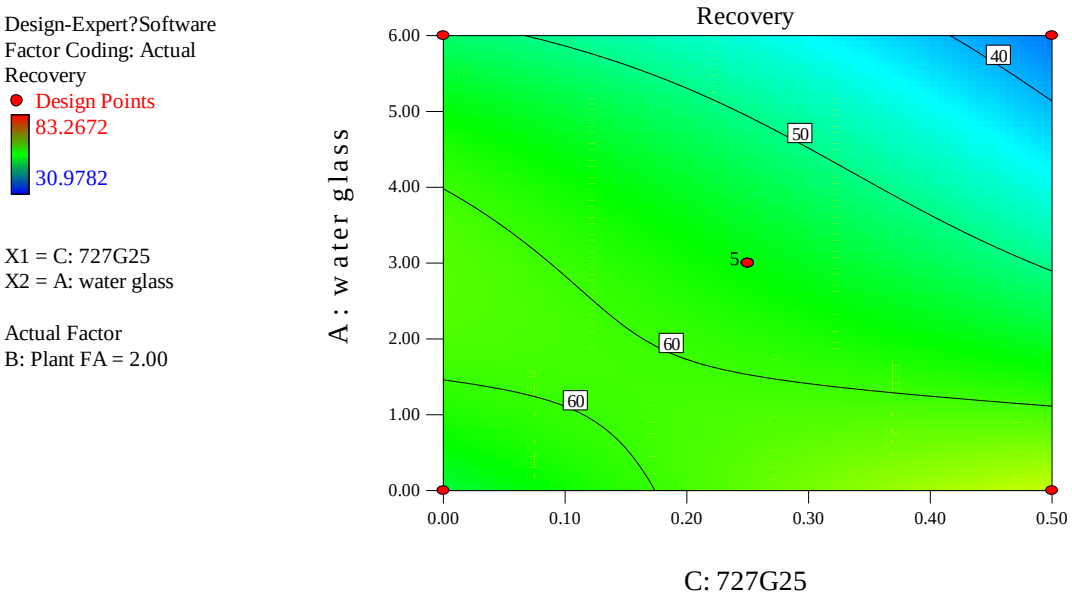

Figure 4.25. Effect of water glass and 727G25 on recovery with 2 kg/t plant fatty acid

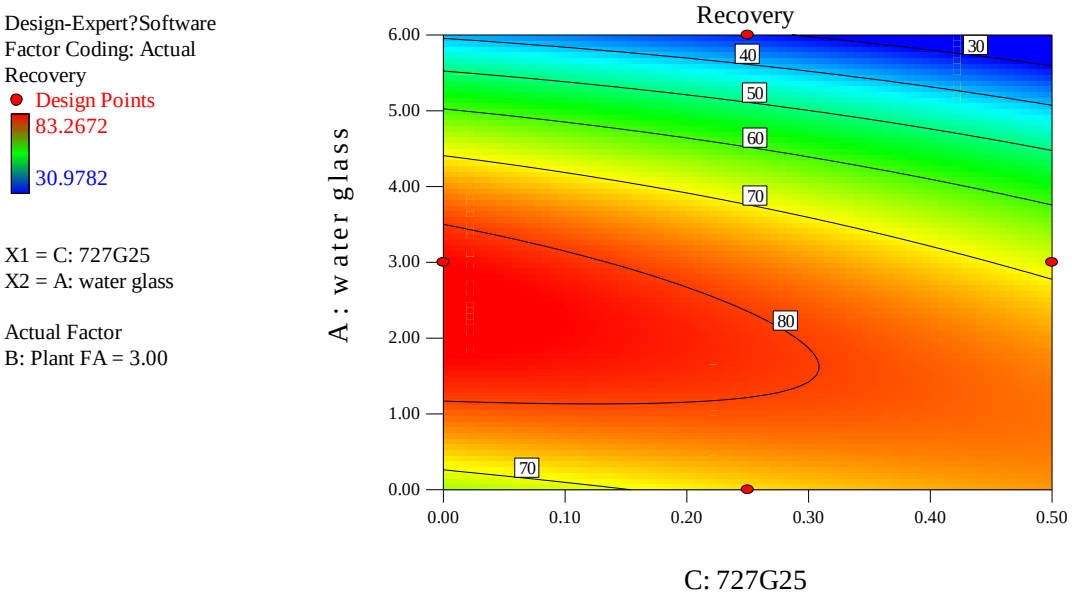

Figure 4.26. Effect of water glass and 727G25 on recovery with 3 kg/t plant fatty acid

Table 4.9 shows the statistical analysis of variance of A.I. rejection and its dependence on the dosage of collector, water glass and clay binder 727G25.

Table 4.9. Analysis of variance of A.I. rejection (%) for flotation tests

Response	A.I. Rejection					
ANOVA for Response Surface Reduced Cubic Model						
Analysis of variance table [Partial sum of squares - Type III]						
Source	**Sum of Squares**	**df**	**Mean Square**	**F Value**	**p-value Prob > F**	
Model	1922.48	9	213.6089	6.392743	0.0115	significant
A-water glass	902.3301	1	902.3301	27.00432	0.0013	
B-Plant FA	573.9661	1	573.9661	17.17727	0.0043	
C-727G25	154.6874	1	154.6874	4.629379	0.0685	
AB	27.45246	1	27.45246	0.821578	0.3948	
AC	65.71406	1	65.71406	1.966646	0.2036	
BC	10.51641	1	10.51641	0.314728	0.5923	
B^2	41.6688	1	41.6688	1.247036	0.3010	
C^2	9.539987	1	9.539987	0.285506	0.6097	
A^2B	638.4365	1	638.4365	19.10669	0.0033	
Residual	233.9	7	33.41428			
Lack of Fit	*166.8974*	*3*	*55.63245*	*3.321211*	*0.1383*	*not significant*
Pure Error	*67.00262*	*4*	*16.75065*			
Cor Total	2156.38	16				

F-value 6.39 in the model implies the model is significant. Only 1.15% chance exists that a "Model F-value" this large could occur due to noise. Value of "Prob>F" 0.0115 that is less than 0.0500 indicate model terms are significant. In this case A, B, A^2B are significant model terms. The "Lack of Fit F-value" is 3.32 meaning that the lack of fit is

not significant relative to the pure error. A 13.83% chance that a "Lack of Fit F-value" could be this large due to noise. According to the statistical analysis of the experimental data, the final equation in terms of coded factors is shown as:

A.I. Rejection =

60.15239	
10.62032	* A
-11.9788	* B
4.397263	* C
-2.61975	* A * B
4.05321	* A * C
1.62145	* B * C
-3.14148	* B^2
1.503154	* C^2
17.86668	* A^2 * B

The final equation in terms of actual factors:

A.I. Rejection =

41.71821	
3.935541	* water glass
11.77209	* Plant FA
-22.4747	* 727G25
-1.7804	* water glass * Plant FA
5.404281	* water glass * 727G25
6.485802	* Plant FA * 727G25
-3.28472	* Plant FA^2
21.75871	* 727G25^2
0.151192	* water glass^2 * Plant FA

Figure 4.27 depicts the normal probability of residual for A.I. rejection. Figure 4.28 shows the relationship between the actual and predicted values of the model designed by Design-Expert software.

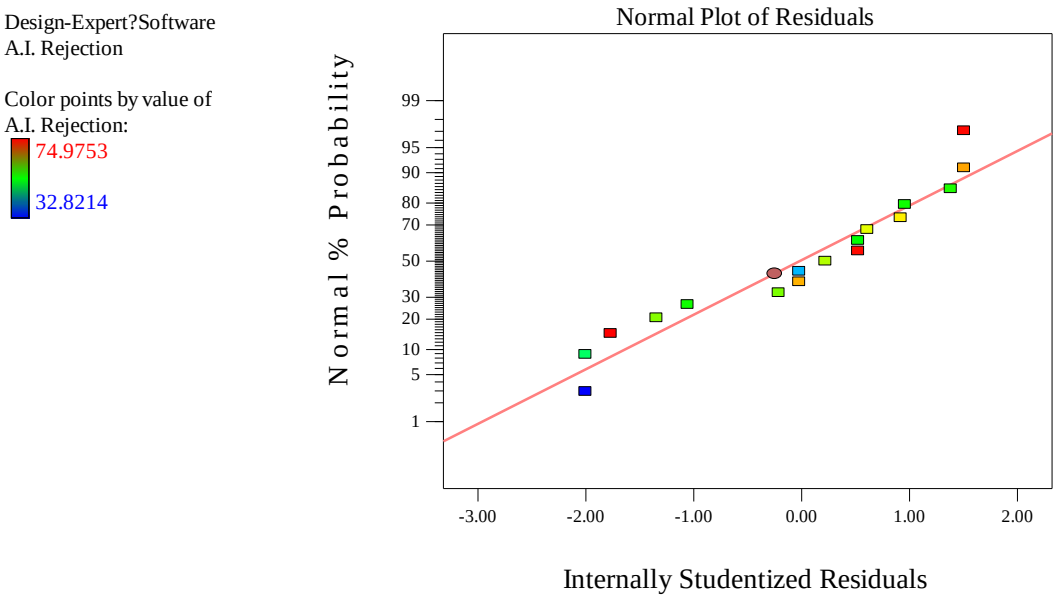

Figure 4.27. Normal probability plot of residual for A.I. rejection of the phosphate flotation

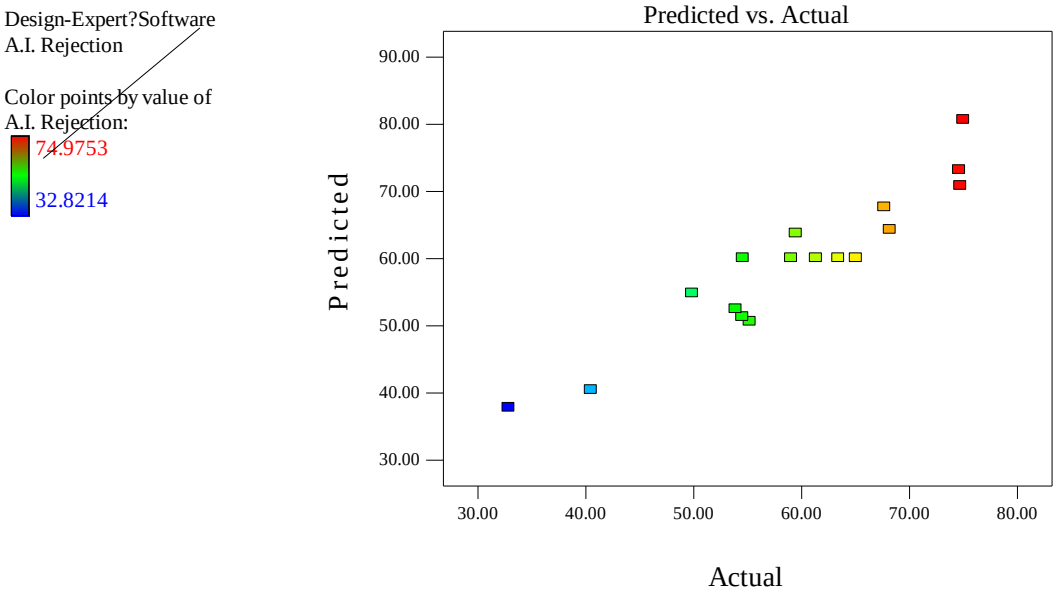

Figure 4.28. Relationship between the actual and the predicted values of the A.I. rejection model

Figures 4.29, 4.30 and 4.31 indicate the effect of water glass and clay binder727G25 on A.I. rejection with dosages at 1, 2, and 3 kg/t. A.I. rejection increased from 40% to 60%

as the dosage of water glass increased from 0 kg/t to 6 kg/t. Figure 4.29 indicates that both water glass and 727G25 can improve A.I. rejection significantly. Water glass can influence this factor more than a clay binder. A.I. rejection is more than 70% when the water glass dosage is greater than 2 kg/t and the dosage of 727G25 is greater than 0.1 kg/t.

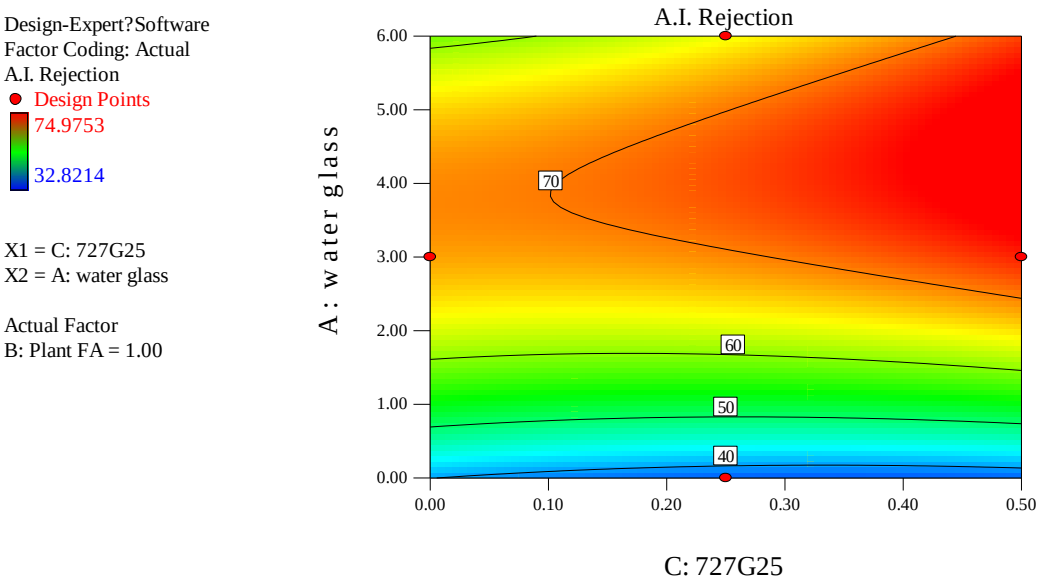

Figure 4.29. Effect of water glass and 727G25 on A.I. rejection with 1 kg/t plant fatty acid

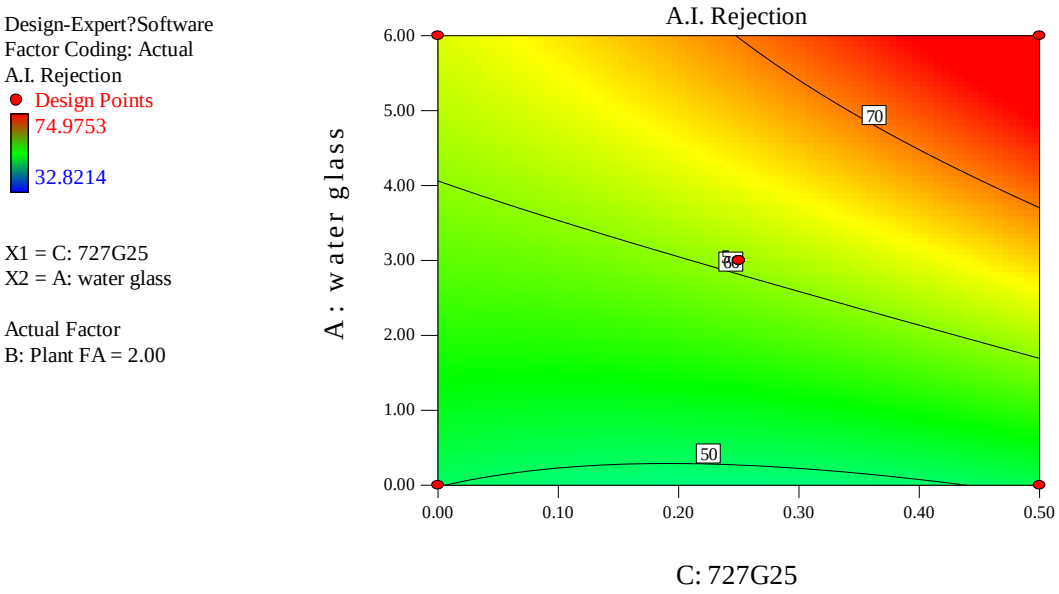

Figure 4.30. Effect of water glass and 727G25 on A.I. rejection with 2 kg/t plant fatty acid

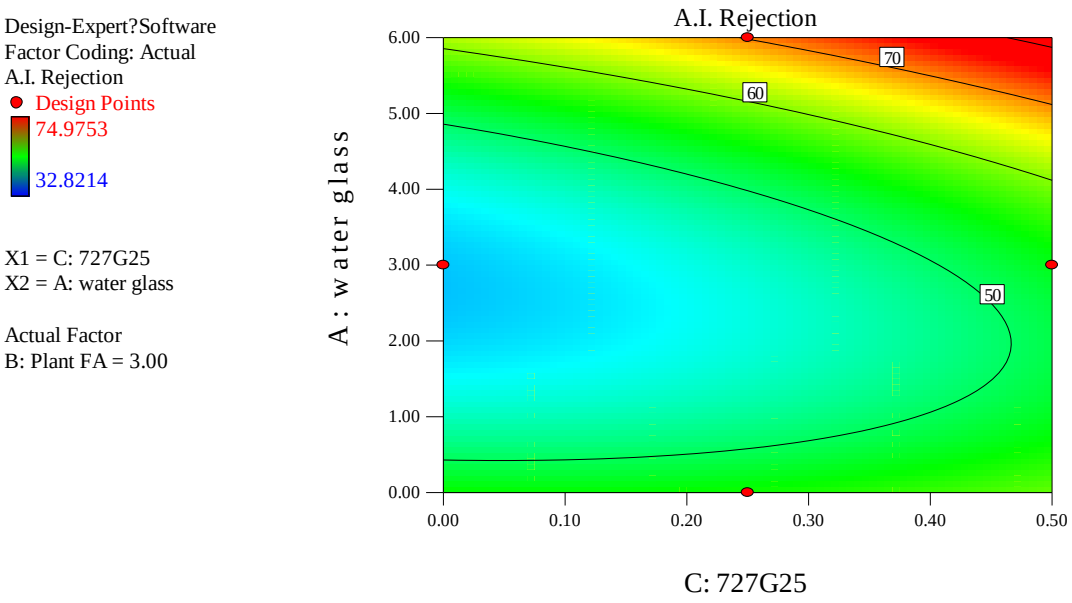

Figure 4.31. Effect of water glass and 727G25 on A.I. rejection with 3 kg/t plant fatty acid

Table 4.10 shows the ANOVA analysis of variance of separation efficiency for flotation tests.

Table 4.10. Analysis of variance of Separation Efficiency (%) for flotation tests

Response	Separation Efficiency					
ANOVA for Response Surface Reduced Cubic Model						
Analysis of variance table [Partial sum of squares - Type III]						
Source	**Sum of Squares**	**df**	**Mean Square**	**F Value**	**p-value Prob > F**	
Model	958.2935	9	106.4771	0.925323	0.5540	not significant
A-water glass	44.3682	1	44.3682	0.385575	0.5543	
B-Plant FA	185.4738	1	185.4738	1.611833	0.2448	
C-727G25	1.02245	1	1.02245	0.008885	0.9275	
AB	5.040025	1	5.040025	0.0438	0.8402	
AC	198.1056	1	198.1056	1.721608	0.2309	
BC	86.21123	1	86.21123	0.749206	0.4154	
A^2	158.5413	1	158.5413	1.37778	0.2789	
B^2	247.7814	1	247.7814	2.153308	0.1857	
C^2	2.344796	1	2.344796	0.020377	0.8905	
Residual	805.4909	7	115.0701			
Lack of Fit	*416.4301*	*3*	*138.81*	*1.427129*	*0.3590*	*not significant*
Pure Error	*389.0608*	*4*	*97.2652*			
Cor Total	*1763.784*	*16*				

The “Model F-value” of 0.93 implies the model is not significant relative to the noise. A 55.4% chance exists that “Model F-value” this large can occur because of noise. Values of “Prob > F” 0.5540 implies that the model terms are not significant. The “Lack of Fit F-value” of 1.43 indicates the Lack of Fit is not significant relative to the pure error. A 35.90% chance happenes that a “Lack of Fit F-value” this large can occur due to noise.

Thus the model fitting is not significant, indicating separation efficiency model cannot describe the three factors very well.

Even though the model is not significant, the effect of water glass and clay binder 727G25 on separation efficiency is shown in Figure 4.32, 4.33 and 4.34. When the dosage of the plant fatty acid increased from 1 kg/t to 3 kg/t, the effect of clay binder became more and more significant. In Figure 3.33, the highest separation efficiency that was more than 15% was achieved with water glass 6 kg/t and plant fatty acid 1 kg/t but no clay binder. However, in Figure 4.34, the maximum separation efficiency area, where separation efficiency could be more than 20%, was achieved with clay binder 0.5 kg/t and plant fatty acid 3 kg/t but without water glass. The clay binder can increase separation efficiency and reduce water glass dosage significantly when the plant fatty acid was 3 kg/t.

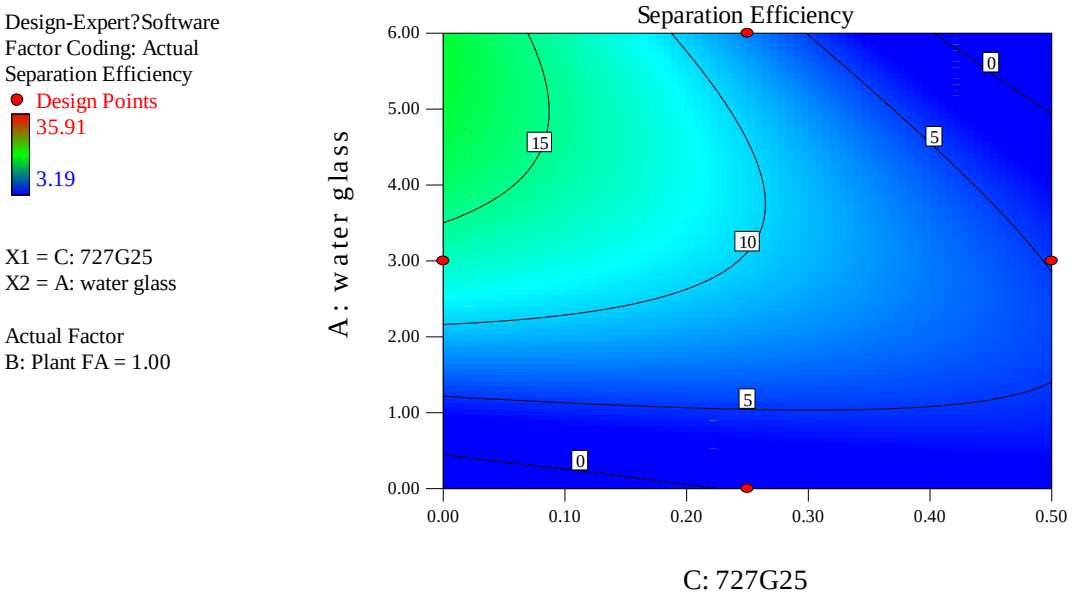

Figure 4.32. Effect of water glass and 727G25 on separation efficiency with 1 kg/t plant fatty acid

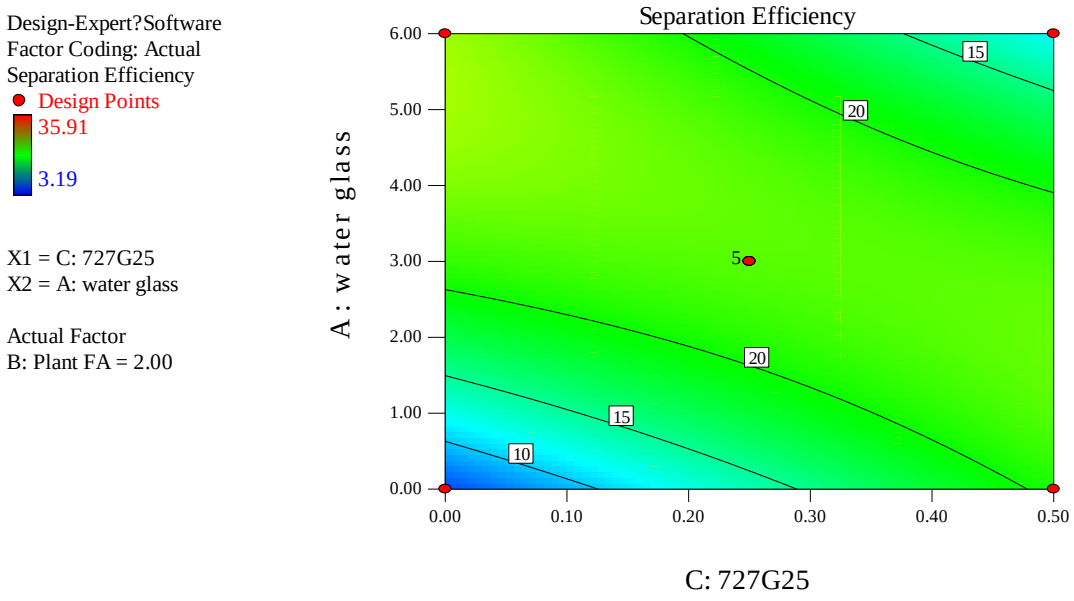

Figure 4.33. Effect of water glass and 727G25 on separation efficiency with 2 kg/t plant fatty acid

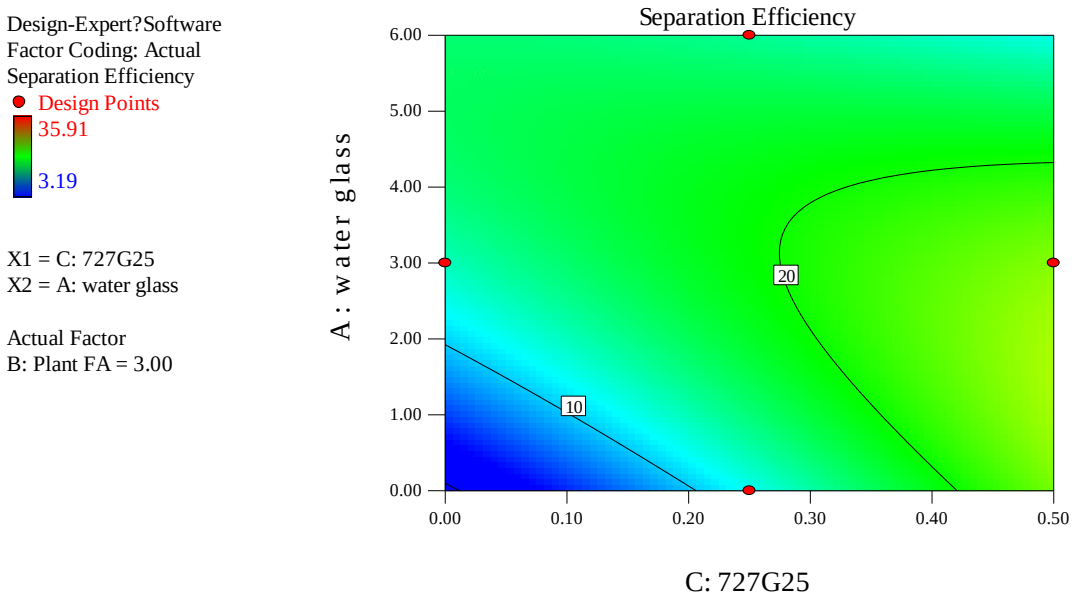

Figure 4.34. Effect of water glass and 727G25 on separation efficiency with 3 kg/t plant fatty acid.

Table 4.11 shows the ANOVA analysis of variance of concentrate grade for flotation tests.

Table 4.11. Analysis of variance of Concentrate Grade (%) for flotation tests

Response	Concentrate Grade				
ANOVA for Response Surface Reduced Cubic Model					
Analysis of variance table [Partial sum of squares - Type III]					
Source	**Sum of Squares**	**df**	**Mean Square**	**F Value**	**p-value Prob > F**	
Model	63.31562	10	6.331562	0.611373	0.7657	not significant
A-water glass	4.89845	1	4.89845	0.472993	0.5173	
B-Plant FA	1.836025	1	1.836025	0.177286	0.6884	
C-727G25	24.0818	1	24.0818	2.32533	0.1781	
AB	1.863225	1	1.863225	0.179912	0.6862	
AC	7.317025	1	7.317025	0.706529	0.4328	
BC	0.783225	1	0.783225	0.075628	0.7925	
A^2	21.01841	1	21.01841	2.02953	0.2041	
B^2	1.622444	1	1.622444	0.156663	0.7059	
C^2	0.231044	1	0.231044	0.02231	0.8862	
A^2B	0.83205	1	0.83205	0.080342	0.7864	
Residual	62.13777	6	10.3563			
Lack of Fit	*22.81165*	*2*	*11.40583*	*1.160127*	*0.4005*	*not significant*
Pure Error	*39.32612*	*4*	*9.83153*			
Cor Total	*125.4534*	*16*				

The “Model F-value” of 0.61 implied the model is not significant relative to the noise. There is 76.57% chance that a “Model F-value” this large can occur because of noise.

Values of "Prob > F" 0.7657 implies that the model terms are not significant. The "Lack of Fit F-value" of 1.16 indicates the Lack of Fit is not significant relative to the pure error. There is a 40.05% chance that a "Lack of Fit F-value" this large can occur due to noise. In this case, the model of concentrate grade is not convincing to describe the effect of three factors including plant fatty acid, water glass and clay binder 727G25.

Even if the model is not significant, Figure 4.35, 4.36 and 4.37 show the effect (as a function of dosage) of water glass and clay binder 727G25 on concentration grade. The presence of clay binder increased concentrate grade by 5% to 8% when plant fatty acid increased from 1 kg/t, 2 kg/t to 3 kg/t, respectively. The presence of water glass decreased the concentrate grade by 3% to 8%. The concentrate grade was more than 26% when the dosage of plant fatty acid was 3 kg/t and the dosage of 727G25 was more than 0.25 kg/t. The clay binder increased concentrate grade significantly. Clay binder 727G25 is a more significant model term than water glass in the model of concentrate grade.

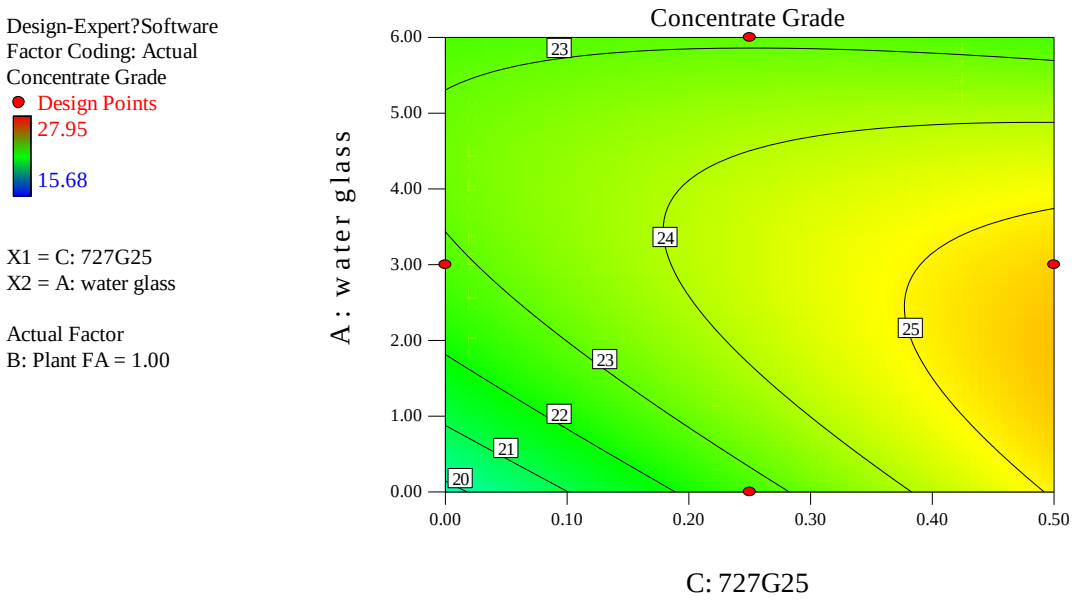

Figure 4.35. Effect of water glass and 727G25 on concentrate grade with 1 kg/t plant fatty acid.

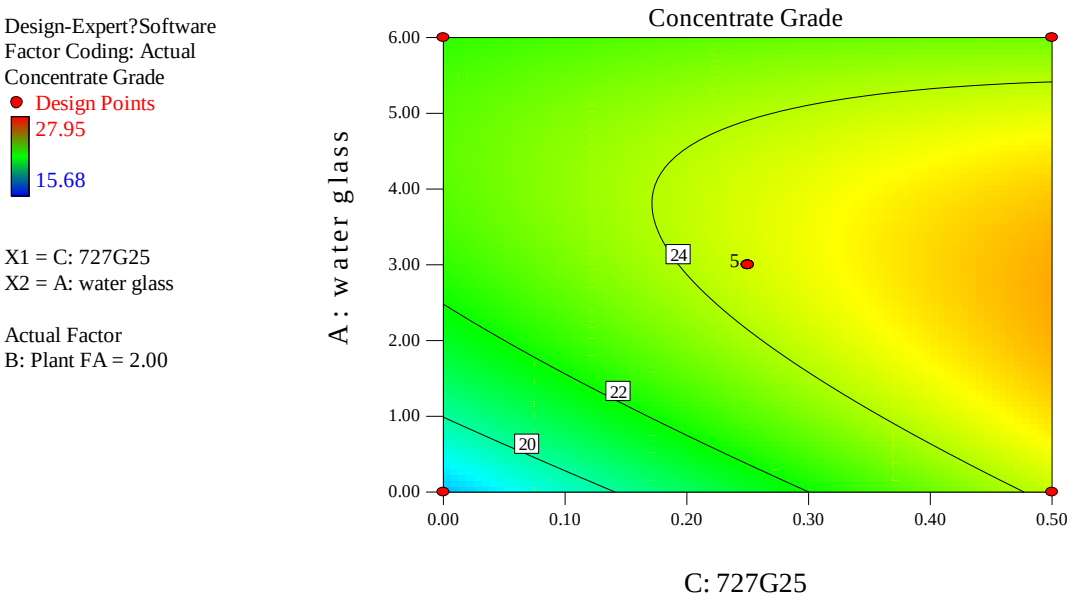

Figure 4.36. Effect of water glass and 727G25 on concentrate grade with 2 kg/t plant fatty acid.

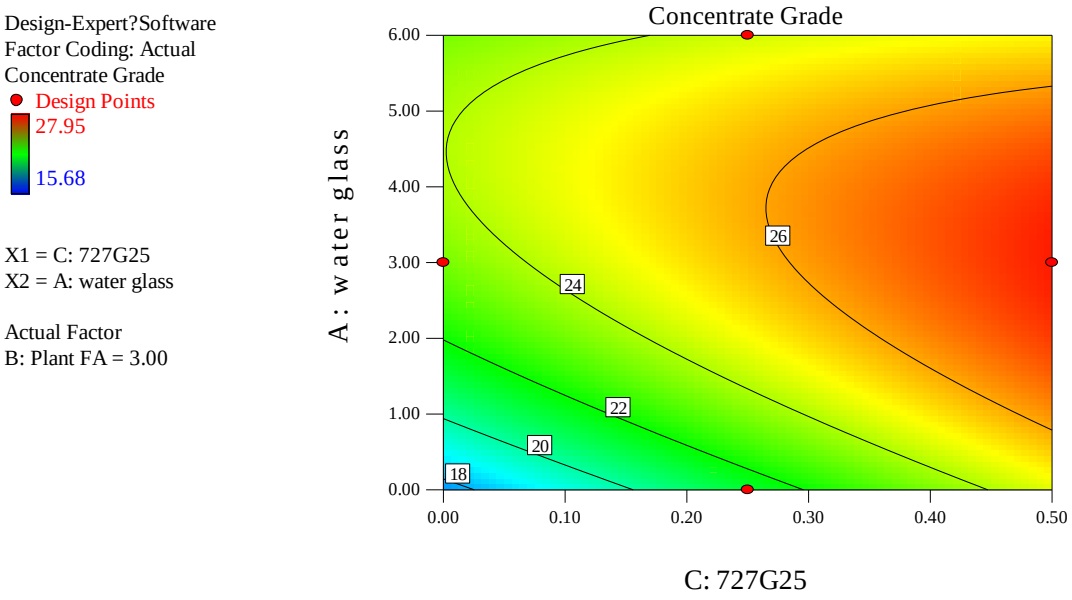

Figure 4.37. Effect of water glass and 727G25 on concentrate grade with 3 kg/t plant fatty acid.

4.4 QCM-D MEASUREMENTS

The conformation of adsorption layer was investigated with QCM-D. Three clay binder concentrations of 250 ppm, 500 ppm and 1000 ppm were investigated with an Al_2O_3 sensor. The adsorption of clay binder on the apatite, silica and Al_2O_3 sensors was compared. The simulation of adsorption in the flotation procedure was conducted using clay binder at 1000 ppm and plant fatty acid at 1000 ppm.

The sensor surfaces were rinsed with purified water and liquid was chased off the surface with a flow of nitrogen gas. A Teflon holder was used to prevent scratching by holding the sensor in a stable position. The sample liquid was degassed in a sonicator bath prior to measurement to reduce the risk of formation of air bubbles in the measurement system. The measurement chamber's working temperature was 25ºC. A pipet tip connected to the temperature-controlled chamber was initially filled with a buffer. Purified water was pumped into the QCM-D chamber. After the baseline for f and D was stable, reagents were separately exposed to different sensor surfaces. When an equilibrium in each connection was obtained, the purified water was filled again. The rinsing speed was 150 µl/min, which allowed the sample liquid enough time for temperature stabilization in the flow module before reaching the sensor surface. The fundamental frequency of the sensor was 4.95 MHz.

4.4.1 Adsorption with clay binder only

The formation of clay binder adsorption was measured with the QCM-D method. The adsorption behavior of a clay binder on Al_2O_3 surface, which can reveal the interaction between clay binder and Al^{3+}, was evaluated in real time as shown in Figures 4.38 and 4.39. The thickness of the adsorbed layer is shown in Figure 4.40. Arrows in Figure 4.38, 4.39 and 4.40 indicate the time when clay binder was added after the step of water rinse.

Figure 4.38 indicates the frequency of the clay binder adsorption on the Al_2O_3 surface using three different concentrations. The plot shows that the increase of $-\Delta f$ is the greatest at a concentration of 1000 ppm. The increase of $-\Delta f$ at 500 ppm was more

than that of the 250 ppm concentration. The increase in $-\Delta f$ means more mass is adding to the surface; if $-\Delta f$ decreases, the surface is losing mass. Thus the adsorption mass at 1000 ppm was the most among the three concentrations.

Dissipation is a parameter to quantify the damping of the system as it relates to the sample's viscoelastic properties. In process that ΔD is increased, the layer on the surface is becoming less rigid, while a decrease of ΔD means the layer is becoming more rigid. After 1300 seconds, a rinsing was performed by replacing the clay binder solution with the purified water.

Figure 4.39 displays the dissipation shift with the third overtone (15 MHz) and its association to a clay binder, at three different concentration, adsorption onto the Al_2O_3 surface. The adsorption of clay binder at 1000 ppm caused a rapid increase in dissipation while the dissipation of 250 ppm and 500 ppm was around at 1×10^{-6} , indicating the adsorption layers of 250 ppm and 500 ppm were rigid and thin and the adsorption layer of 1000 ppm was more viscoelastic or softer. The main reason for the change of 1000 ppm might be that the adsorption layer was soft and porous with hydro-dynamically coupled water.

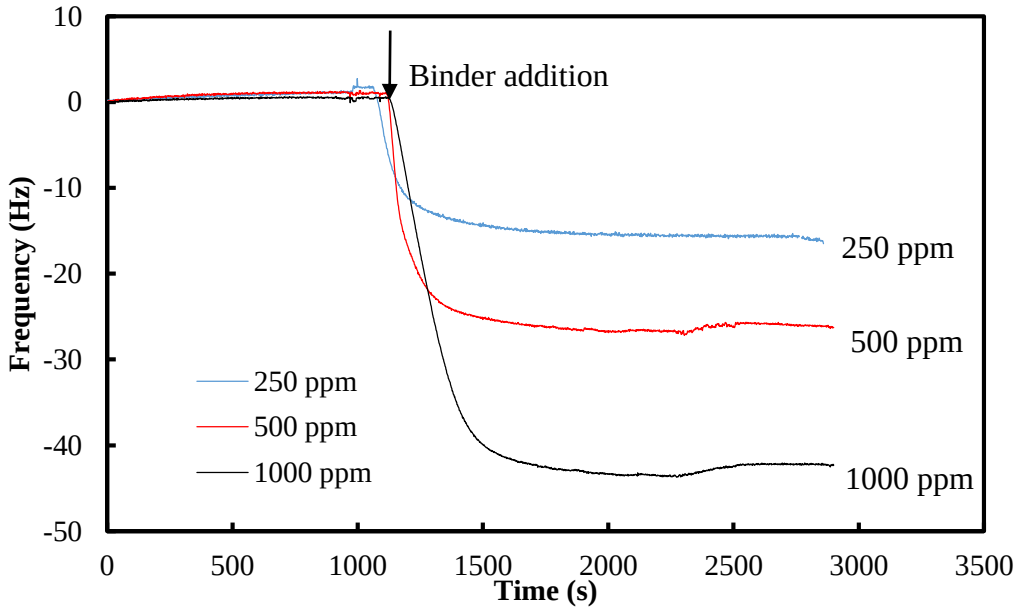

Figure 4.38. Frequency with the third overtone (15 MHz) of the QCM-D resonator for different concentrations of clay binder adsorption on Al_2O_3 surface.

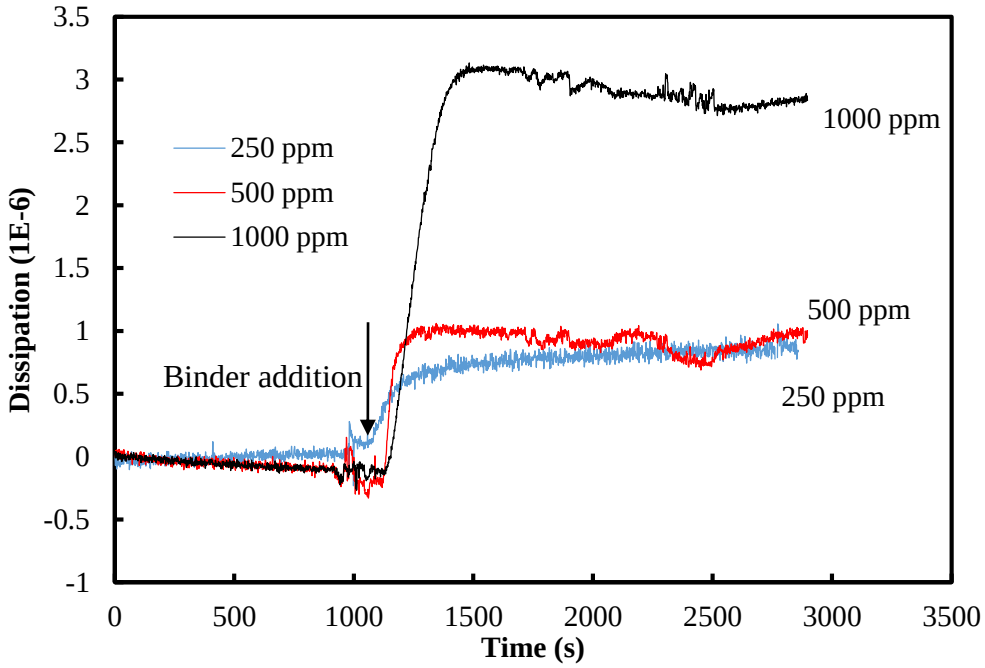

Figure 4.39. Dissipation with the third overtone (15 MHz) of the QCM-D resonator for different concentrations of clay binder adsorption on Al_2O_3 surface.

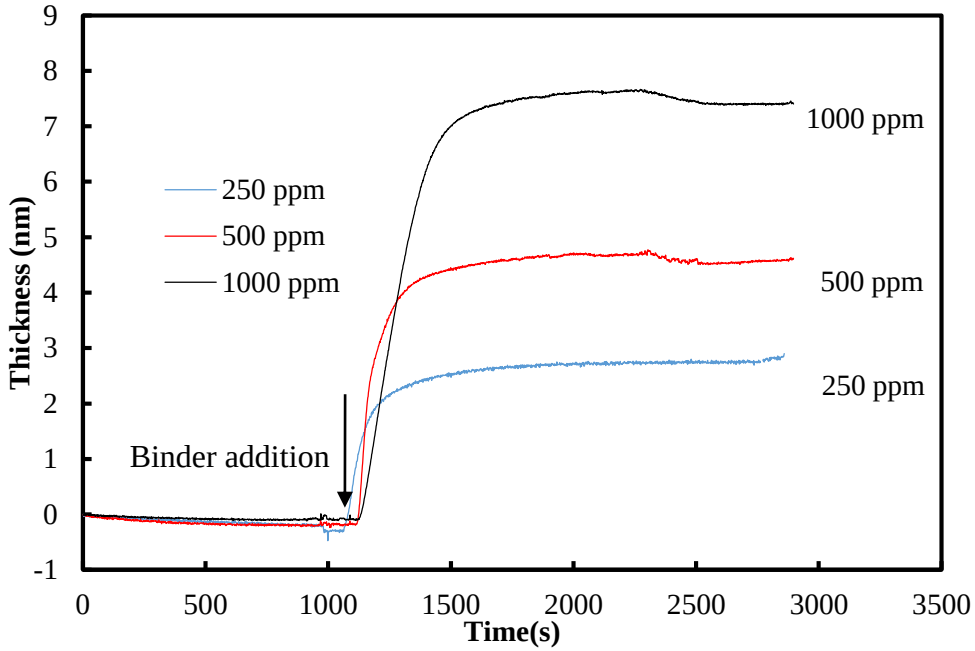

Figure 4.40. Thickness of the adsorption layer with the third overtone (15 MHz) of the QCM-D resonator for different concentrations of clay binder adsorption on Al_2O_3 surface.

Figure 4.41 shows the relationship between Δf and ΔD when the Al_2O_3 surface was exposed to a clay binder solution at different concentrations. Observations were made based on the trend of the curves representing the kinetic and structural alternations taking place during the adsorption process (Paul et al., 2008). A small K value reveals a more rigid and compact adsorption mass, while a higher K value means a soft and dissipated layer was formed. One slope is indicative adsorption without conformational or kinetic change, while more than one slope indicates direct adhesion and change in orientation with hydro-dynamically coupled water. Since the K of 250 ppm was the smallest, the formation of the adsorbed layer was most rigid suggesting that the initially-formed layer was the least dissipated. The K of 1000 ppm was the largest which implied that the layer was viscoelastic and dissipated. The layer thickness of 1000 ppm was the most of the three concentrations shown in Figure 4.40. Since the adsorption of 250 ppm was persistent and the adsorbed layer was rigid and thin, it is probable that the interaction between a clay binder and an Al_2O_3 surface is chemical adsorption. Comparing the results of 500 ppm and 1000 ppm tests, it is found that K_1 is higher than K_2. By decreasing frequency, the increase of the dissipation shift became slower indicating that the loss of water was caused by the compression of layer or the change in orientation of the molecules. The adsorbed layer of 1000 ppm was viscoelastic and water rich while the adsorbed layer of 500 ppm was more rigid.

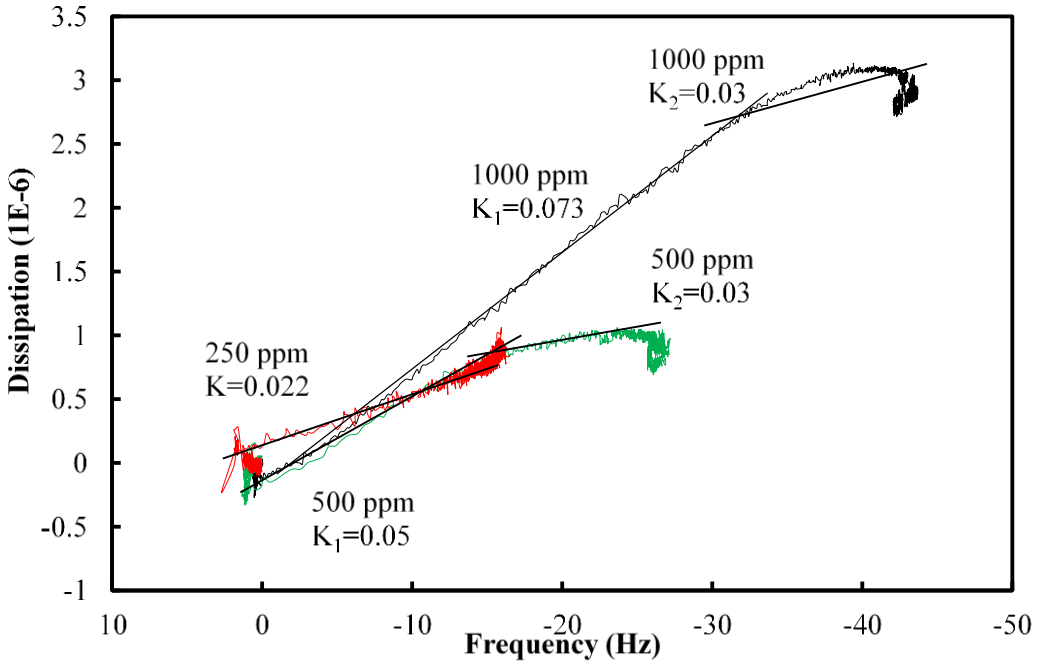

Figure 4.41. $\Delta f - \Delta D$ plot of the adsorption layer with the third overtone (15 MHz) of the QCM-D resonator for different concentrations of clay binder adsorption on Al_2O_3 surface.

Figure 4.42 shows the frequency with an overtone of 35 MHz for clay binder adsorption as a function of time on apatite, silica and Al_2O_3 surfaces. Arrow A in Figure 4.42, 4.43 and 4.44 indicates the beginning time for clay binder addition after water rinse on sensor surface and arrow B represents the time clay binder solution was switched to pure water. The frequency decreased most significantly for the clay binder adsorption on Al_2O_3 surface while the frequency changed least significantly on the silica surface, revealing that the adsorption mass on Al_2O_3 is more than that of the silica and apatite surface. Thus the clay binder was adsorbed on Al_2O_3 surfaces more readily which means that a clay binder can remove clay particles from apatite and silica easily during the flotation procedure. This is consistent with the conclusion that a clay binder can improve flotation test results.

Figure 4.43 shows the dissipation shift with 35 MHz for clay binder adsorption on the three surfaces. The Al_2O_3 surface had the most significant change of dissipation more than 1×10^{-6} indicating the adsorbed layer on Al_2O_3 surface was softest or most

viscoelastic determined through Kevin-Voigt model. The thickness of the layer on Al_2O_3 surface was larger than that of apatite and silica (Figure 4.44). Thus the adsorbed layer on Al_2O_3 surface was thick and viscoelastic, on silica and apatite surface, it was relatively thin and rigid. It is possible that the adsorbed layer on Al_2O_3 surface was porous and contained amounts of water molecule.

The molecules adsorb rather quickly, and then start to organize themselves onto the layer below (they form a more packed structure leading to water being release from the film). The adsorption on the silica and apatite surface was saturated quickly once the dissipation shift became stable. The apatite surface formed a more rigid adsorbed layer than that of silica surface. The results indicated that a clay binder can help remove clay minerals from both apatite and silica particles more readily.

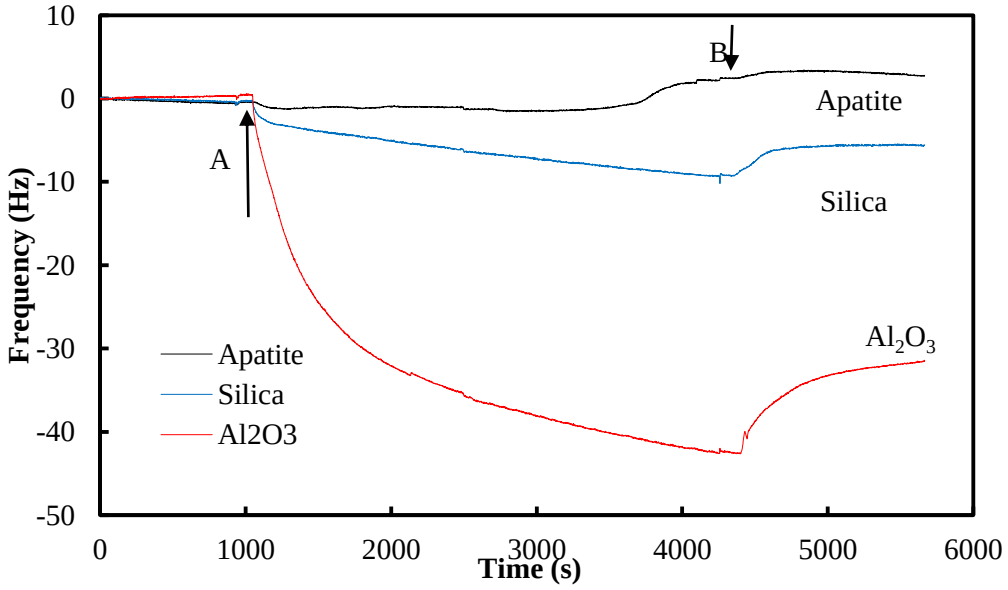

Figure 4.42. Frequency with the seventh overtone (35 MHz) of the QCM-D resonator for clay binder 727G25 adsorption at 500 ppm on different surfaces.

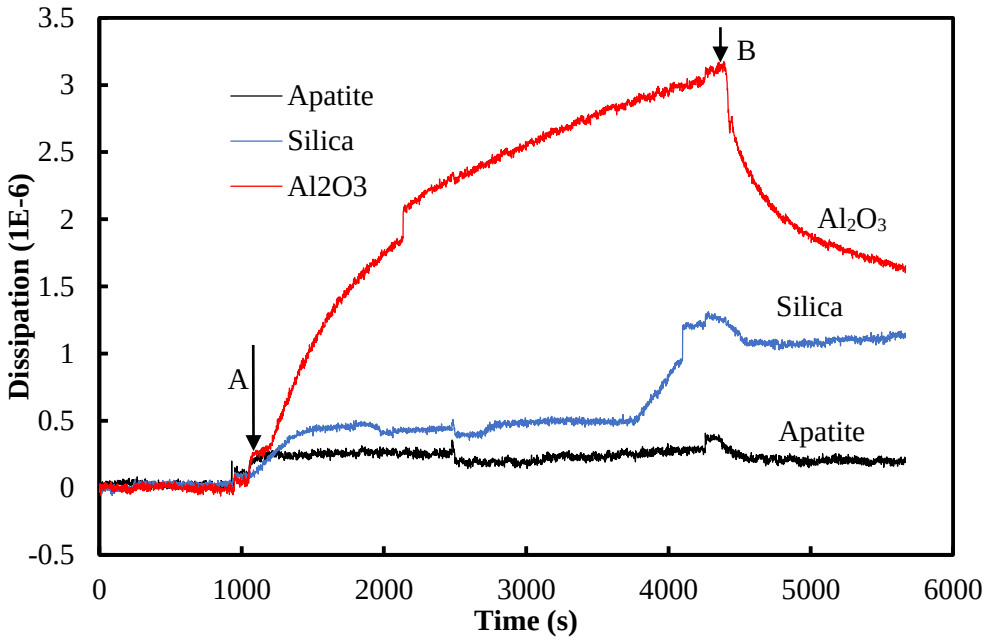

Figure 4.43. Dissipation with the seventh overtone (35 MHz) of the QCM-D resonator for clay binder 727G25 adsorption at 500 ppm on different surfaces.

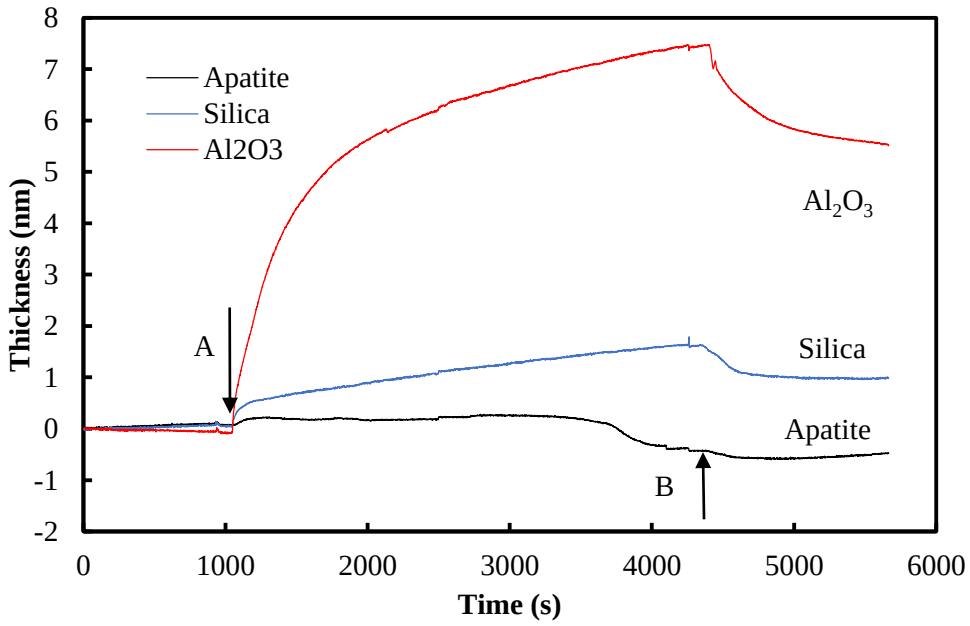

Figure 4.44. Thickness of the adsorption layer with the seventh overtone (35 MHz) of the QCM-D resonator for different concentrations of clay binder adsorption on Al_2O_3 surface.

4.4.2 Adsorption with collector and clay binder

Adsorptions of plant fatty acid and clay binder were monitored in real time to investigate the interactions between the reagents and mineral particles in flotation. The results are shown in Figure 4.45.

Clay binder was injected into the QCM-D chamber first, and after the adsorption of clay binder was saturated, plant fatty acid was injected into the chamber then. It was the same with the reagent order in the flotation tests. The addition of clay binder started at arrow A after water rinse. The plant fatty acid was injected into the solution at arrow B after the frequency became stable. Arrow C indicates the time when the collector addition stopped. The frequency of the responses indicates that the adsorption of clay binder on the Al_2O_3 surface was much more than it was on apatite or silica surfaces, and the adsorption of collector on apatite was the most compared to the adsorption on the other two surfaces (Figure 4.45). Figure 4.46 shows that the dissipation for the adsorption of a clay binder on an Al_2O_3 surface was more than that obtained on the apatite or silica surface. The adsorption mass of clay binder on Al_2O_3 surface was the most through Sauerbrey model since the dissipation was less than 1×10^{-6} that means the adsorption layer was rigid. When the conditions during a measurement are changed, there are internal stresses upon sensor crystal loaded with a substantial amount of mass (several hundred nanometers thick) that may lead to the negative D value. After the collector was injected into the chamber, the decrease of frequency on apatite surface was greater than that of silica and Al_2O_3, and the dissipation of apatite surface kept increasing, revealing that the adsorbed mass of the collector on apatite surface was increasing and the adsorption layer was becoming thicker. In the flotation process, a clay binder can remove the clay minerals around the apatite particles but it does not influence the adsorption of the collector on apatite particles. Therefore, use of a clay binder can help improve phosphate flotation performance.

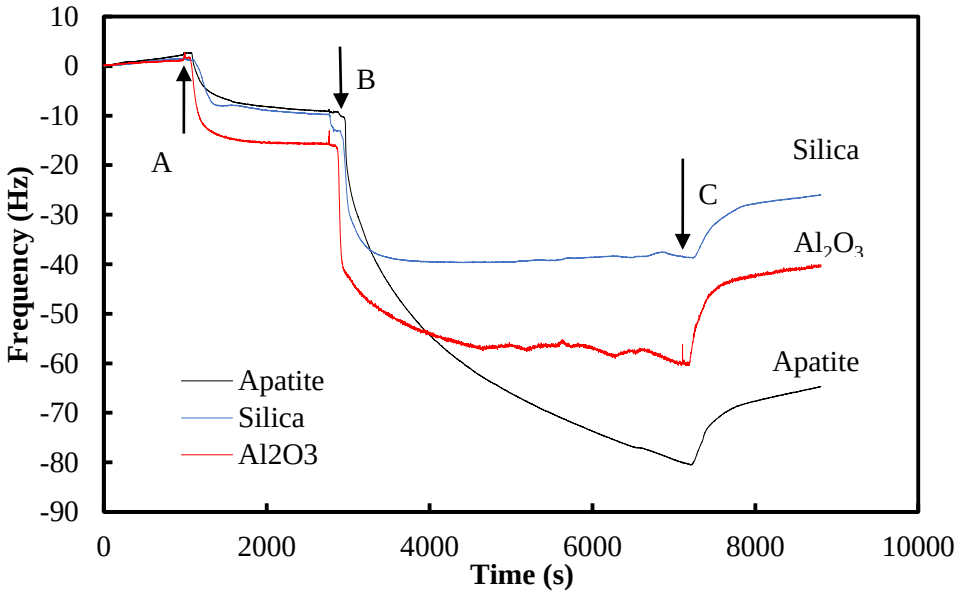

Figure 4.45. Frequency of the adsorption layer with the third overtone (15 MHz) of the QCM-D resonator for clay binder and collector adsorption on different surfaces.

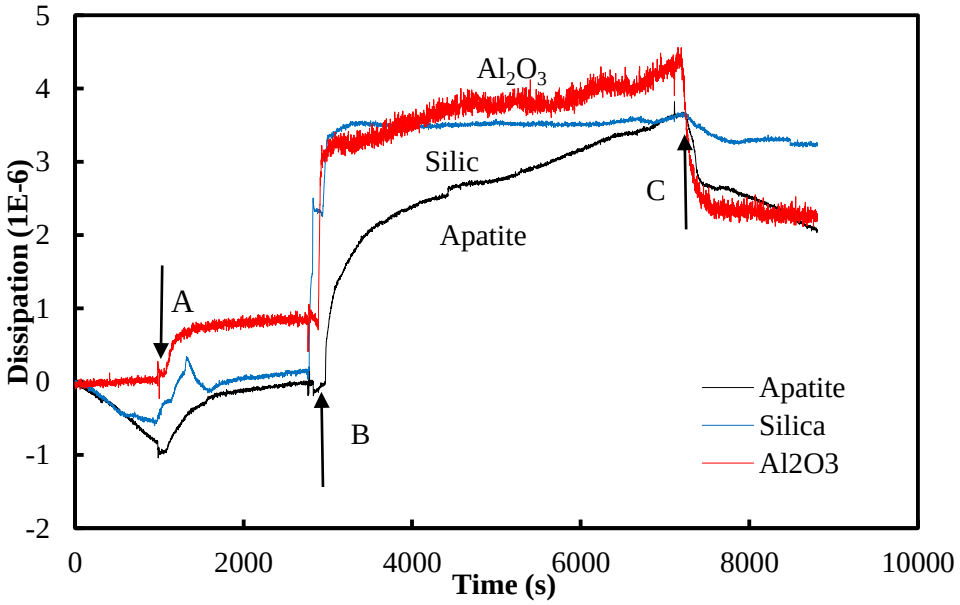

Figure 4.46. Dissipation of the adsorption layer with the third overtone (15 MHz) of the QCM-D resonator for clay binder and collector adsorption on different surfaces

Copyright © Lingyu Zhang 2013

CHAPTER 5 CONCLUSION AND RECOMMENDATION

5.1.CONCLUSION

The results of the flotation tests indicated that the presence of clay binder significantly improved Yunnan phosphate flotation separation performance. Several baseline flotation tests were done to establish the optimal pH value for the plant fatty acid, the optimal GP collector type and dosage, and the optimal clay binder type and dosage. A depressant combination of clay binder and water glass (sodium silicate) was evaluated to examine the flotation performance of plant fatty acid with clay binder and water glass. Zeta potential and QCM-D measurements were used to interpret the adsorption behavior of clay binder and collector on different minerals in the flotation process.

The following major conclusions were established from this study:

1. The main size fraction of the as-received sample was less than 200 mesh (0.074 mm) that accounts for 57.2% of the sample. The D_{50} was approximately 18 μm and more than 95% of the particles were smaller than 70 μm after grinding. The major minerals identified by XRD were fluorapatite ($Ca_{10}(PO_4)_6F_2$) and quartz (SiO_2). The main chemical compositions determined by XRF analysis were: 19.32% apatite, 36.18% silica, and 30.99% calcite.

2. The zeta potential measurements with apatite, silica, and clay minerals indicate that the repulsive electrostatic force between clay minerals and quartz was stronger than it was between clay minerals and apatite, meaning the removal of clay from apatite particles was more difficult.

3. The optimal pH value for the plant fatty acid collector was pH 11. The best fatty acid collector was XTOL 100. Compared to the plant collector at similar dosages, XTOL 100 resulted in a higher phosphate recovery but lower A.I. rejection. The optimal dosage for collectors was 3 kg/t.

4. The optimal clay binder was 727G25 at 0.25 kg/t, which showed the higher separation efficiency, higher recovery, and higher A.I. rejection than the other four clay binders.

5. The model system of reagents designed by Design-expert software shows the effect of 727G25 and water glass when plant fatty acid was used as a collector. Water glass is used as a dispersant in the phosphate flotation. When collector dosage was 1 kg/t, the clay binder increased recovery by approxiametely 15% without the use of water glass. Thus the presence of a clay binder can reduce collector and water glass usage significantly. A.I. rejection increased by 40-60% as the dosage of water glass was increased from 0 kg/t to 6 kg/t. The separation efficiency that was more than 15% was achieved with water glass 6 kg/t and plant fatty acid 1 kg/t but no clay binder. However, when the clay binder was 0.5 kg/t and plant fatty acid was 3 kg/t without water glass, the separation efficiency could be more than 20%. This indicates that the clay binder can increase separation efficiency and reduce water glass dosage significantly when the plant fatty acid was 3 kg/t. The presence of clay binder increased concentrate grade by 5% to 8% while water glass decreased the concentrate grade by 3% to 8% when plant fatty acid increased from 1 kg/t, 2 kg/t to 3 kg/t, respectively.

6. QCM-D analysis measured the adsorption behavior of clay binder 727G25 and plant fatty acid on apatite, silica, and Al_2O_3 surfaces. When the concentration of 727G25 was 1,000 ppm, the adsorption layer on the Al_2O_3 surface was the most viscoelastic and thickest when compared to concentrations of 250 ppm and 500 ppm. The adsorption mass at 1000 ppm was more than at the other two concentrations. When the clay binder 727G25 was adsorbed on different surfaces (including apatite, silica, and Al_2O_3), the adsorption mass of clay binder on the Al_2O_3 surface was greatest and the adsorption layer was the thickest and most viscoelastic, indicating that 727G25 could remove clay minerals from apatite and silica particles easily thus improving flotation selectivity. In simulating the interaction between reagents and minerals in flotation procedure through QCM-D, the results indicated that the adsorption of the clay binder 727G25 on Al_2O_3 was significant. 727G25 had no influence on the

adsorption of plant fatty acid collector when used on the apatite surface. This result is consistent with the flotation results using clay binders.

5.2. RECOMMENDATION

The study proved that clay binders improved flotation performance significantly. However, more study of clay binders is needed in the future. For instant, the comparison between GP clay binders and other clay depressants can be studied; the effect of clay binders in reverse phosphate flotation should be demonstrated; the adsorption procedure and construction of clay binder should be investigated using other methods such as AFM, SEM, FTIR and so on. Furthermore, economic evaluation is also needed so that the application of clay binder can be more extensively practiced in the phosphate processing industry.

Copyright © Lingyu Zhang 2013

REFERENCES

Abdel-Khalek, N.A., 2000. Technical note evaluation of flotation strategies for sedimentary phosphates with siliceous and carbonates gangues, Minerals Engineering, Vol. 13, No.7, pp. 789-793.

Al-Fariss T.F., Ozbelge.H.O.and Abdulrazik A.M., 1991. Phosphorus and Potassium, Vol.171, pp. 28-30.

Abromov, A.A., Abromov, Al. Al., Onal, G., Atak, S., and Celik, M.S., 1993. "Mechanism of Reverse Flotation of Calcareous Phosphate Ores", in Beneficiation of Phosphates: Theory and Practice, El-Shall, H., Moudgil, B., Wiegel, B., eds., SME, Littleton, CO, pp. 281-288.

Abu-Eishah, S.I., et al. 1991. "Beneficiation of Calcareous Phosphate Rocks Using Dilute Acetic Acid Solutions," International Journal of Minerals Processing, 31 pp. 115-126.

Adbel-Zaher, M.A., 2008. Physical and thermal treatment of phosphate ores-an overview. Int. J. Miner, Process. 85, pp. 59-84.

Al-Thyabat Salah, Yoon Roe-Hoan, Shin Dongcheol, 2011. A comparison of anionic and cationic flotation of a siliceous phosphate rock in a column flotation cell, Mining Science and Technology (China) 21, pp. 147-151.

Albuquerque Rodrigo O., Antonio E.C. Peres, Jose A. Aquino, Plinio E. Praes, Carlos A. Pereira, 2012. Pilot Scale Direct Flotation of a Phosphate Ore with Silicate-Carbonate Gangue. Procedia Engineering 46, pp. 105-110.

Anazia, I.J. and Hanna, J., 1987. New flotation approach for carbonate phosphate separation, Minerals and Metallurgical Processing, November, 4(4), pp. 196-202.

Anderson, B and Somasundaran, P., 1993. "Mechanisms Determining Separation of Phosphatic Clay Waste by Selective Flocculation", Miner. Metall. Process., 10(4), pp.200-205.

Atalay, V., 1985. "Beneficiation of Low Grade Tasit Phosphate Ore from Turkey", In Proceedings, World Congress on Non-Metallic Minerals, Belgrade, Yugoslavia, April, pp. 389-396.

Baudet, G., Save, M., 1999. Phosphoric esters as carbonate collectors in the flotation of sedimentary phosphate ores. In: Beneficiation of phosphate: Advances in research and practice, pp, 163-185.

Brown, G, 1954. Soil morphology and mineralogy: A qualitative study of some gleyed soils from North-west England: Jour. Soil Sci., vol. 5, pp. 145-155.

Brown D.J., Smith H.G., 1954. Colliery Eng., vol. 31, pp. 245-250.

Buttry, D.; Ward, M. Chemical Review, 1992. 92, pp. 1355-1379.

Cisse L. and Mrabet T., 2004. "World phosphate production: overview and prospects," Phosphorus Research Bulletin, Vol. 15, pp 21-25.

Churaev N V, Sergeeva I P, Sobolev V D, et al., 2000. Modification of quartz surfaces using cationic surfactant solution. In Colloids and Surfaces A: Physicochemical and Engineering Aspects, 164, pp. 121-129.

Chibowski E, Holysz L., 1985. Correlation of surface free energy changes and floatability of quartz[J]. Journal of Colloid and Interface Science, 112, pp. 15-23.

Clerici, C., 1984. "Flotation of a Phosphate Rock with Carbonate-Quartz Gangue", Reagents in the Mineral Industry, Jones, M.J. and Oblatt, R., eds., IMM, London, pp. 221-225.

Du Rietz C., 1957. Progress in Minerals Dressing, Transactions of the International Mineral Dressing Congress, Stockholm, Almqvist & Wiksell, Stockholm, pp. 417.

Doheim, M.A., M.M. Tarshan, and M.M. El-Gendy., 1978. "Calcination of Phosphate Rock in a Fluidized Bed Furnace," Journal of Applied Chemistry and Biotechnology, 28(8), pp. 531-538.

El-Mofty, H. E., and P. Somasundaran., 2002. “Surface Chemical Characteristics and Adsorption Properties of Calcite as One of the Gangue Minerals of Phosphate Ores,” Beneficiation of Phosphates -- Fundamental and Technology, Society for Mining, Metallurgy and Exploration, pp. 239-246.

El-Shall H., Zhang P., Khalek N.A., Ei-mofty S., 2003. Beneficiation technology of phosphate: challenges and solutions, SME annual meeting.

El-Shall, H., Zhang, P., and Snow, R., 1996. Comoparative analysis of dolomite-francolite flotation techniques. Minerals and Metallurgical Processing, 13(3), pp. 135-140.

El-Shall, H. and Bogan, M., 1994. “Evaluation of Dolomite Separation Techniques”, Publication No. 02-094-108, Florida Institute of Phosphate Research.

Elgillani, D.A. and Abouzeid, A.Z.M., 1993. Flotation of carbonates from phosphate ores in acidic media, International Journal of Mineral Processing, 38(3-4), pp. 235-256.

Everhart, D.L., 1971. Soc. Econ. Geol. Meeting, New York.

Fertilizers-Sustaining Global Food Supplies, U.S., Geological Survey

Fleming B.D., E.J. Wanless, 2000. Soft-contact Atomic Force Microscopy Imaging of Adsorbed Surfactant and Polymer Layers. In Microscopy and Microanalysis, vol 6, issue 02, March, pp. 104-112.

Frazier, A.W. and Lee, R.G., 1972. Fert. Solut, 16(4).

Fuerstenau D.W., 2007. A century of developments in the chemistry of flotation processing. In Froth Flotation. A century of innovations, M.C. Fuerstenau, G.Jemason and R.H.Yoon Editors, SME Ed. Littleton, Colorado, USA, pp. 3-64,

Fuerstenau. C. Maurice and Han N. Kenneth, 2003. Principles of Mineral Processing.

Gaudin, 1957. A.M.Flotation, 2nd Ed.; McGraw-Hill: New York.

Gharabaghi M., Noaparast M., Irannajad M., 2009. Selective leaching kinetics of low-grade calcareous phosphate ore in acetic acid, Hydrometallurgy, Vol. 95, No. 3-4.

Gibbs J.W., 1928. Collected Works. In Longmans Green and Company, London, pp. 325.

Gruber GA. 1995. Phosphate rock treatment for waste reduction. Florida Institute of phosphate research. Publication No. 01-112-125.

Gruber G, Somasundaran P. 1996. Understanding the basics of anionic conditioning in phosphate flotation. FIPR Publication; 2(9): pp. 121.

Gu Zhengxing, Gao Zhizhong, and Zheng Shibo, 1999. Beneficiation of Florida dolomitic phosphate pebble with a fine-particle flotation process, Beneficiation of phosphates: advances in research and practice, pp 155-162.

Gu, B and Doner, H.E., 1993. "Dispersion and Aggregation of Soil as Influenced by Organic and Inorganic Polymers", Soil Science Society of America Journal, 57 (3), pp 709-716.

Guan C., May 2009. Theoretical background of the crago phosphate flotation process, Minerals and Metallurgical processing, Vol 26, No.2.

Harbort, G.J., Cowburn, J., Manlapig, E., 2004. Recovery interactions between the froth zone, pulp zone and downcomer within a Jameson cell, in 10th Australian Coal Prep Conf., 17-21 October.

Hann, W.M. and Natoli, J., 1984. "Acrylic Polymer and Its Use in Combating Particulate Matter Formation or As a Dispersant in an Aqueous System", European Patent Application, EP 122, 789.

Henchiri Ammar, Sempso, Tunis, Tunisia, 1993. A contribution to carbonates-phosphate separation by flotation technique. In: Beneficiation of phosphate: Theory and Practice.

Holmes G.G., Lishmund S.R. & Oakes G.M. 1982. A review of industrial minerals and rocks in New South Wales. Geological Survey of New South Wales, Bulletin.

Hosseini S. Hamid and Forssberg Eric, 2006. XPS & FTIR study of adsorption characteristics using cationic and anionic collectors on smithsonite. In Journal of Minerals & Materials Characterization & Engineering, Vol.5, No.1, pp 21-45.

H.Sis, S.Chander, 2003. Improving froth characteristics and flotation recovery of phosphate ores with nonionic surfactants, Minerals Engineering 16, pp. 587-595.

Jasinski, S.M. 2009. Phosphate Rock, Mineral Commodity Summaries. US Geological Survey. Mineral Commodity Summaries.

Jasinski. S.M, 2011. Phosphate Rock, U.S. Geological Survey, Mineral Commodity Summaries.

Jasinski. S.M, 2013. Phosphate Rock, U.S. Geological Survey, Mineral Commodity Summaries.

Joseph Goldstein, Dale E. Newbury, David C.Joy, Charles E.Lyman, Patrick Echlin, Eric Lifshin, L.C.Sawyer, J.R.Michael, 2007. Scanning Electron Microscopy and X-ray Microanalysis

Klein Cornelis and Dutrow Barbara, 2008. Mineral Science.

Kou J., Tao D., Xu G., 2010. A study of adsorption of dodecylamine on quartz surface using quartz crystal microbalance with dissipation. Colloids and Surfaces A: Physicochemical and Engineering Aspects.

Kou J., Tao D., Xu G., 2010. Fatty acid collectors for phosphate flotation and their adsorption behavior using QCM-D, International Journal of Mineral Processing, 95(2010), pp. 1-9.

Kou J., Tao D., Sun T., Xu G., 2012. Application of the quartz crystal microbalance with dissipation method to a study of oleate adsorption onto a hydroxyapatite surface, in Minerals & Metallurgical Process, 2012, Vol.29, No.1, pp. 47-55.

Lamont, W.E., McLendon, J.T., Clements L.W. and Field, I.L. 1975. Characterization studies of Florida Phosphate Slimes, Report of Investigations 8089, U.S. Dept. of Interior, Bureau of Mines, Washington, D.C.

Levenspiel, O., 1972. Chemical Reaction Engineering, Wiley, New York.

Leal Filho, L.S., and A.P. Chaves, 1993. The influence of corn starch on the separation of apatite from gangue minerals via froth flotation. In Beneficiation of Phosphate: Theory and Practice. Edited by H.El-Shall, B.M.Moudgil, and R.Wiegel. Littleton, CO: SME, pp. 147-155.

Lehr, J and G.H. McClellan, 1973. Paper presented at Cento Symposium on Mining and Beneficiation of Fertilizer Materials, Cento, Italy.

Leja J.. 1982. Surface Chemistry of Froth Flotation. Plenum Press, New York. A division of plenum publishing corporation ed., Chapter 5, Flotation Surffactants, Chapter 10, Inorganic Regulator Agents, Activators, Depressants, pp. 205-339 and 611-681.

Li D., 1991. A study on the mechanism of apatite flotation at ambient temperature using synergists, Master thesis, Wuhan Iron and Steel University.

Lu Shouci and Sun Keji, 1999. Developments of phosphate flotation reagents in China, Beneficiation of phosphates: advances in research and practice.

Luttrell, G.H. and Yoon, R.-H., 1992. J.Colloid Interface Sci., 154, pp. 129-137.

Marisa Martins and Laurindo de Salles Leal Filho, 2010. Surface tension of solution and its influence on the selectivity of the separation between apatite and gangue minerals by flotation with long chain anionic collector, in Beneficiation of phosphates: technology advance and adoption.

Mankosa M.J., Luttrell G.H., Adel G.T. and Yoon R.H., 1992. A study of axial mixing in column flotation, International Journal of Mineral Processing, 35, pp. 51-64.

Mcnamee C E, Butt H J, Higashitani K, et al. 2009. Interaction of cationic hydrophobic surfactants at negatively charged surfaces investigated by atomic force microscopy [J], Langmuir, vol 25, pp. 11509-11515.

Mcnamee C E, Matsumoto M, Hartley P G., et al. 2001. Interaction forces and zeta potentials of cationic polyelectrolyte coated silica surfaces in water and in ethanol: effects of chain length and concentration of perfluorinated anionic surfactants on their binding to the surface[J]. Langmuir, vol. 17, pp. 6220-6227.

Meneze J.L., Yan J. and Sharma M.M., 1989. The mechanism of alteration of macroscopic contact angles by the adsorption of surfactant, Colloids and Surfaces, 38, pp. 365-390.

Miller, J.D., Wang, X., Li, M., 2001. A new collector chemistry for phosphate flotation, Preprint 01-46, SME annual meeting, Denver, Colorado, February 26-28.

Miller, J.D., Ning Liu and Yongqiang Lu, 2001. Improved phosphate flotation with nonionic polymers, Final report prepared for Florida Institute of Phosphate Research.

Mohammadkhani, M., Noaparast, M., Shafaei, S. Z., Amini, A., Amini, E. and Abdollahi, H., 2011. Double reverse flotation of a very low grade sedimentary phosphate rock rich in carbonate and silicate. International Journal of Mineral Processing, 100 3-4, pp. 157-165.

Namasivayam C., Kavitha D., 2006. IR, XRD and SEM studies on the mechanism of adsorption of dyes and phenols by coir pith carbon from aqueous phase, in Microchemical Journal 82, pp. 42-48.

Novich B.E., Ring T.A., 1985. A predictive model for the alkylamine-quartz flotation system, Langmuir 1, pp. 701-708.

Orphy M.K., Yousef A.A., and Lawendy T.A.B., 1969. Mining Magazine, Vol.121, No.3, pp. 195-201.

Paul, S., Paul, D., Tamara, B., Ray, A.K., 2008. Studies of adsorption and viscoelastic properties of proteins onto liquid crystal phthalocyanine surface using quartz crystal microbalance with dissipation technique. J. Phys. Chem. C. 112, pp. 11822–11830.

Pan, Q., 1984. "Depression and Dispersion Effects of Humates on Some Minerals", Kuangye Gongcheng (Ch.), 4(4), pp. 23-28.

Peng F, Gu Z. 2005. Processing Florida dolomitic phosphate pebble in a double reverse fine flotation process. Minerals & Metallurgical Processing; 22(1), pp. 23-30.

Rodahl M., Hook F., Fredriksson C., Keller C.A., A. Krozer, P. Brzezinski, M. Voinova, B. Kasemo, 1997. Simulaneous frequency and dissipation factor QCM measurements of biomolecular adsorption and cell adhesion, Faraday Discuss, 107, pp. 229-246

Rabinovich Ya.I., R-H, Yoon, 1994. Use of atomic force microscope for the measurements of hydrophobic forces, Colloids Surfaces A: Physicochem, Eng. Aspects 93, pp. 263-273

Rao K H, Forssberg K S E. Mechanism G [J]. 1991. In Minerals Engineering, 4(7-11): pp 879-890.

Rao K H, Antti B M, Forssberg K S E. 1988. Mechanism of oleate interaction on salt type minerals Part I, adsorption and electrokinetic studies of calcite in the presence of sodium oleate and sodium metasilicate [J]. In Colloids and Surfaces, 34: pp. 227-239.

Rao K H, Cases J M, Donato P D, et al. 1991. Mechanism of oleate interaction on salt type minerals Part IV, adsorption, electrokinetic and diffuse reflectance FTIR studies of natural fluorite in the presence of sodium oleate [J]. In Journal of colloid and interface science, 145(2): pp. 314-329.

Rao K H, Cases J M, Donato P D, et al. 1991. Mechanism of oleate interaction on salt type minerals Part V, adsorption and precipitation in relation to the solid/liquid

ratio in the synthetic fluorite-sodium oleate [J]. Journal of Colloid and Interface Science, 145(2): 330-348.

Rao K H, Antti B M, Forssberg K S E. 1990. Mechanism of oleate interaction on salt type minerals Part II, adsorption and electrokinetic studies of apatite in the presence of sodium oleate and sodium metasilicate [J]. International Journal of Mineral Processing, 28, pp. 59-79.

Rao K H, Forssberg K S E. 1991. Mechanism of oleate interaction on salt type minerals Part III, adsorption, zeta potential and diffuse reflectance FTIR studies of scheelite in the presence of sodium oleate [J]. Colloids and Surfaces, 54, pp. 161-187.

Reed, C. E.; Kanazawa, K.K.; Kaufman, J.H. 1990. Journal of Applied Physics 68, pp. 1993-2001.

Samani, M., S., Blazy, P., and Cases, J.M., 1975. Transactions AIME, Vol. 258, Part I-V, pp. 168-182.

Sengul. H., Kadir Ozer. A., Sahin Gulaboglu. M., 2006. Beneficiation of Mardin-Mazida gi (Turkey) calcareous phosphate rock using dilute acetic acid solutions, Chem. Eng. J. 122, pp. 135-140.

Sharmistha Paul, Deepen Paul, Tamara Basova, and Asim K.Ray, 2008. Studies of Adsorption and Viscoelastic Properties of Proteins onto Liquid Crystal Phthalocyanine Surface Using Quartz Crystal Microbalance with Dissipation Technique, J.Phys. Chem. C, Vol. 112, No.31.

Straaten, P.V., 2002. Rocks for Crops, Agro minerals of sub-Sahara Africa. (CD), ICRAF, Nairobi, Kenya, ISBN: 0-88955-512-5, pp. 7-24.

Straaten, P.V., 2007. Agrogeology, The use of rocks for crops. Enviroquest (pub.), (Chapter 4), pp. 87-164.

S.Song, A. Lopez-Valdivieso, C.Martinez-Martinez, R.Torres-Armenta, 2006. Improving fluorite flotation from ores by dispersion process, In Minerals Engineering, 19, pp. 912-917.

Somasundaran P. and Lei Zhang, 1999. Role of surface chemistry of phosphate in its beneficiation, advances in research and practice, pp. 141-154.

Somasundaran P., B.Markovic, S.Krishnakumar and X.Yu, 1997. Colloidal Systems and Interfaces: Stability of Dispersions through polymer and Surfactant Adsorption, Handbook of Surface and Colloid Chemistry, K.S.B.irdied, CRC Press.

Sotillo F.J., Wang Guoxin, and Parker D.T., 2009. The role of surfactants on collectors and modifiers for improving phosphate flotation, Beneficiation of phosphates: Technology advance and adoption.

Swapp Susan, Scanning Electron Microscopy (SEM), in Integrating Research and Education website

Tao D. and Zhou X., Dopico P.G. Hines J. and Kennedy D., 2010. Evaluation of novel Georgia Pacific clay binders in iron ore flotation, Mineral and Metallurgical process, Vol 27, No. 1.

Tao D., Zhou Xiaohua, Kennedy Dennis, Dopico Pablo and Hines John, 2010. Improved Phosphate flotation using clay binder, Separation science and technology, pp. 604-609.

Tao D., Zhou X.H., Zhao C., Fan M.M., Chen G.L., Aron M. and Wright J., 2007. Coal and potash flotation enhancement using a clay binder, Canadian Metallurgical Quarterly, Vol 46, No.3, pp. 243-250 (8).

Tao D., Zhou X., Zhao C., Aron M. and Wright J., 2008. Clay binders for enhanced potash mineral beneficiation using froth flotation, SME annual meeting.

Tao D., 2004. Role of Bubble size in Flotation of coarse and fine particles-a review, separation science and technology, Vol 39, NO. 4, pp. 741-760.

Theys, 2003. Influence of the rock impurities on the phosphoric acid process, products and some downstream uses. Presented at the IFA meeting of the technical committee at the Hilton Abu Dhabi.

Teague A.J., Lolback M.C., 2012. The beneficiation of ultrafine phosphate, Mineral Engineering, pp. 52-59.

Unkelbach, K.H., and H.D.Wasmuth. 1991. "A High Intensity Drum-Equipped Magnetic Separator with Superconducting Magnet," Industrial Minerals Supplement, pp. 48-54.

Voinova M.V., M.Rodahl, M.Jonson, B. Kasemo, 1999. Viscoelastic acoustic response of layered polymer films at fluid-solid interfaces: continuum mechanics approach, Phys. Scr. 59, pp 391-396.

Wang and Gu, 2010. Collector development for beneficiating different phosphate ores with carbonate impurities.

Walzak M.J., Davidson R. and Biesinger M., 1998. The use of XPS, FTIR, SEM/EDX, Contact angle, and AFM in the characterization of coatings. In Journal of Materials Engineering and Performance, Vol 7(3), pp. 317-323.

Young T., 1805. An essay on the cohesion of fluids, Philos. Trans. R.Soc. London 95, pp. 65-87.

Yoon, R.-H. 2000. The role of hydrodynamic and surface forces in bubble-particle interaction. Inter. J. Miner. Proces. 58, pp. 129-143.

Zhang F, Yu Y, Bogan M. 1997. Challenging the "Crago" double float process II. Amine-fatty acid flotation of siliceous phosphates. Mineral Engineering, 10(9), pp. 983-994.

Zhang.P, Yu, Y, Hanson, H, Snow, R. 1999. Fundamentals and practical implications of the role of polymers in separating silica from phosphate, Beneficiation of phosphate: advances in research and practice, pp. 41-52.

Zhang, Jinhong and Zhang Wei, 2010. Applying an atomic force microscopy in the study of mineral flotation, Microscopy: Science, Technology, Application and Education, pp. 2028-2034.

Zhang, Patrick; Snow, Robert; Yu, Yingxue, 2002. Challenging the Crago Double Float Process III. Beneficiation of Phosphate using the FIPR/SAPR Process, Beneficiation of Phosphates-Fundamentals and Technology.

Zhang, Patrick; Snow, Robert; Yu, Yingxue and Michael D. Bogan, 2002. A Screening Study on Phosphate Depressants for Beneficiating Florida Phosphate Minerals, Final Report for Florida Institute of Phosphate Research, Bartow, Florida.

Copyright © Lingyu Zhang 2013

VITA

Author's name: Lingyu Zhang

Birthplace: P.R. China

EDUCATION:

- Master of Science in Mining Engineering, University of Kentucky, Lexington, September 2009 − present
- Bachelor of Science in Mineral Processing Engineering, China University of Mining and Technology (Beijing), Beijing, September 2005 − July 2009

PROFESSIONAL POSITION:

- Research Assistant, University of Kentucky, Lexington, KY, September 2009 − present
- Assistant Technician, China University of Mining and Technology (Beijing), May 2008 – 05/2009

ORAL PRESENTATION

- Enhanced phosphate flotation using novel depressants, SME Annual Conference 2013, Denver, February 2013

MEMBER

- SME – Society of Mining, Metallurgy and Exploration

Copyright © Lingyu Zhang 2013